Anaerobic digestion of excess sludge by cascade digesters

Guo, H.

DOI
10.4233/uuid:3a1703bb-38e1-4449-9551-92367c3d416b

Publication date
2024

Document Version
Final published version

Citation (APA)
Guo, H. (2024). *Anaerobic digestion of excess sludge by cascade digesters*. [Dissertation (TU Delft), Delft University of Technology]. https://doi.org/10.4233/uuid:3a1703bb-38e1-4449-9551-92367c3d416b

ANAEROBIC DIGESTION OF EXCESS SLUDGE BY CASCADE DIGESTERS

Hongxiao GUO

ANAEROBIC DIGESTION OF EXCESS SLUDGE BY CASCADE DIGESTERS

DISSERTATION

for the purpose of obtaining the degree of doctor

at Delft University of Technology

by the authority of the Rector Magnificus, Prof.dr.ir. T.H.J.J. van der Hagen

chair of the Board for Doctorates

to be defended publicly on

February 27th, 2024

by

Hongxiao GUO

Master of Environmental Engineering, Beijing Forestry University, China

born in Beijing, China

This dissertation has been approved by the promotors.

Composition of the doctoral committee:

Rector Magnificus	Chairperson
Prof. Dr. Ir. M. de Kreuk	Delft University of Technology, promotor
Prof. Dr. Ir. J.B. van Lier	Delft University of Technology, promotor

Independent members:

Prof. Dr. Ir. D. Brdjanovic	Delft University of Technology / IHE Delft, the Netherlands
Prof. Dr. Ir. X. Zhan	National University of Ireland, Galway, Ireland
Prof. Dr. Ir. L. Appels	Katholieke Universiteit Leuven, Belgium
Prof. Dr. Ir. W. Parker	University of Waterloo, Canada
Dr. Ir. S. Scherrenberg	Royal HaskoningDHV, the Netherlands
Prof. Dr. Ir. H.M. Jonkers	Delft University of Technology, reserve member

The research presented in this thesis was performed at the Sanitary Engineering Section, Department of Water Management, Delft University of Technology. Hongxiao Guo acknowledges the PhD scholarship awarded by the China Scholarship Council (China) and Lamminga Fund (the Netherlands).

Printed by: proefschrift-aio.nl
Cover by: Chun TANG/Hongxiao GUO
ISBN: 978-94-93353-61-9

An electronic version of this dissertation is available at https://repository.tudelft.nl/

This book is dedicated to my family, for their endless support and patience.

谨以此书献给我的家人，感谢你们一直以来对我无尽的 支持和包容。

Table of Content

SUMMARY

The management and disposal of excess sludge is one of the main challenges for wastewater treatment facilities across the world. Anaerobic digestion (AD) is a widely accepted treatment method for stabilizing excess sludge due to its robustness, ability to reduce pathogens, and capacity to convert the biochemical energy enclosed in organic compounds into biogas. However, the efficiency of converting excess sludge organics into biogas using conventional continuous stirred tank reactors (CSTR) is relatively low, primarily due to the slow hydrolysis rate. Various enhancement technologies, including thermal, chemical, and enzymatic methods, have been developed to accelerate the hydrolysis rate. Among these, enzymatically enhanced hydrolysis has attracted attention for its advantages, such as the absence of toxic by-product formation and the ability to operate under moderate conditions. However, the scaling-up of these methods to industrial scale presents ongoing challenges. The research in this dissertation explored the feasibility of an innovative cascade anaerobic digestion (CAD) technology, consisting of differently sized CSTR digesters in series. The overall objective of the CAD technology is to achieve enzymatically enhanced hydrolysis of excess sludge in the first reactor stages.

In **chapter** 2 of this thesis the study on the feasibility of the CAD configuration to improve WAS hydrolysis and subsequent digestion is described. This research assessed the process performance, enzyme activities, and microbial community composition at different solids retention times (SRTs). The CAD system increased the sludge treatment capacity by 30-35% compared to a conventional sludge digester of the same volume, with a total SRT of only 12 days, indicating its potential for efficient, cost-effective excess sludge treatment. Hydrolytic enzyme activity tests revealed higher enzyme activities in the CAD system, particularly at short SRTs, attributable to the enhanced specific hydrolysis rate. Certain enzymes targeting the hydrolysis of structural extracellular polymeric substance (SEPS) related organic compounds exhibited reversed distribution and increased activity in the final stages of the CAD system. This, along with the increased relative abundance of key hydrolytic bacteria in the first three reactors of the CAD system contributed to enhanced enzymatic hydrolysis and sludge reduction. Results also showed a shift in relative abundance from hydrogenotrophic methanogens to acetoclastic methanogens when decreasing the SRT.

Chapter 3 describes the examined impact of digestate recirculation strategies on WAS hydrolysis in the CAD process, applying low recirculation ratios. A digestate recirculation ratio of only 10% led to an average total chemical oxygen demand reduction efficiency of 40% at a total SRT of 12 days. It was hypothesized that recycling trace metals, such as Mn and Zn, from later stages to the first reactor is of importance for enhanced enzyme production and thus for regulating WAS hydrolysis rates. The solids fraction of the digestate served as a source of active hydrolytic microorganisms, as demonstrated by comparative microbial analyses.

The full-scale CAD system, being an upgrade of the lab-scale reactor discussed in chapters 2 and 3, was constructed at wastewater treatment plant Tollebeek in the Netherlands. The research in the full-scale system focused on the impact of primary sludge (PS) on sludge hydrolysis performance. In **chapter 4**, we report the assessment of long-term reactor performance by studying the sludge biodegradability, hydrolytic enzyme activities, and metagenome composition. The full-scale CAD system consisted of a CSTR divided into three smaller pie-shaped reactors, operated in series at a low SRT and a small recycle between the third and first reactors, followed by one large existing CSTR in series. This CAD system yielded a significant sludge reduction efficiency of approximately 56% and showed enhanced enzymatic activity of protease and cellulase in the first reactors. Unlike the lab experiments, however, a less pronounced separation of microbial populations was observed in the full-scale cascade AD system, possibly due to level-equalisation holes in the inner walls of this first full-scale pie-shaped design.

The research described in **chapter 5 and 6** compared the anaerobic biodegradability of waste aerobic granular sludge (AGS) with WAS and PS from full-scale municipal WWTPs, focusing on differences in biomethane potential (BMP) and physicochemical composition, such as related to the carbohydrates, proteins, and lipids content. The waste AGS consisted of two fractions: the more flocculent AGS selection discharge (AGS-SD) and the granular AGS fraction for solids retention time control (AGS-RTC). AGS-RTC had a significantly lower BMP than WAS, while the BMP of AGS-SD matched that of PS and surpassed AGS-RTC, likely due to the presence of highly biodegradable cellulose-like fibres. SEPS degradation patterns showed that SEPS from granules had a lower degradation rate than SEPS from WAS, which can be potentially enhanced by the cascade AD process.

The final chapter summarizes the primary findings from each preceding chapter and outlines recommendations for future research pertaining to the use of cascade configurations for AD of excess sludge. These recommendations are:

1) Enhance our understanding of hydrolysis kinetics in CAD systems.

2) Conduct more comprehensive experiments to understand the role of trace metals in regulating enzymatic hydrolysis of excess sludge in CAD systems.

3) Undertake more in-depth studies on conversion processes, kinetics, microbial consortia, and operational conditions in full-scale CAD applications, such as the Ephyra® technology that was further developed with the results of this thesis.

4) In terms of WAS management using the cascade AD process, there is a need to investigate technologies that could enhance the decomposition of structural EPS. Furthermore, it's of interest to explore the potential of the CAD process to effectively digest aerobic granules for both biogas production and volatile fatty acids production in the first stage of the CAD system for enhanced nutrients removal.

Chapter 1

INTRODUCTION

Activated sludge processes (ASP) are widely implemented for the treatment of municipal sewage and are characterised by a relatively easy operation and high treatment efficiency. Despite these benefits, managing sewage sludge, a by-product generated during the ASP, has become an unprecedentedly challenge in recent years. The current daily production of dry solids (DS), ranging from 60 to 90 g of DS per population equivalent, equals nearly 10 million tons of dry sludge annually in the European Union alone (Appels et al., 2008). With an increasing number of wastewater treatment plants (WWTPs) globally, sludge production is expected to grow very substantially in the foreseeable future. Considering the development of population, urbanization and industrialization, finding effective solutions for sewage sludge treatment is of increasing global concern (Peccia & Westerhoff, 2015).

According to the Dutch roadmap for WWTPs towards 2030, which was announced by the Dutch Foundation for Applied Water Research (STOWA), the transition of WWTPs in the Netherlands to 'Energiefabrieken' (energy plants) started in 2010. The aim is to produce and recover energy, such as biogas, to the extent that WWTPs become energy neutral or even energy positive (Ampe et al., 2020). Given the energy content of sewage sludge, it is considered a proper energy source, and energy recovery from sewage sludge complies with sustainability principles (Shaddel et al., 2019).

The potential benefits of utilizing sewage sludge to maximize the energy recovery in Dutch WWTPs can only be realised through appropriate technological solutions. In order to achieve a sustainable transition, a research program aiming at the development of next-generation sewage sludge treatment technologies was granted by Dutch Foundation for Applied Water Research (STOWA). This PhD thesis describes the research conducted as part of this program, especially focusing on process enhancement in anaerobic digestion of waste activated sludge (WAS). The research was performed in close collaboration with Royal HaskoningDHV, technology providers, and water authorities. This research shows that fundamental research can be translated into practical applications for full-scale WWTP installations.

1.1 Basic principles of anaerobic digestion

As the world's fossil fuel reserve declines, anaerobic digestion (AD) is commonly suggested as a sustainable technology for sewage waste sludge treatment. AD not only reduces the sludge quantity with 30 to 40 %, it also generates energy through the production of methane. AD is considered a preferred treatment for municipal sewage sludge due to its lower cost and comparably moderate performance when compared to aerobic digestion. The World Biomass Association estimated the potential of biogas production of sewage sludge alone at 6 billion m^3 for the

European Union, which amounts 1.2% of total use of natural gas in Europe (Scarlat et al., 2018). In the absence of oxygen, AD leverages anaerobic microorganisms to transform organic material into biogas. This biogas generally comprises 55 - 75 vol% of methane and 25 - 40 vol% of carbon dioxide (Van Lier et al., 2020). AD consists of four interdependent, complex sequential and parallel biological steps:

Hydrolysis: Hydrolysis is the first step in AD, during which particulate organic compounds, like proteins, carbohydrates and nucleic acids, are converted into soluble substrates, such as amino acids and sugars, by hydrolytic bacteria using membrane-bound and extracellular enzymes. Important hydrolytic bacteria involved in this process, belong to the phyla *Clostridium, Bacteroides, Microbispora, Ruminococcus,* and *Firmicutes* (Jain et al., 2015). Hydrolysis is broadly viewed as the bottleneck in the anaerobic digestion of particulate organic material (Gonzalez et al., 2018). The process of hydrolyzing particulate organic matter has commonly been modeled using first-order kinetics, which encapsulates the cumulative impacts of all micro-level processes taking place in the initial stage of anaerobic digestion (Eastman & Ferguson, 1981). Studies by Feng et al. (2009) and Mahmoud et al. (2004) have demonstrated that also the hydrolysis of particulate chemical oxygen demand (COD) from WAS and primary sludge (PS), could be described using first-order kinetics. Several factors, such as pH, temperature, enzyme types and exact substrate composition, may affect the hydrolysis process of WAS. Previous research proposed a linear relation between hydrolysis rate and the concentration of biodegradable substrate present in the anaerobic digestor at constant pH and temperature (Vavilin et al., 2008).

Acidogenesis: The molecules produced during the hydrolysis phase are subsequently transformed into volatile fatty acids (VFA) by specific bacteria known for their acidogenic or fermentative properties. These bacteria include members of genera *Clostridium, Lactobacillus, Geobacter,* and *Bacteroides* (Guo et al., 2015). These fermentative organisms can survive in a wide pH range between 4 and 8.5. Along with VFA, minor by-products, such as ammonia, H_2, and CO_2 are formed during this conversion.

Acetogenesis: The organic acids created by fermentative bacteria are further metabolized by acetogens into acetic acid, CO_2, and H_2. The partial pressure of hydrogen is critical in facilitating this conversion. These reactions are thermodynamically favorable only under particularly low concentrations of the reaction products, specifically acetate and H_2. This means acetate concentrations should be between 10^{-4} - 10^{-1} mol/L, and the required H_2 partial pressures for propionate and butyrate should be between 10^{-6} - 10^{-4} bar and (1.0 - 7.0) $\times$ 10^{-3} bar, respectively (Dhar et al., 2015).

Methanogenesis: Methanogenesis represents the final stage in anaerobic digestion, resulting in the production of methane. Methanogens either reduce CO_2 with H_2 as an electron donor or transform acetate into CH_4 and CO_2. Acetate decarboxylation, also known as acetoclastic methanogenesis, accounts for approximately 70% of methane production in anaerobic digestion processes. Methanogens are highly sensitive to pH changes and can only flourish within a pH range of 6.5 - 8.0. They maintain the balance in hydrogen partial pressure, necessary for the acetogenic transformations, by consuming hydrogen. Hence, a well-regulated digestion process should result in a balance between acidogenesis and methanogenesis (Pasalari et al., 2021).

1.2 Types of chemical composition of excess sludge and their bio-methane potential in anaerobic digestion

Biological excess sludge, also known as WAS, is made up of microbial clusters, filamentous bacterial species, organic and inorganic particles, extracellular polymeric substances (EPS), and a significant quantity of water. Organic compounds found in wastewater, including cellulose and humic acids, can become integrated into the activated sludge flocs. The organic fraction of WAS is mainly composed of proteins, polysaccharides, nucleic acids, humic substances, and lipids (Gonzalez et al., 2018).

EPS in activated sludge primarily derive from the secretion of microbial byproducts and cell lysis. Depending on their location within the sludge floc matrices, EPS are typically classified into three types: slime EPS (S-EPS), loosely bound EPS (LB-EPS), and tightly bound EPS (TB-EPS). S-EPS primarily resides in the bulk liquid surrounding the sludge flocs. In contrast, LB-EPS and TB-EPS are associated with the sludge flocs and generally display a highly porous and dispersed structure. Particularly, TB-EPS adheres to the surface of bacterial cells within the sludge flocs (Sheng et al., 2010). The presence of these three-dimensional, negatively charged biopolymers, which behave like hydrogels, determines the surface physicochemical characteristics of sludge matrices. EPS provide a protective layer and influence the functional integrity, strength, flocculation, dewaterability, and even biodegradability of sludge flocs (More et al., 2014). Moreover, microbial cells themselves have a rigid cell envelope made up of glycan strands cross-linked by peptides, creating a physical and chemical barrier for anaerobic digestion. As a result, waste activated sludge (WAS) can be challenging to hydrolyze and convert during the AD process within the established timeframe. This leads to a volatile solids (VS) destruction efficiency of 30 to 50% for raw sludge in conventional mesophilic anaerobic digesters, even with extended retention times of 20 – 30 days (Cao & Pawlowski, 2012).

One of the first steps of municipal sewage treatment is usually primary clarification producing a PS fraction. This fraction consists of settleable organic solids from

kitchen and toilet waste. The biomethane production rate and extend of PS in AD is usually higher than that of WAS, which is related to its composition of biodegradable fats, carbohydrates and proteins, and lack of bacterial structures like described above (Bernat et al., 2017). Champagne and Li (2009) attributed the high methane production efficiency of PS specifically to the higher content of easily biodegradable cellulosic fibers and lipids in PS than in WAS, considering the theoretical average methane production for carbohydrates of 0.42 m^3 CH_4/gVS, proteins of 0.50 m^3 CH_4/g VS, and lipids of 1.01 m^3 CH_4/gVS (Angelidaki et al., 2004).

Over recent years, the aerobic granular sludge (AGS) process has emerged as a favored method for biological wastewater treatment, with successful deployment at over a hundred large-scale wastewater treatment plants worldwide (Pronk et al., 2015). Aerobic granules are dense and compact bacterial aggregates, bound together by its EPS. The unique morphological differences between aerobic granular sludge (AGS) and activated sludge (AS) are dictated by the varied chemical and mechanical characteristics of the EPS that form their structure or gel (Lin et al., 2013). So far, Bernat et al. (2017) studied the biogas potential of AGS grown in laboratory conditions. According to this study the content of hard-to-biodegrade lignocellulosic substances determined the biogas potential of AGS, that was 1.8 time lower than that of AS. In the study, it is unclear why the AGS of the laboratory scale reactor contained a considerable higher fraction of lignin than the WAS and PS obtained from a full scale WWTP. Moreover, it was suggested to improve the biogas potential for AGS by co-digestion of AGS with PS. However, AGS installations usually don't install primary clarification, and therefore this suggestion seems not very useful.

1.3 Strategies to enhance hydrolysis of excess sludge

While the potential of using WAS and PS from WWTPs as a means for sustainable energy generation has attracted great interest, the efficiency of excess sludge digestion, in particular of WAS and AGS, remains low due to the low hydrolysis rates. To enhance the biodegradability and accelerate degradation of sludge, several hydrolysis enhancement methods for excess sludge have been developed. Their common main goal is to disintegrate the sludge particles, and thus to destroy its structural EPS and bacterial cell walls in order to liberate its biodegradable fraction. Techniques of enhancing sludge hydrolysis can be either of physical (thermal and mechanical), chemical (acid or alkaline) or biological nature (such as hydrolytic enzyme treatment) (Gonzalez et al., 2018). The advantages and disadvantages of different enhancement methods have been summarized in Table 1.1. Physical and chemical enhancement methods are usually energy intensive or need chemicals leading to the formation of waste byproducts. This can result in economic constraints and limitations to their scale up and commercialization (Carballa et al., 2011).

Microorganisms and prokaryotes break down organic matter in wastewater with the help of hydrolytic enzymes. Due to their catalytic nature, the enzymes of hydrolytic and fermentative organisms in AD hydrolyze complex molecules at mild pH values and temperatures, without the production of hazardous waste products, which is very different from physical or chemical enhancement methods (Chen et al., 2018). Sludge hydrolysis by enzymes can be represented by two conceptual models (Batstone et al., 2002): (a) the organisms secrete hydrolytic enzymes to the bulk solution, where it adsorbs onto a particle or reacts with a soluble substrate, and (b) the organisms attach to a particle, while membrane-bound enzymes perform hydrolysis reactions at the surface of the particle. Usually, hydrolytic enzymes are prone to self-degradation in their free form. Therefore, in biological systems they are usually immobilized onto solid media such as EPS or sludge flocs in order to increase their stability (Lu et al., 2016). Common ways to enhance the enzymatic hydrolysis of sludge include addition of active enzymes (Pei et al., 2010), and/or bioaugmentation (Agabo-Garcia et al., 2019). Unlike externally adding enzymes, bioaugmentation accelerates the generation of endogenous enzymes (or enzyme-producing microorganisms) in the digester, for example by adjustment in temperature from mesophilic 35 °C to thermophilic 55 °C conditions (Hendriks et al., 2018). This example is put into practice by the development of temperature phased AD processes for sludge treatment (Wu et al., 2015). However, researches on bioaugmentation via changing reactor design are still limited so far (Nabaterega et al., 2021).

1.4 Scope of this thesis

The aim of this Ph.D. thesis was to develop a new enzymatic hydrolysis enhancement method for excess sludge by applying four CSTRs in series. Based on the research gaps that were described in the previous paragraphs, this thesis has been divided in the following chapters and their corresponding research questions:

Research question 1: how does a cascade anaerobic digestion (CAD) configuration affect the enzymatic hydrolysis rate and efficiency, and the reduction of WAS compared to a conventional digester?

In chapter 2, the feasibility of using a CAD configuration to enhance WAS hydrolysis and the subsequent anaerobic sludge digestion was researched. The process performance, as well as enzyme activities were evaluated at different solids retention times (SRTs), and the microbial community was analyzed. Governing hydrolysis kinetics in this system were preliminarily explored as well.

Table 1.1 Summary of the benefits and drawbacks of different pretreatment methods (modified from Zhen et al. (2017) and Gonzalez et al. (2018))

Hydrolysis enhancement method		Fundamental mechanisms	Operational parameters	Energy demand	Chemicals dosage	Waste byproduct formation
Physical						
Heating	Mild temperature	Thermal effect at 60 - 100 °C	Temperature, exposure time,	Medium	No	Recalcitrant compounds from Maillard reaction
	High temperature	Thermal effect at 100 - 180 °C	Temperature, exposure time, pressure	High	No	
Microwave		Thermal effect to break up hydrogen bonds, etc.	Power input, frequency, exposure time	High	No	Recalcitrant compounds from Maillard reaction
Ultrasonication		Cavitation (hydro-mechanical shear forces, oxidizing effect)	Power input, exposure time	High	No	No
Feeze- thaw		Volume difference between water and ice	Power input, exposure time	High	No	No
Chemical						
Acidic		Hydrolysis of hemicellulose	Dose, exposure time	Low	Yes	Residual acid in the sludge
Alkaline		Solvation, saphonication	Dose, exposure time	Low	Yes	Residual alkaline in the sludge
Fenton/H_2O_2		Hydroxyl radicals	Dose, Fe^{2+}/H_2O_2 ratio, exposure time, pH	Low	Yes	Fe sludge
Ozonation		Formation of hydroxyl radicals	Dose, exposure time	Medium	Yes	Ozone gas emission
Activated persulfate		Sulfate free radicals	Dose, exposure time, pH	Low	Yes	Residual sulfate
Biological						
Thermophilic digestion		Hydrolysis and acidogenesis in thermophilic stage	Thermophilic temperature, HRT	Medium	No	Aromatic compounds
Enzyme addition		Addition of hydrolytic enzymes	Dose, temperature	Medium	Yes	No

Research question 2: how does the digestate recirculation ratio regulate WAS hydrolysis in a high-rate CAD system?

Chapter 3 focuses on the effect of digestate recirculation strategies on the performance of WAS hydrolysis in the CAD process. A novel control method was

developed and evaluated, using low recirculation ratios rather than high ratios as commonly reported in literature. Using this method, the mechanisms that related to trace-metals supplements and changes in the microbial structure were discussed.

Research question 3: what are the sludge hydrolysis and sludge reduction efficacies of the CAD process at full-scale fed with a PS - WAS mixture with fluctuating compositions?

Being upgraded from lab-scale studies presented in chapter 2 and 3, a full-scale cascade sludge AD system was constructed in WWTP Tollebeek, the Netherlands. This installation was studied in detail, of which the results are reported in chapter 4. In this full-scale process, special emphasis was given to the impact of the presence of PS on the sludge hydrolysis performance. Full-scale sludge AD processes are typically operated by the co-digestion of WAS and PS rather than the treatment of WAS alone. Long-term reactor performance in terms of sludge biodegradability, hydrolytic enzyme activities and a genome analysis was investigated, respectively.

Research question 4: can Waste AGS (WAGS) also be a potential substrate for treatment by the CAD process, considering the differences in physicochemical properties of sludge between WAGS and WAS?

AGS technology is an alternative to conventional activated sludge processes to reduce the process footprint and energy consumption. Strategies for efficient management of its produced biomass, characterized by a combination of flocculent and granule morphologies, need further development. The studies of chapter 5 and chapter 6 systematically compared the anaerobic biodegradability of WAGS with WAS as well as PS from full-scale municipal wastewater treatment plants. Difference in biomethane potential (BMP) and in the physicochemical composition were investigated, with special attention to differences in carbohydrates (cellulosic fibers), proteins, and lipids composition between WAGS, WAS and PS. Especially, the biodegradation mechanism of the structural EPS generated in WAGS and WAS were elucidated by using Fourier transformed infrared spectroscopy (FT-IR), three-dimensional excitation and emission matrix analysis (3D-EEM) and dynamic mechanical analysis. The results led to an evaluation on potential advantages of WAGS digestion using the CAD process.

Chapter 7 gives concluding remarks on the thesis, and describes the outlook for this field of research.

References

Agabo-Garcia, C., Perez, M., Rodriguez-Morgado, B., Parrado, J., Solera, R. 2019. Biomethane production improvement by enzymatic pre-treatments and enhancers of sewage sludge anaerobic digestion. Fuel, 255.

Ampe, K., Paredis, E., Asveld, L., Osseweijer, P., Block, T. 2020. A transition in the Dutch wastewater system? The struggle between discourses and with lock-ins. Journal of Environmental Policy & Planning, 22(2), 155-169.

Angelidaki, I., Sanders, W.J.R.V.i.E.S., Bio/Technology. 2004. Assessment of the anaerobic biodegradability of macropollutants. 3(2), 117-129.

Appels, L., Baeyens, J., Degreve, J., Dewil, R. 2008. Principles and potential of the anaerobic digestion of waste-activated sludge. Progress in Energy and Combustion Science, 34(6), 755-781.

Batstone, D.J., Keller, J., Angelidaki, I., Kalyuzhnyi, S.V., Pavlostathis, S.G., Rozzi, A., Sanders, W.T.M., Siegrist, H., Vavilin, V.A. 2002. The IWA Anaerobic Digestion Model No 1 (ADM1). Water Science and Technology, 45(10), 65-73.

Bernat, K., Cydzik-Kwiatkowska, A., Wojnowska-Baryla, I., Karczewska, M. 2017. Physicochemical properties and biogas productivity of aerobic granular sludge and activated sludge. Biochemical Engineering Journal, 117, 43-51.

Cao, Y.C., Pawlowski, A. 2012. Sewage sludge-to-energy approaches based on anaerobic digestion and pyrolysis: Brief overview and energy efficiency assessment. Renewable & Sustainable Energy Reviews, 16(3), 1657-1665.

Carballa, M., Duran, C., Hospido, A. 2011. Should We Pretreat Solid Waste Prior to Anaerobic Digestion? An Assessment of Its Environmental Cost. Environmental Science & Technology, 45(24), 10306-10314.

Champagne, P., Li, C.J. 2009. Enzymatic hydrolysis of cellulosic municipal wastewater treatment process residuals as feedstocks for the recovery of simple sugars. Bioresource Technology, 100(23), 5700-5706.

Chen, J.H., Liu, S.H., Wang, Y.M., Huang, W., Zhou, J. 2018. Effect of different hydrolytic enzymes pretreatment for improving the hydrolysis and biodegradability of waste activated sludge. Water Science and Technology, 592-602.

Dhar, B.R., Elbeshbishy, E., Hafez, H., Lee, H.S. 2015. Hydrogen production from sugar beet juice using an integrated biohydrogen process of dark fermentation and microbial electrolysis cell. Bioresource Technology, 198, 223-230.

Eastman, J.A., Ferguson, J.F. 1981. Solubilization of Particulate Organic-Carbon during the Acid Phase of Anaerobic-Digestion. Journal Water Pollution Control Federation, 53(3), 352-366.

Feng, L.Y., Yan, Y.Y., Chen, Y.G. 2009. Kinetic analysis of waste activated sludge hydrolysis and short-chain fatty acids production at pH 10. Journal of Environmental Sciences, 21(5), 589-594.

Gonzalez, A., Hendriks, A., van Lier, J.B., de Kreuk, M. 2018. Pre-treatments to enhance the biodegradability of waste activated sludge: Elucidating the rate limiting step. Biotechnol Adv, 36(5), 1434-1469.

Guo, J.H., Peng, Y.Z., Ni, B.J., Han, X.Y., Fan, L., Yuan, Z.G. 2015. Dissecting microbial community structure and methane-producing pathways of a full-scale anaerobic reactor digesting activated sludge from wastewater treatment by metagenomic sequencing. Microbial Cell Factories, 14.

Hendriks, A.T.W.M., van Lier, J.B., de Kreuk, M.K. 2018. Growth media in anaerobic fermentative processes: The underestimated potential of thermophilic fermentation and anaerobic digestion. Biotechnology Advances, 36(1), 1-13.

Jain, S., Jain, S., Wolf, I.T., Lee, J., Tong, Y.W. 2015. A comprehensive review on operating parameters and different pretreatment methodologies for anaerobic digestion of municipal solid waste. Renewable & Sustainable Energy Reviews, 52, 142-154.

Lin, Y.M., Sharma, P.K., van Loosdrecht, M.C.M. 2013. The chemical and mechanical differences between alginate-like exopolysaccharides isolated from aerobic flocculent sludge and aerobic granular sludge. Water Research, 47(1), 57-65.

Lu, F., Wang, J.W., Shao, L.M., He, P.J. 2016. Enzyme disintegration with spatial resolution reveals different distributions of sludge extracellular polymer substances. Biotechnology for Biofuels, 9.

Mahmoud, N., Zeeman, G., Gijzen, H., Lettinga, G. 2004. Anaerobic stabilisation and conversion of biopolymers in primary sludge - effect of temperature and sludge retention time. Water Research, 38(4), 983-991.

More, T.T., Yadav, J.S.S., Yan, S., Tyagi, R.D., Surampalli, R.Y. 2014. Extracellular polymeric substances of bacteria and their potential environmental applications. Journal of Environmental Management, 144, 1-25.

Nabaterega, R., Kumar, V., Khoei, S., Eskicioglu, C.J.J.o.E.C.E. 2021. A review on two-stage anaerobic digestion options for optimizing municipal wastewater sludge treatment process. 105502.

Ortega, S., T. 2023. Conversion of Polymeric Substrates by Aerobic Granular Sludge.Ph.D. dissertation, TU Delft.

Pasalari, H., Gholami, M., Rezaee, A., Esrafili, A., Farzadkia, M. 2021. Perspectives on microbial community in anaerobic digestion with emphasis on environmental parameters: A systematic review. Chemosphere, 270, 128618.

Peccia, J., Westerhoff, P. 2015. We Should Expect More out of Our Sewage Sludge. Environmental Science & Technology, 49(14), 8271-8276.

Pei, H.Y., Hu, W.R., Liu, Q.H. 2010. Effect of protease and cellulase on the characteristic of activated sludge. Journal of Hazardous Materials, 178(1-3), 397-403.

Pronk, M., de Kreuk, M.K., de Bruin, B., Kamminga, P., Kleerebezem, R., van Loosdrecht, M.C. 2015. Full scale performance of the aerobic granular sludge process for sewage treatment. Water Research, 84, 207-17.

Scarlat, N., Dallemand, J.F., Fahl, F. 2018. Biogas: Developments and perspectives in Europe. Renewable Energy, 129, 457-472.

Shaddel, S., Bakhtiary-Davijany, H., Kabbe, C., Dadgar, F., Osterhus, S.W. 2019. Sustainable Sewage Sludge Management: From Current Practices to Emerging Nutrient Recovery Technologies. Sustainability, 11(12).

Sheng, G.P., Yu, H.Q., Li, X.Y. 2010. Extracellular polymeric substances (EPS) of microbial aggregates in biological wastewater treatment systems: A review. Biotechnology Advances, 28(6), 882-894.

Van Lier, J.B., Mahmoud, N., Zeeman, G. 2020. Anaerobic Wastewater Treatment Biological Wastewater Treatment: Principles, Modelling and Design, Second Edition, Chapter 16, IWA Publishing, London, UK, 701-756.

Vavilin, V.A., Fernandez, B., Palatsi, J., Flotats, X. 2008. Hydrolysis kinetics in anaerobic degradation of particulate organic material: An overview. Waste Management, 28(6), 939-951.

Wu, L.J., Qin, Y., Hojo, T., Li, Y.Y. 2015. Upgrading of anaerobic digestion of waste activated sludge by temperature-phased process with recycle. Energy, 87, 381-389.

Zhen, G.Y., Lu, X.Q., Kato, H., Zhao, Y.C., Li, Y.Y. 2017. Overview of pretreatment strategies for enhancing sewage sludge disintegration and subsequent anaerobic digestion: Current advances, full-scale application and future perspectives. Renewable & Sustainable Energy Reviews, 69, 559-577.

Chapter 2

FEASIBILITY OF CASCADE DIGESTER IN IMPROVING ENZYMATIC HYDROLYSIS OF WASTE ACTIVATED SLUDGE IN ANAEROBIC DIGESTION

This Chapter is based on:

Guo, H., Oosterkamp, M. J., Tonin, F., Hendriks, A., Nair, R., van Lier, J. B., & de Kreuk, M. (2021). Reconsidering hydrolysis kinetics for anaerobic digestion of waste activated sludge applying cascade reactors with ultra-short residence times. Water Research, 202, 117398.

Abstract

Hydrolysis is considered to be the rate-limiting step in anaerobic digestion of waste activated sludge (WAS). In this study, an innovative 4 stages cascade anaerobic digestion (CAD) system was researched to (1) comprehensively clarify whether cascading configuration enhances WAS hydrolysis, and to (2) better understand the governing hydrolysis kinetics in this system. The CAD consisted of three 2.2 L ultra-short solids retention times (SRT) continuous stirred tank reactors (CSTRs) and one 15.4 L CSTR. The CAD was compared with a reference conventional CSTR digester (22 L) in terms of process performance, hydrolytic enzyme activities and microbial community dynamics under mesophilic conditions (35°C). The results showed that the CAD achieved a high and stable total chemical oxygen demand (tCOD) reduction efficiency of 40-42%, even at 12 days total SRT that corresponded to only 1.2 days SRT each in the first three reactors of the cascade. The reference-CSTR converted only 31% tCOD into biogas and suffered process deterioration at the applied low SRTs. Calculated specific hydrolysis rates in the first reactors of the CAD were significantly higher compared to the reference-CSTR, especially at the lowest applied SRTs. The activities of several hydrolytic enzymes produced in the different stages revealed that protease, cellulase, amino peptidases, and most of the tested glycosyl-hydrolases had significantly higher activities in the first three small digesters of the CAD, compared to the reference-CSTR. This increase in hydrolytic enzyme production by far exceeded the increase in specific hydrolysis rate, indicating that hydrolysis was limited by solids-surface availability for enzymatic attack. Correspondingly, high relative abundances of hydrolytic-fermentative bacteria and hydrogenotrophic methanogens as well as the presence of syntrophic bacteria were found in the first three digesters of the CAD. However, in the fourth reactor, acetoclastic methanogens dominated, similarly as in the reference-CSTR. Overall, the results concluded that using multiple CSTRs that are operated at low SRTs in a cascade mode of operation significantly improved the enzymatic hydrolysis rate and extend in anaerobic WAS digestion. Moreover, the governing hydrolysis kinetics in the cascading reactors were far more complex than the generally assumed simplified first-order kinetics.

2.1 Introduction

Waste activated sludge (WAS) is an inevitable by-product generated in biological wastewater treatment plants (WWTPs). Due to quantitative and qualitative extension of wastewater treatment, the annual WAS production has increased in the European Union during the last two decades, from 10 million tons in 2008 to 11.5 million tons in 2015, and is expected to approach 13 million tons by 2020 (Rorat et al. 2019). Anaerobic digestion (AD) is a proven key technology for both stabilization of WAS and recovery of the biochemical energy stored in the sludge in the form of biogas. WAS usually contains complex particulate organics, such as proteins, polysaccharides, lignocellulosic matters, and fats (Gonzalez et al. 2018). Hydrolysis of WAS into soluble substrates is the first step in AD and is generally regarded as the rate-limiting step in this process (Appels et al. 2008). Therefore, conventional digesters using continuous stirred tank reactors (CSTRs) have to be operated under prolonged sludge retention times (SRTs) exceeding 20 days for an acceptable WAS conversion.

To accelerate the conversion rate of WAS and decrease these long SRTs, process optimisation has been applied as well as the development of hydrolysis enhancement technologies, including thermal, chemical and enzymatic methods (Zhen et al. 2017). Enzymatic hydrolysis enhancement seemingly offers unique advantages compared to chemical or physical processes, as it neither causes generation of toxic substances, nor needs operations under extreme conditions, thus receiving an increased attention in the recent years (Gonzalez et al. 2018). Most of these studies focused on the direct addition of highly active hydrolytic enzymes into the digester (Yang et al. 2010) or on pre-fermentation by specific hydrolytic bacteria prior to AD (Agabo-Garcia et al. 2019). These proof-of-concept methods showed remarkable improvement in WAS hydrolysis and bio-degradation; however, full scale applications require a continuous purchase of enzymes and/or the need for preservation of specific biomass while working with poorly defined substrates.

Hydrolysis of organic matter during AD is performed by extracellular and/or membrane-bound hydrolytic enzymes (Kim et al. 2012). Enhancement of WAS hydrolysis also can be achieved by accelerating the reaction rates and/or increasing the activity of these hydrolytic enzymes instead of adding external hydrolytic enzymes or applying pre-fermentation. A commonly applied strategy is to perform WAS digestion under thermophilic (55°C) conditions, which roughly results in a doubling of the enzymatic reaction rates compared to the commonly applied mesophilic (35 °C) conditions (Ge et al. 2011a). Nevertheless, decreased process performance was often observed under thermophilic conditions due to the accumulation of organic intermediates to a toxic level, or to a drop in pH (Kim et al. 2003),

negatively impacting the actual enzymatic reaction rates. In addition, other constraints of thermophilic WAS digestion include higher energy requirement, poor effluent quality and a poorer digestate's dewaterability (De la Rubia et al. 2013). Thus, there is a great interest to search for alternative technologies.

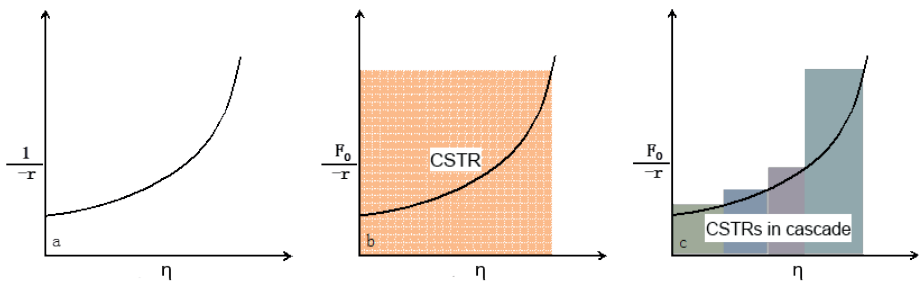

Figure 2.1 Theoretical reactor volume reduction by applying a cascade CSTR configuration versus a single stage CSTR (Levenspiel 2006). (a) Relationship between the substrate conversion ratio (η) and the reciprocal first order conversion reaction rate (-r), (b) required reactor volume of a single stage CSTR for a required conversion ratio η, indicated by the total surface area of the rectangle, and (c) required reactor volume for the cascade CSTR configuration for the same η, by summing the 4 subsequent surface areas

The enzymatic hydrolysis of WAS is commonly described by empirical first-order kinetics (Vavilin et al. 2008), meaning that the observed solids conversion rate is dependent on the solid substrate concentration and the first-order hydrolysis rate constant (Eq. 2.1).

$$\frac{dS}{dt} = -k_H S \qquad \text{(Eq. 2.1)}$$

Where S = substrate concentration, t = time, and k_H = first-order hydrolysis rate constant.

Theoretically, in a CSTR, the concentration S in the reactor equals the effluent S concentration, indicating that in-reactor conversion rates decrease with decreasing S (Eq. 2.1), agreeing with an increased conversion ratio (η) (Figure 2.1a). Based on Eq. 2.2, the required volume of a CSTR at a given inlet feeding rate (F_0) is fully determined by the required η and is graphically presented by the large rectangular area shown in Figure 2.1b (Levenspiel 2006). On the contrary, by cascading CSTRs, small reactor volumes in series are applied that result in high intermediate S concentrations. Consequently, the first CSTRs can be operated at high reaction rates, whereas the last CSTR of the CAD will have a similar reaction rate as the single stage CSTR. Thus, the series of small CSTRs will eventually reach to a similar η but to a significant

smaller working volume, compared to the single stage CSTR (Figure 2.1c). The overall required volume of the CAD is reciprocally correlated to the number of CSTRs.

$$V = F_0 \frac{1}{-r}\eta \qquad \text{(Eq. 2.2)}$$

Where V = volume of the CSTR (m^3), F_0 = substrate feeding rate (kg COD/day), -r = substrate conversion rate (kg COD/m^3/day), and η = substrate conversion ratio (0-100 %).

Cascade CSTR configurations are commonly applied to accelerate catalytic substrate conversions that are characterised by Eq. 2.1 (Miyawaki et al. 2016). In case reaction rates are substrate dependent, such as for soluble substrates in Michaelis-Menten and/or Monod kinetics, the impact of reactor cascading will even be higher. However, for solid substrates such as WAS, concentration dependent reaction rates are rarely documented (Miron et al. 2000) and generally first-order reaction rate constants are considered (Blumensaat and Keller 2005).

Up to now, application of the cascade CSTR configurations for WAS has been mainly reported in the scope of co-digestion in food waste (Liu et al. 2013) or agricultural waste (Zhou et al. 2019), in which WAS contributed to improved buffer capacities and more balanced nutrient profiles. In the past decade, several researchers found higher WAS conversion efficiencies by using two-stage (two CSTRs in series) mesophilic AD systems, either with or without addition of primary sludge, for which no clear mechanistic explanation was given (Athanasoulia et al. 2012, Maspolim et al. 2015b). Ge et al. (2011b) and Wu et al. (2015) observed an improved hydrolysis rate in temperature-phased (thermophilic CSTR–mesophilic CSTR) WAS anaerobic digestion processes. Nonetheless, the authors attributed the enhanced hydrolysis merely to the thermophilic conditions applied. Despite the fact that staging has resulted in improved WAS digestion, it remains unclear whether accelerated enzyme activities, increased surface area of the solid substrates, and/or other factors were determinative. However, the published wide range of assessed hydrolysis rate constants for WAS (Batstone et al. 2002), gives room for further research and process optimisation.

In order to (1) comprehensively clarify whether a cascade configuration enhances WAS hydrolysis, and to (2) better understand the governing hydrolysis kinetics in this system, a novel CAD system for WAS treatment was researched in this study, which consisted of four CSTRs in series, i.e., three small-volume CSTRs and a large-volume CSTR. Considering that digestate recycle improves process stability in staged anaerobic digestion (Qin et al. 2019), the CAD was equipped with a modest digestate recirculation, applying a much lower ratio than reported in literature (Wu et al. 2015). As such, the

whole system can be interpreted as a semi plug-flow device with only a negligible hydraulic impact of the recycle flow. Reactor performance in the different steps of the system were investigated. Detailed research on prevailing specific hydrolysis rates, activities of key hydrolytic enzymes and the bacterial/archaeal community structure was performed to explain the results of the reactor performance and unveil the impact of cascading on hydrolysis kinetics. All results from the CAD were compared to those obtained from a reference conventional CSTR system operated under the same conditions with regard to feeding regime, total organic loading and temperature.

2.2 Materials and Methods

2.2.1 Source and characteristics of inoculum and substrate

All reactors were seeded with anaerobic sludge collected from a full-scale mesophilic anaerobic digester (SRT of 20 days) at the municipal WWTP Harnaschpolder, The Netherlands, treating primary sludge and centrifuge-thickened WAS from an enhanced biological phosphorus removal (EBPR) process. More information regarding the configuration and the operational parameters of the EBPR process can be found elsewhere (Guo et al. 2020b). The inoculum characteristics were: pH 8.1 ± 0.4, total solids (TS) 3.3 ± 0.1 wt%, and volatile solids (VS) 2.3 ± 0.0 wt%. The WAS from the same WWTP was collected weekly as feed sludge, and was characterized by a total chemical oxygen demand (tCOD) concentration between 40-70 g/L. The tCOD concentration of the feed sludge was adjusted to approximately 53 g/L by centrifugation or dilution with the fresh centrifuged supernatant obtained from the same WWTP, and stored at 4 °C before use.

2.2.2 Experimental set-up and operation

The experiments were carried out using two digestion systems operated in parallel: 1) a CAD system consisting of three CSTRs with 2.2 L each (R1, R2, R3) and a 15.4 L CSTR (R4); 2) a conventional CSTR as the reference with a working volume of 22 L (Figure 2.2). The experimental set-ups were both equipped with feed pumps (Watson-Marlow 120U/DV-220Du, USA), temperature & pH sensors (Endress & Hauser, The Netherlands), and biogas flow meters (Ritter Milligas Counter MGC-1-PMMA, Germany). The digestate was discharged from all reactors in both systems via overflow. In addition, for the CAD a sludge recirculation system from R3 to R1 with a flow ratio of 10% (recirculation/feed) was implemented using a recirculation pump (Watson-Marlow 120U/DV-220Du, USA). The temperature of all water-jacket equipped CSTRs was 35 ± 1 °C, controlled by thermostatic water baths (Tamson Instruments, The Netherlands). Both systems were monitored via a computer running LabView software (National Instruments, USA).

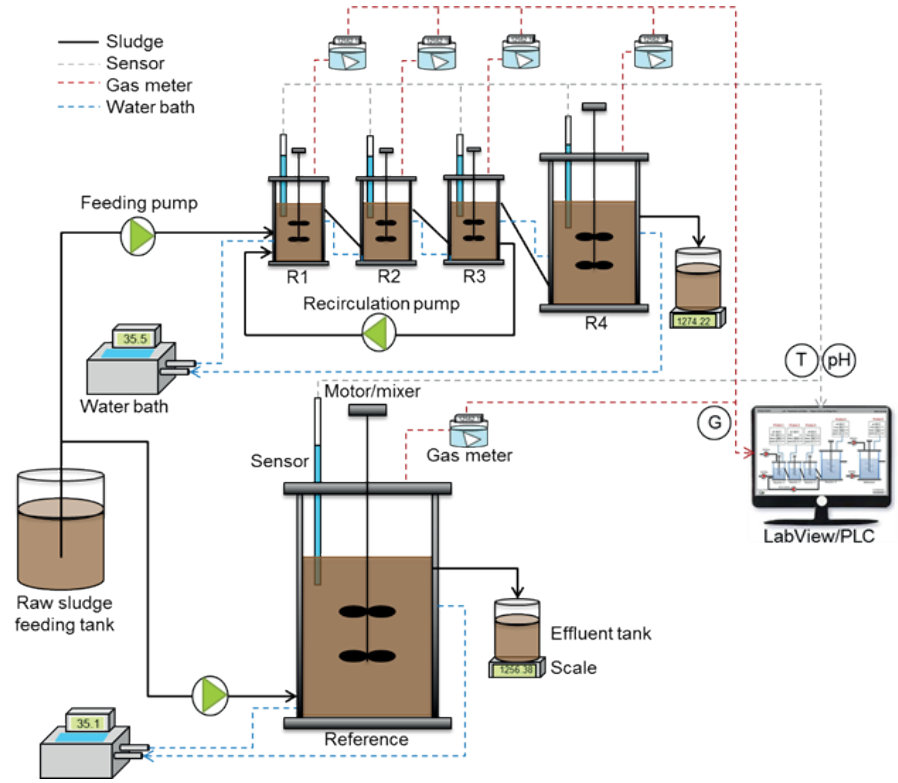

Figure 2.2 Schematic illustration of the experimental set-ups

The total SRT of both systems was decreased from 22 to 12 days in four phases. The operational conditions during all these phases are shown in Table 2.1.

Table 2.1 Operational conditions of the CAD system and the reference-CSTR

Experimental time (day)	SRT (days) CAD	Reference-CSTR	Total organic loading rate (g COD/L/d)	Phase
0-71	R1-R3: 2.2 each R4: 15.4	Reference: 22	2.41	I
72-152	R1-R3: 2.2 each R4: 15.4	Reference: 22	2.41	II
153-259	R1-R3: 1.5 each R4: 10.5	Reference: 15	3.54	III
260-330	R1-R3: 1.2 each R4: 8.4	Reference: 12	4.41	IV

2.2.3 Analysis and calculation methods

The tCOD and soluble COD (sCOD) were measured using spectrophotometry-based test kits (Hach Lange LCK, Germany). TS and VS were analysed according to standard protocols (APHA, 2005). The pH was determined with a multi-functional meter (WTW Multi 720, Germany). VFAs were measured by a gas chromatograph (GC) equipped with a flame ionisation detector (FID) (Agilent 7890A, USA) and a column (Agilent 19091F-112). Helium was used as carrier gas (1.8 mL/min); injection port and oven temperatures were 240 °C and 80 °C, respectively. Methane content of the biogas was analysed using a GC (Varian CP 4900, USA) with thermal conductivity detector (TCD) and columns, i.e. Mol-Sieve-5A-PLOT and argon as carrier gas (1.47 mL/min, 80 °C) and PoraPlot-U and helium as carrier gas (1.47 mL/min, 65 °C).

The specific hydrolysis rate, referring to the hydrolysis rate constant k_H (Yasui et al. 2008), was calculated by Eq. 2.3 based on Wu et al. (2015). As the AD system was equipped with a digestate recirculation of 10% from R3 to R1, the recycled sCOD and the recycle flow were also considered in the calculation of the specific hydrolysis rates for these three reactors.

$$\text{Specific hydrolysis rate (g COD/g VS/day or 1/day)} = \frac{\left(\frac{\text{mass\_sCOD} + \text{mass\_COD}_{CH_4}}{\text{day}}\right)_{\text{eff.}} - \left(\frac{\text{mass\_sCOD}}{\text{day}}\right)_{\text{inf.}}}{\text{mass of VS within reactor}} \quad \text{(Eq. 2.3)}$$

Where mass_sCOD = sCOD weight (g); mass_COD_{CH4} = CH_4 weight calculated as COD (g); eff. = effluent + methane; inf. = influent. It should be noted that inf. for R1 is composed of both the feeding and the recirculated digestate; inf. for R2 is the effluent from R1; inf. for R3 is the effluent from R2; inf. for R4 is composed of the effluent from R3, without the recycle flow.

2.2.4 Hydrolytic enzyme activity

Sampling and enzyme extraction

Triplicate sludge samples, including feed and digestates, were collected for enzyme extraction at the end of Phase-II (day 145 and 151), Phase-III (day 252 and 258) and Phase-IV (323 and 329) of the individual reactors of both digestion systems. The hydrolytic enzymes were separated into free and sludge-attached fractions. The free enzymes are defined as the enzymes that are present in the WAS's supernatant, whereas the sludge-attached enzymes are either membrane-bound or in other ways attached to the sludge particles. The extraction method of the hydrolytic enzymes was implemented according to Zhang et al. (2007) with a slight modification for sludge samples. Briefly, 1 mL sludge sample was centrifuged in a 1.5-mL tube

(Eppendorf, Germany) at 14,000 rpm for 1 min. The supernatant was transferred to a clean tube and was used for the measurement of free enzyme activities. The pellet was washed twice, using potassium dihydrogen phosphate buffer (pH 7.0, 0.1 mol/L) and was subsequently resuspended in sodium acetate buffer at pH 6.0 to the original volume to release sludge-attached enzymes. After centrifugation the suspension at 3,000g for 10 min, the supernatant was used for the determination of sludge-attached enzyme activities.

Quantification of enzyme activity

This work mainly focused on two hydrolytic enzymes: protease and cellulase. The activities of protease and cellulase were individually analysed by Pierce fluorescent protease assay kit (Thermo Fisher, USA) and MarkerGene fluorescent cellulase assay kit (MarkerGene, USA), using a 96-well microplate spectrophotometer (BioTek Synergy-HTX, USA). Meanwhile, API ZYM® strip (BioMerieux, France) was used to determine the activities of specific amino peptidases (leucine arylamidase, valine arylamidase and cystine arylamidase) and glycosyl-hydrolases (α-galactosidase, β-galactosidase, β-glucuronidase, α-glucosidase, β-glucosidase, n-acetyl glucosamidase, α-mannosidase and α-fucosidase). This commercial semi-quantitative micro-cell method works via colour development, with a numerical level of 1-5 (from low, 5 nmol, to high, >20 nmol) assigned to each sample, based on the colour chart provided by the manufacturer. The measurements of enzyme activity for both methods were performed at 35 °C.

Microbial community analysis

During the experiment, duplicate biomass samples were analysed to evaluate the microbial community dynamics, including one inoculum sample, two feed samples and 15 digestate samples from the digestion systems. The feed samples were taken individually on day 79 (summer season) and day 235 (winter season), and the digestates were sampled from R1, R2, R3, R4 and reference-CSTR at the end of each phase, i.e. days 151, 258, and 329. The FastDNA® SPIN-Kit-for-Soil (MP Biomedicals, USA) was used to extract DNA according to the manufacturer's instructions. The obtained DNA's quality was checked by Qubit3.0 DNA detection (Qubit® dsDNA-HS-Assay-Kit, Life Technologies, USA). High throughput sequencing was performed using the HiSeq Illumina platform and a universal primer 515F/806R (5'-GTGCCAGCMGCCGCGGTAA-3'/5'-GGACTACHVGGGTWTCTAAT-3') for bacterial and archaeal 16S rRNA genes (Novogene, UK). Raw reads were deposited in the European Nucleotide Archive under accession number PRJEB40450. Sequences were analysed by the QIIME pipelines (Version 1.7.0) to pair forward and reverse sequences, and removal of chimeras' sequences was performed by UCHIME algorithm.

Sequences with ≥ 97% similarity were clustered into one operational taxonomic unit (OTUs) by UCLUST algorithm. Singletons were removed, and OTUs with an occurrence less than three times in at least one sample were excluded. Taxonomic assignment was performed in Mothur software against the SILVA Database.

Statistical analysis

Student's t-test was used for variance analysis by SPSS Statistics 25 (IBM, USA), with the threshold for significance set at a P-value < 0.05. Shannon index and principal coordinate analysis (PCoA) based on the ordination of Bray-Curtis similarities were used to evaluate Alpha diversity and Beta diversity, respectively, by "vegan" microbial community ecology package in R software (version 4.0.2). Prediction of functional pathways from 16S rRNA gene sequences were conducted by "Tax4Fun2" software package that provides functional annotations based on the Kyoto Encyclopedia of Genes and Genomes (KEGG) pathway database.

2.3 Results and discussion

2.3.1 Performance comparison between the CAD system and the reference-CSTR

During the start-up phase, the effluent tCOD concentrations and methane production rate fluctuated in all reactors (Figure 2.3a). Both parameters gradually stabilised from day 71 onward, after which the cascade and reference system were both operated under stable conditions for 81 days (Phase-II). During both Phase-I and Phase-II, the CAD and the reference-CSTR were operated with an SRT of 22 days. The tCOD removal efficiency of the entire CAD was 43 ± 6%, versus 40 ± 5% of the reference-CSTR during this period. Both removal efficiencies were within typical ranges of mesophilic WAS digestion, reported by previous studies (Maspolim et al. 2015b). On average, the methane production rate was around 8% higher in the CAD than in the reference-CSTR (Figure 2.3b).

After the total SRT was lowered to 15 days (Phase-III), effluent tCOD concentrations of both R4 and the reference-CSTR increased due to the sudden increase in total organic loading rate (OLR) from 2.4 to 3.5 g COD/L/d. This reduction in tCOD removal efficiency was also observed at the start of Phase-IV, when the total SRT was further decreased to 12 days and the total OLR correspondingly increased to 4.4 g COD/L/d. Strikingly, only the CAD recovered to a tCOD removal efficiency between 40% and 42% at the applied increased OLR, whereas the tCOD removal efficiency in the reference-CSTR reduced to around 38% in Phase-III and 31% in Phase-IV. The difference in treatment performance was reflected by the increasing difference in methane production (Figure 2.3b). The CAD showed an average 13% higher methane

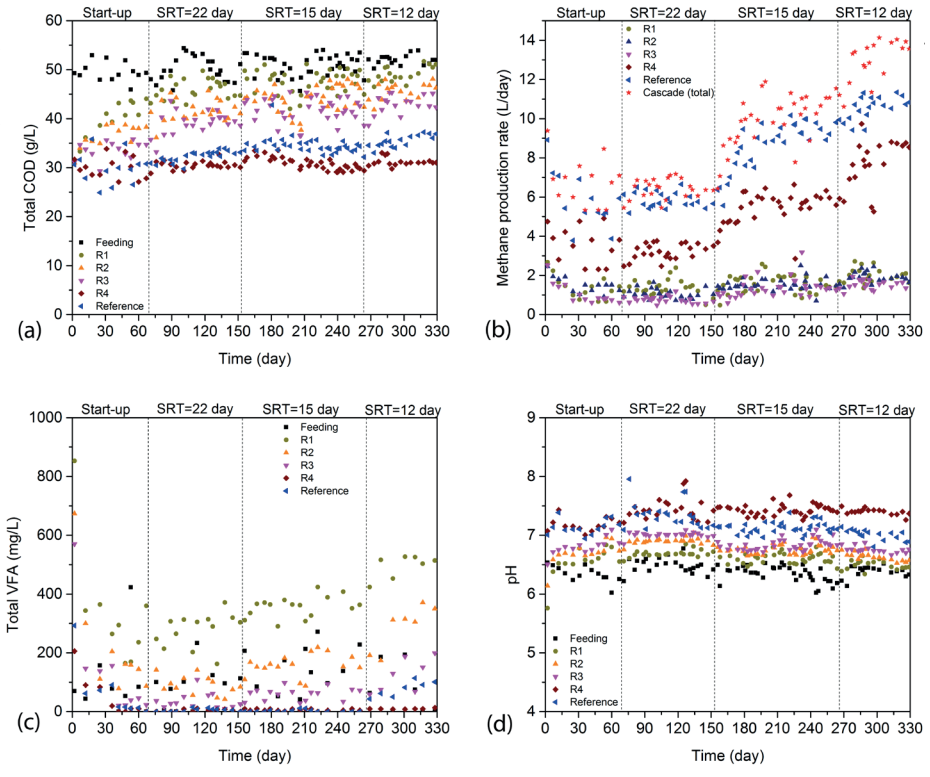

Figure 2.3 Operational performance of the CAD system and the reference digester, respectively. **(a)** tCOD concentration, **(b)** methane production rate, **(c)** total VFA concentration and **(d)** pH

Zooming into the separate reactors of the CAD reveals that the reactors R1, R2 and R3, with an SRT of 2.2 days each (Phase-II), contributed to 20-24% of the total methane volume that was produced in the CAD (Figure 2.3b). These results agree with a reported study on two staged AD systems under similar SRT conditions, which showed that the methane production in the first CSTR was on average 25% of the total (Maspolim et al. 2015b). When the SRT in the cascade reactors R1, R2 and R3 was decreased to 1.5 and 1.2 days each in Phase-III and Phase-IV, respectively, the methane production stayed between 12 and 16% of the overall total methane production. The biogas in these three reactors contained 46-53% methane, while the methane content of the biogas of R4 and of the reference-CSTR was 56-62%. Negligible hydrogen partial pressure was found in all the anaerobic reactors (< 0.01%). These observations showed that, despite their short SRT and most probably due to the 10% recirculation flow, active methanogens were present in R1, R2 and R3.

VFA concentrations and pH are commonly used as indicators for process perturbation and/or reactor control (Franke-Whittle et al. 2014). The total VFA concentration in the feed and all reactors is presented in Figure 2.3c. As expected, the VFA concentration was always the highest in R1 and was gradually reduced along the system. Acetate and propionate accounted for 60-80% of the total VFAs, showing their predominance in all reactors (Figure S2.1 in supplementary data). With increased OLR, or decreased SRT, an elevation in VFA concentration in R1, R2 and R3 was observed, from 310, 100 and 60 mg/L at SRT 22 days to 590, 380 and 175 mg/L at SRT 12 days, respectively. Very low total VFAs (< 5 mg/L) were found in reactor R4 in all phases, demonstrating that all VFAs were eventually converted to methane in the last step of the CAD. In the reference-CSTR there was no VFA accumulation observed, even at the shortest SRT (12 days) when total VFA concentration slightly increased to around 110 mg/L. Clearly, the VFA concentrations remained far below the inhibition threshold for methanogenic activity (Wang et al. 2009), and thus cannot explain the difference in WAS degradation between the CAD and the reference-CSTR at short SRTs. However, the pH in both R1 and R2 of the CAD was between 6.3 and 6.5, somewhat lower than the pH in the rest of the reactors. The lower pH coincided with the somewhat higher VFA concentrations in R1 and R2 and can be attributed to increased acidifying activity and reduced methanogenic activity in the first reactors of the cascade (Maspolim et al. 2015b). In reactors R3 and R4, as well as in the reference system, the pH remained neutral (Figure 2.3d). Nonetheless, the relatively stable pH in R1 and R2 could be ascribed to alkalinity supplementation by digestate recirculation from R3 to R1, introducing sufficient buffer capacity as presented in Figure S2.2 in Supplementary data.

To be able to explain the different tCOD removal efficiencies between the cascade and the reference system, the specific hydrolysis rates were calculated using Eq. 2.3, the tCOD and sCOD variations (Figure 2.1 and Figure S2.3 in Supplementary data), and the methane production (Figure 2.3b) in each reactor. Computed specific hydrolysis rates, resembling the first-order hydrolysis rate constant k_H (Eq. 2.1), are shown in Figure 2.4. Under all tested operational conditions, the specific hydrolysis rate was highest in R1 of the CAD, and steadily decreased throughout the subsequent reactors of the cascade. During Phase-II, the specific hydrolysis rate calculated for the reference-CSTR was slightly higher than that in R3 of the CAD. Reducing the SRT from 22 to 12 days led to approximately a doubling of the specific hydrolysis rate in the reactors of the CAD, while it increased only 1.5 times in the reference-CSTR. It should be noted that the bar-presented specific hydrolysis rates are in fact underestimates of the actual values, since these were calculated using Eq. 2.3, which includes both the substrate and biomass VS in each reactor. However, particularly in reactors R1-3, the contribution of the substrate VS to the total VS is relatively large. We, therefore,

recalculated the apparent k_H values using the VS content in R4, which resembles the non-digestible VS fraction in the entire CAD. The corrected k_H values are presented above each bar of R1-3 in Figure 2.4, showing an even higher increase in specific hydrolysis rates in the first stages of the cascade reactor.

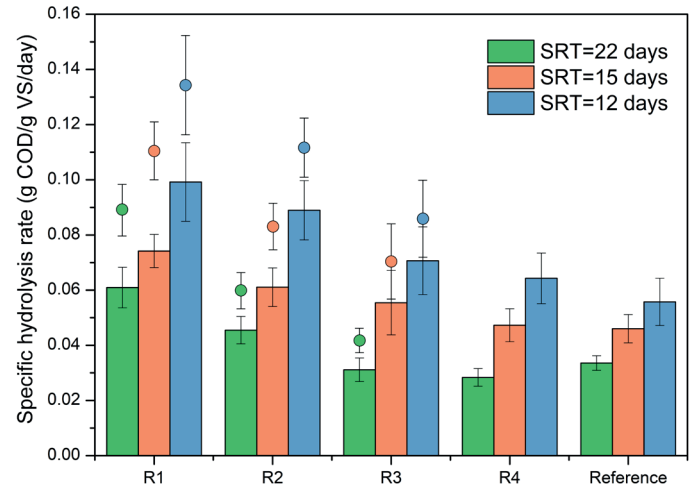

Figure 2.4 Specifichydrolysis rate calculated based on the COD balance and the VS concentration of each reactor (bars). The circles displayed above the bars of R1, R2 and R3 represent the calculated specific hydrolysis rate using the stabilized VS concentration of R4 at each SRT, which resembles the non-digestible VS fraction in the CAD

Strikingly, under all loading conditions, the assessed specific hydrolysis rates in R4 of the CAD and the reference-CSTR were very similar. Nonetheless, at the highest OLR, the overall specific hydrolysis rate in the reference-CSTR was significantly lower (p-value < 0.05) than the separate specific hydrolysis rates in all reactors of the CAD. Apparently, the specific hydrolysis rate was process-condition dependent and results in Figure 2.4 showed that in all reactors the specific hydrolysis rate increased with increasing OLRs. Similar observation were previously done by Miron et al. (2000). Our present results clearly indicate that the potential volume reduction, which can be attained by implementing cascade configurations, is indeed much more than based on solely the theoretical considerations as explained in Figure 2.1 (Levenspiel 2006), where the same first-order reaction rate is applied for all individual reactors in the CAD and the single stage CSTR. Moreover, at the applied low SRTs, or imposed extreme OLRs, the specific hydrolysis rates increased significantly more (p-value < 0.05) in the first reactors of the CAD compared to that in the reference-CSTR (Figure 2.4). Most likely, the maximum organic loading potentials of the CAD were not reached yet, as process performance remained stable even at an SRT of 12 days (Figure 2.3).

Results further indicate that for increasing the sludge treatment capacity at a common WWTP, the present AD installation can be upgraded in a relatively easy manner to a very compact cascade reactor system via retrofitting existing parallel-fed large-scale conventional CSTR-based sludge digesters. For instance, one CSTR digester could be divided into a sequence of several compartments and subsequently be connected with another digester in series.

2.3.2 Hydrolytic enzyme activity

To explain the large differences in observed specific hydrolysis rates between the different reactors, the hydrolytic enzyme activities were assessed (Parawira et al. 2005). Cellulosic fibres and proteins are identified as the two predominated organic components in WAS (Guo et al. 2020b). Therefore, the activity of cellulase and protease were chosen as representative enzyme activities for a first characterisation of WAS hydrolysis in both systems, applying a widely reported enzymes extraction protocol for anaerobic samples (Zhang et al. 2007). Meanwhile, automatic measurements in a 96-well microplate reader rather than manual measurements were conducted for the analysis of enzyme activities in this study (Bonilla et al. 2018), with the duplicate extraction of enzymes from the same reactor at three inconsecutive days. Results in Figure 2.5 showed that both free and sludge-attached enzymes are present in the digester, regardless of the configuration type, i.e. cascade or single CSTR. The results showed that protease activities were two orders of magnitude higher than cellulase activities, which could be possibly due to the significant higher proportion of protein than cellulose in WAS (Guo et al. 2020b). Highest protease and cellulase enzyme activities were present in the sludge-attached fraction of both reactor configurations. Enzyme activities are proportionally related to the enzyme's amount (Kim et al. 2012), suggesting that the hydrolytic enzymes were mainly adsorbed on, or attached to the sludge matrix, in line with a previous publication by Maspolim et al. (2015a).

In both free and sludge-attached fractions, the activity of hydrolytic enzymes distinctly increased from the feed to R1, especially at short SRTs, indicating that hydrolysis in R1 was indeed accelerated owing to increased presence of hydrolytic enzymes. Significant higher enzyme activities (p-value < 0.05) were observed in the three small reactors in comparison with the reference-CSTR: the protease activities in R1 were double the activities in the reference-CSTR; even the protease activities in R4 were slightly higher than those in the reference-CSTR. Meanwhile, the cellulase activities in R1, R2 and R3 were statistically higher than those in R4, while the digestate of R4 showed a similar cellulase activity as the reference-CSTR (Figure 2.5d). The observed higher hydrolytic enzyme activities in the CAD system, compared to those of the reference-CSTR, could be attributed to the imposed high

OLRs (corresponding to short SRTs) in reactors R1, R2 and R3. Following first order reaction kinetics (Eq. 2.1), the application of increased OLRs results in accelerated hydrolytic enzyme activities (Menzel et al. 2020, Xiao et al. 2017). Results showed that enzyme activities, especially the sludge-attached ones, in all reactors increased over three times when the total SRT was reduced from 22 to 12 days (Figure 2.5). Notably, the increase in the enzyme activities in both systems exceeded the increase in the calculated specific hydrolysis rates in each reactor (Figure 2.4). This mismatch strongly indicates that the actual solids hydrolysis in the CAD was limited by the available free surface for enzymatic attack, rather than by the presence of sufficient hydrolytic conversion capacity.

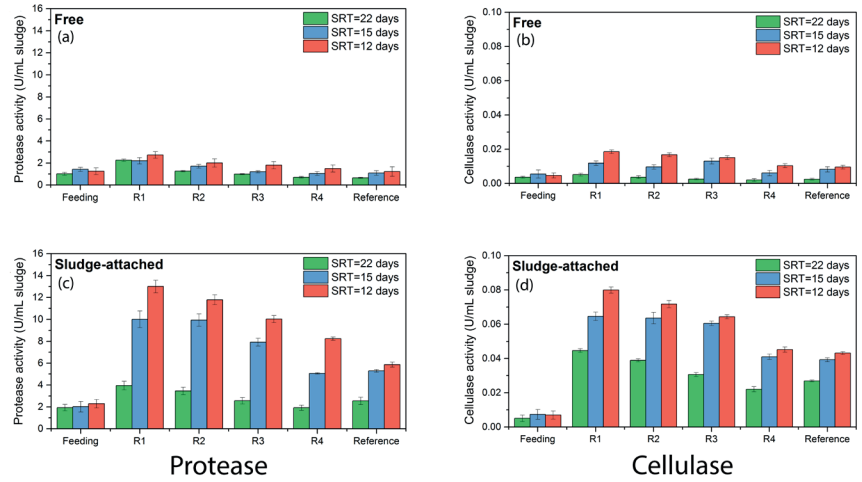

Figure 2.5 Enzyme activity in U per mL of sludge from the feeding and each reactor. The TS concentration of the feeding was: 4.1-4.2 wt%, and of each individual reactor: 3.9-4.1, 3.7-4.0, 3.0-3.7, 2.8-3.0 and 3.1-3.3 wt% for R1, R2, R3, R4 and the reference-CSTR, respectively. **(a)** Free protease. **(b)** Free cellulase. **(c)** Sludge-attached protease. **(d)** Sludge-attached cellulase. Samples for each measurement were taken during stabilised performance at each operational period. Error bars refer to the standard deviation (n = 6)

A more detailed semi-quantitative analysis of amino peptidases and glycosyl-hydrolases in both free and sludge-attached fractions using API ZYM® strips, were carried out at the same moments as described above (Figure 2.6). Similar to protease and cellulase activities, the activities of all hydrolases tested with this method increased at short SRTs, and showed a downward trend in activity from R1 to R4 of the cascade digester. Surprisingly, however, the β-glucuronidase, α-mannosidase and α-fucosidase activities increased stepwise along the CAD, which indicates that the hydrolysis of target substrates of these enzymes occurs later in the process. The

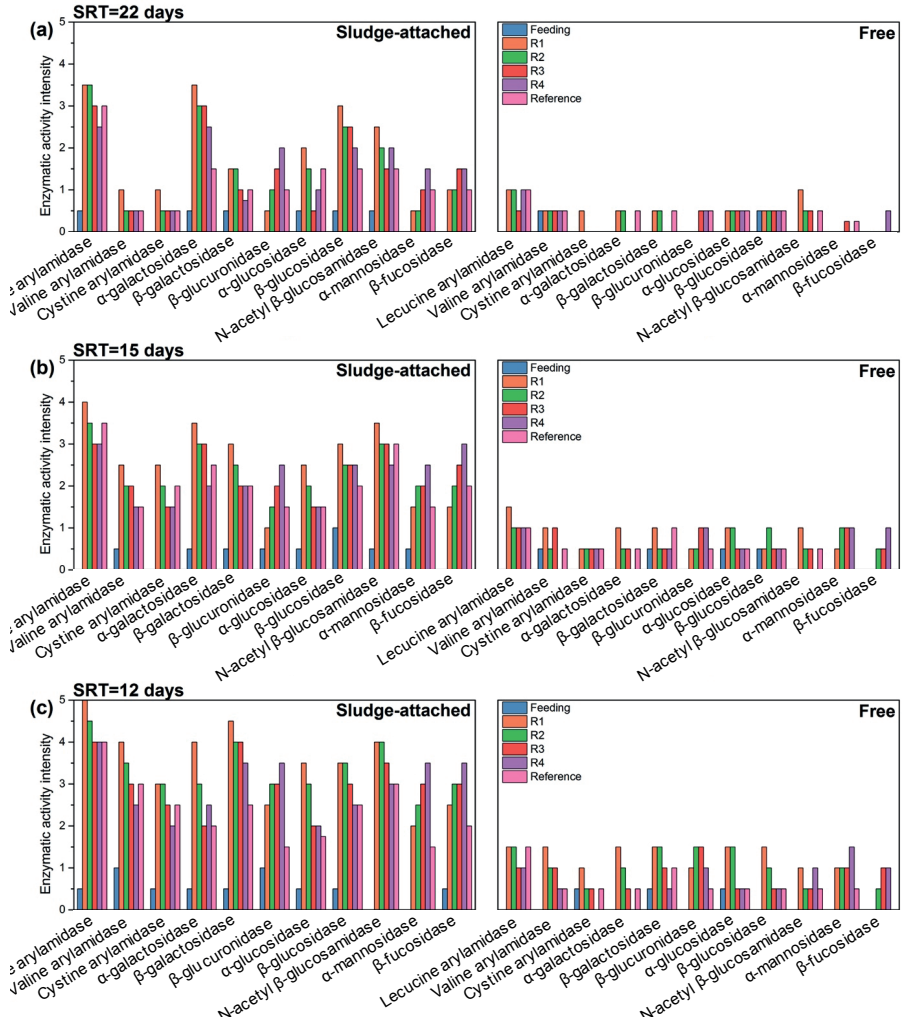

Figure 2.6 Average (n = 3) enzyme intensity of specific amino peptidases and glycosyl-hydrolases in both CAD and reference-CSTR, which were analysed using API ZYM® strips for sludge-attached and free enzymes collected at the end of **(a)** SRT = 22 days, **(b)** SRT = 15 days and **(c)** SRT = 12 days

presence and the role of the target substrates, namely, glucuronic acid, mannose and fucose in the sludge matrix have been researched in several studies, showing that they act as main building blocks in the structural extracellular polymeric substances (SEPS) that form the gel-like structures of the sludge (Guo et al. 2020a). Regarding the degradation of SEPS in both digestion systems (Figure S2.4 in Supplementary data), results showed that SEPS were mostly converted in R4, irrespective of changes in SRT, which was in line with the distributions of the β-glucuronidase, α-mannosidase and

α-fucosidase activities. In addition, observations from the CAD reveal that in the first reactors the more easily biodegradable (poly-)saccharides and (poly-)proteins were degraded, while in the remaining of the CAD, the more refractory organic residuals in WAS, such as SEPS related saccharides, were degraded. As a consequence, the CAD revealed a more stepwise and improved reduction of different types of organics, which e.g. resulted in 14% more SEPS reduction at the total SRT of 22 days compared to the reference-CSTR. At the shortest tested SRT of 12 days, SEPS reduction was even 64% higher (Figure S2.4 in Supplementary data).

2.3.3 Pyrosequencing analysis of the microbial communities

Diversity indices

The results of Alpha diversity based on Shannon diversity were listed in Table S2.1 in Supplementary data. Substrate sample 1 & 2, and the inoculum had the highest and lowest values, respectively, meaning that the WAS substrate contained the most diverse bacterial communities, whereas the anaerobically grown inoculum had the least biodiversity. Shannon diversity decreased in both AD systems when operated at the total SRT of 22 days and slightly increased as the SRT was reduced. This indicates that the initial microbiome members that were present in the feed partially disappeared in the CAD process and thus, a narrowed AD community was eventually formed.

A microbial dynamic transition alongside with the CAD from R1 to R4 could be clearly demonstrated by the Beta diversity described via PCoA based on the matrix distance between the samples (Figure 2.7). In all operational conditions, R1, R2 and R3 were clustering closely to each other, while R4 was obviously separated from R1-3 and near the inoculum, revealing a different microbial composition presented in R4 compared to other reactors in the CAD. The microbial structure of the reference-CSTR and the R1-3 was similar to that of WAS under the reduced SRTs, suggesting less cell decay of the fed WAS at this short SRT, which is possibly linked to the deterioration in tCOD reduction efficiency (Figure 2.3a).

It should be noted that the applied CAD system was equipped with a digestate recirculation system operating at a recirculation ratio of 10%. It has been reported that recycling the digestate from a methanogenic reactor to an acidogenic reactor at a recycling ratio of 100% resulted in a changed and improved diversity of bacteria and archaea in the acidogenic reactor (Wu et al. 2016). Thus far, the effect of only 10% recycling is unknown. Nonetheless, in our present study, considerable methane production was observed in R1, R2 and R3 (Figure 2.3b), which might be ascribed to the

supplement of methanogens via digestate recirculation. However, based on the PCoA results, showing the clear microbial shift within the CAD from R1 to R4 (Figure 2.7), it seems that this impact of 10% recycling was limited.

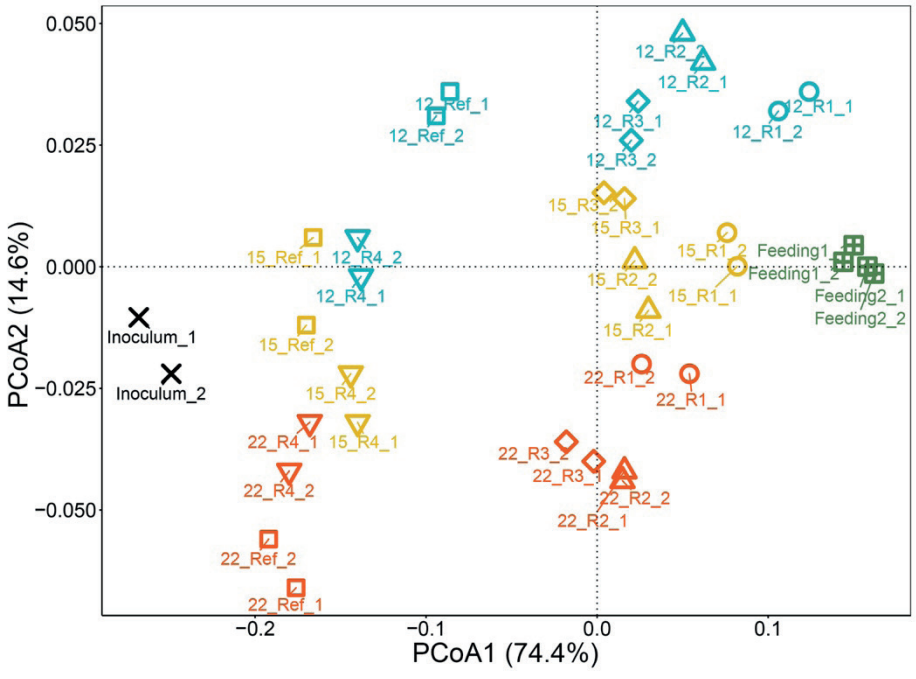

Figure 2.7 PCoA analysis for the microbial community of feed sludge, inoculum and digestates from all reactors operated at the different SRTs. The samples analysed for PCoA were plotted in duplicates grouped by the same symbol and colour. Symbols in black and green represented the inoculum and the feed, respectively. Symbols in blue, yellow and red refer to the reactors operated at SRT of 12 days, 15 days and 22 days, respectively

Bacterial communities

The bacterial species taxonomy at phylum level is shown in Figure 2.8a. Proteobacteria (55-60%), followed by Bacteroidetes (8-10%) and Actinobacteria (7-9%) were the most dominant phyla in the raw WAS, which is in line with previous studies (Westerholm et al. 2016). The changes in microbial composition between samples were most pronounced for Proteobacteria, because the total reduction in the relative abundance of this phylum was distinctly higher than for the other phyla in both CAD and reference-CSTR. The relative abundance of the genus *Candidatus_Competibacter* belonging to the phylum Proteobacteria was reduced by approximately 30% in R1, R2 and R3 together, while it was declined by 60% in the post digester (R4) of the CAD system. A similar observation was also found for other genera from this phylum, such

as *Candidatus_Accumulibacter* related to phosphorus removal and *Dechloromonas sp.* for denitrification (Luo et al. 2020), even though the fractions in WAS were relatively low in this study (Figure 2.8b). The results imply that the aforementioned dominant phyla largely disappeared due to cell decay in the AD process. Considering that 9-24 % of WAS consists of microorganisms (Gonzalez et al. 2018), the released amount of intracellular organics due to endogenous decay of cells cannot be ignored in the CAD and would become part of the tCOD that was available as substrate for the investigated hydrolytic enzymes (Figure 2.5 and 2.6). Firmicutes were not predominant in the WAS, but clearly, the relative abundance of this phylum increased in R1, R2 and R3 to approximately 6.7% compared to 4.5% in the feed sludge at the total SRT of 22 days, Furthermore, the relative abundance of Firmicutes increased to 8.8% and 11.3% as the SRT reduced to 15 and 12 days, respectively. Firmicutes have been identified to hydrolyse and ferment large numbers of organic compounds under a variety of conditions in AD systems (Karthikeyan et al. 2016, Liu et al. 2019). The increase in relative abundance of this type of species implies that the role of hydrolysis and acidogenesis processes in R1, R2 and R3 of the CAD became increasingly more important as the SRTs decreased, in line as was reported by Zhang et al. (2019).

To relate the identified microbes to hydrolysis and acidogenesis of WAS in the CAD system under different operational conditions, the top 10 genera that governed the hydrolysis/acidogenesis of the organic compounds in both systems were selected and ranked by the relative abundance, while the changes in relative abundance were shown in Figure 2.8c. Bacteria affiliated to genera *VadinBC27_wastewater-sludge_group*, *Clostridium_sensu_stricto_1*, *Enterococcus*, *Gelria*, *Bivil28_wastewater-sludge_group* and *Sedimentibacter* had significantly higher (p-value < 0.05) relative abundance in R1, R2 and R3 than in the reference-CSTR at the SRT of 22 days. This might have been due to the greater abundance of non-hydrolysed substrates that were present in R1, R2, and R3, since these genera have been frequently reported as the prevalent fermenters that were capable of hydrolysing protein or carbohydrate in AD (Kirkegaard et al. 2017, Liu et al. 2016, Wang et al. 2020). Possibly, the mentioned genera can be recognised as the main contributors to the enhanced hydrolysis rate in the cascade digester system. Moreover, lowering the total SRT of these reactors further increased the relative abundance of the aforementioned bacteria, which implies their higher metabolic activities in the degradation of WAS at higher loading rates. On the other hand, an upward trend in relative abundance of *Smithella*, *Candidatus_Cloacamonas* and *Thermovirga* was detected in the CAD, especially in R1, R2 and R3, at the short SRTs. These recently characterized microorganisms might oxidize propionate and ferment sugars and amino acids to produce hydrogen and carbon dioxide, indicating that these species may possibly constitute acidifying and

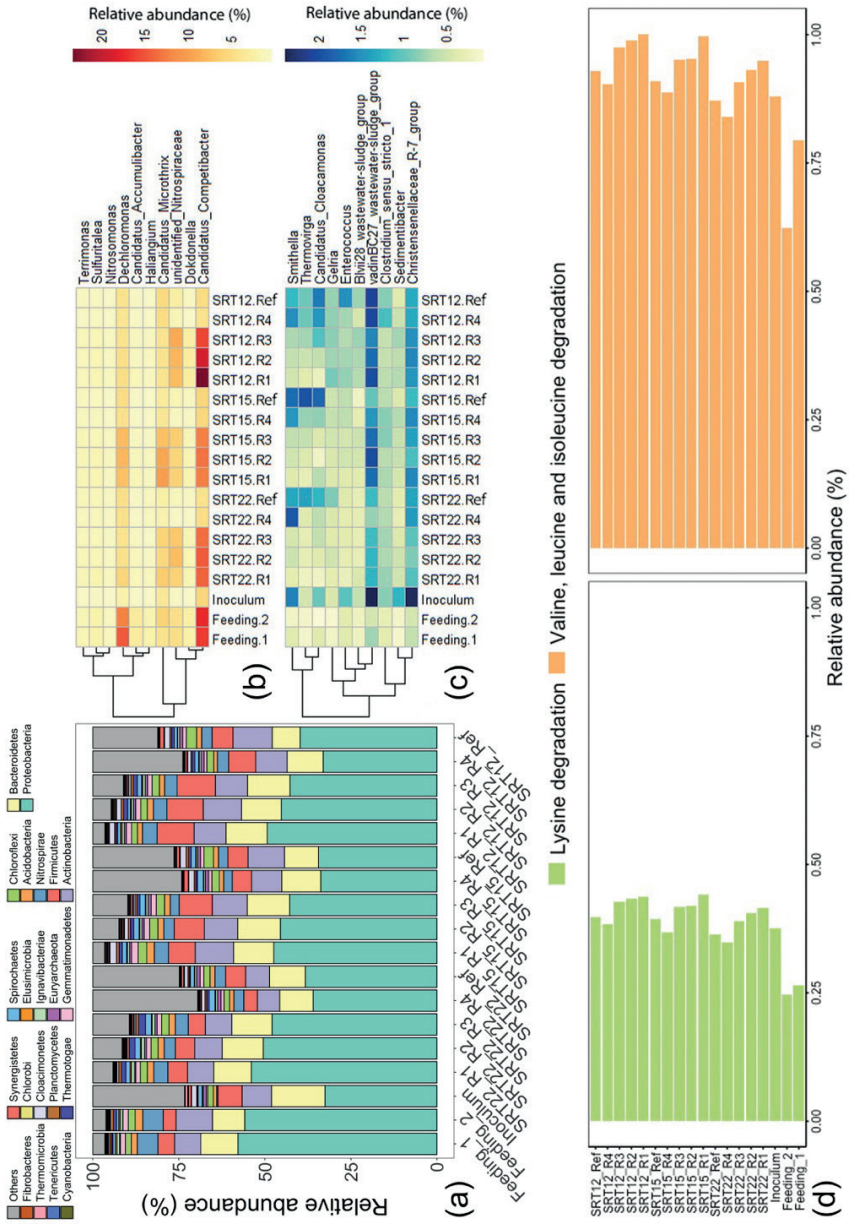

Figure 2.8 (a) Species taxonomy of bacteria at the phylum level: the species, whose sums of percentage in all the samples are less than 1%, are classified as "the others", **(b)** relative abundance of taxa related to feeding dominated bacteria of interest (top 10 species that presented in feeding), **(c)** anaerobic hydrolytic bacteria (top 10 species that appeared in all anaerobic reactors) at the genus level and **(d)** prediction of functional pathways related to amino acids degradation (average value, n = 2)

syntrophic associations (Stolze et al. 2015, Zamanzadeh et al. 2013). It should be noted that a small proportion of *VadinBC27_wastewater-sludge_group* and *Bivil28_wastewater-sludge_group* was also found in WAS. These strains directly might have contributed to the hydrolysis and degradation of WAS when they entered the CAD. Moreover, because of their continuous seeding, they might have persisted as functional biomass in R1-3, where short SRTs were applied (Kim and Speece 2002). However, the exact role of the WAS-related cultures in the CAD needs further studies.

Besides the investigation on the relative abundance of the functional bacteria, the microbial functional pathways including amino acid and carbohydrates metabolisms in different experimental phases were also researched and the results were summarized. It was found that lysine degradation (Ko00310) as well as valine, leucine and isoleucine degradation (Ko00280) were the dominant pathways related to biomass conversion. The relative abundance of these metabolic pathways in the different reactors indeed increased when the reactor SRT dropped from 22 to 12 days. Moreover, they showed a similar trend as the activities of valine and leucine arylamidase that catalyse the hydrolysis of valine and leucine from peptide chains (Figure 2.8d and Figure 2.6). These findings suggest that applying a CAD results in an enhanced microbial metabolism of hydrolytic/acidogenic bacteria that caused the observed acceleration in hydrolytic enzyme activity and subsequent enhanced sludge reduction compared to the reference-CSTR. Obtained results also illustrated the microbial complexity of WAS hydrolysis, which is difficult to capture in first-order hydrolysis kinetics, particularly under high loading conditions.

Methanogenic archaeal communities

As for the archaeal domain displayed in Figure 2.9, *Methanobrevibacter* and *Methanosaeta* were equally dominant in the feed (around 28% each in relative abundance). In Phase-II, when the CAD was operated at an SRT of 22 days, *Methanobrevibacter*, a hydrogenotrophic methanogen, was the most abundant methanogen in R1, but gradually became the minor species in favour of *Methanosaeta* that utilize acetate as the sole substrate from R2 to R4 (Maspolim et al. 2015c). This means a clear microbial shift from hydrogenotrophic methanogens towards acetoclastic methanogens alongside the CAD. Also, at the low SRTs of 15 and 12 days in Phase-III and Phase-IV, the composition of methanogens in R1-4 followed a similar trend as in Phase-II, whereas the proportion of hydrogenotrophic methanogens was at a higher level. The predominance and importance of hydrogenotrophic methanogens in the acidogenic first stage reactors of phased AD systems have been described in literature. The very high OLR in the first stages of the CAD resulted in a very high acidogenesis rate, with a concomitant high hydrogen and carbon

dioxide production rate (Huang et al. 2015, Liu et al. 2019, Shimada et al. 2011, Zhang et al. 2019). The increased hydrogen/carbon dioxide flux in reactors R1-3 resulted in an increased yield of hydrogenotrophic methanogens, leading to an increase and eventual dominance of hydrogenotrophic methanogenic subpopulations. Considering the maximum growth rate (μ_{max}) of hydrogenotrophic methanogens in the range between 2.00-2.85 d^{-1}, which is around 3-9 folds that of *Methanosaeta* species (0.33-0.71 d^{-1}) (Batstone et al. 2002, Van Lier et al. 2020), and the very short SRTs of reactors R1-3, the microbial abundancy of hydrogenotrophic methanogens could outcompete the acetoclastic *Methanosaeta* species. In contrast, the applied SRT in R4 and the prevailing acetate flux resulted in a pre-dominance of *Methanosaeta* in the final reactor of the cascade. Notably, the acetate concentrations in R1, R2 and R3 were all significantly higher (p-value < 0.05) than the threshold (< 600 µg/L) for *Methanosaeta* survival (Klocke et al. 2008). Therefore, unlike the reference-CSTR and R4, methane production from hydrogen and carbon dioxide, rather than from acetate, was most likely the dominating methanogenic pathway in R1, R2 and R3.

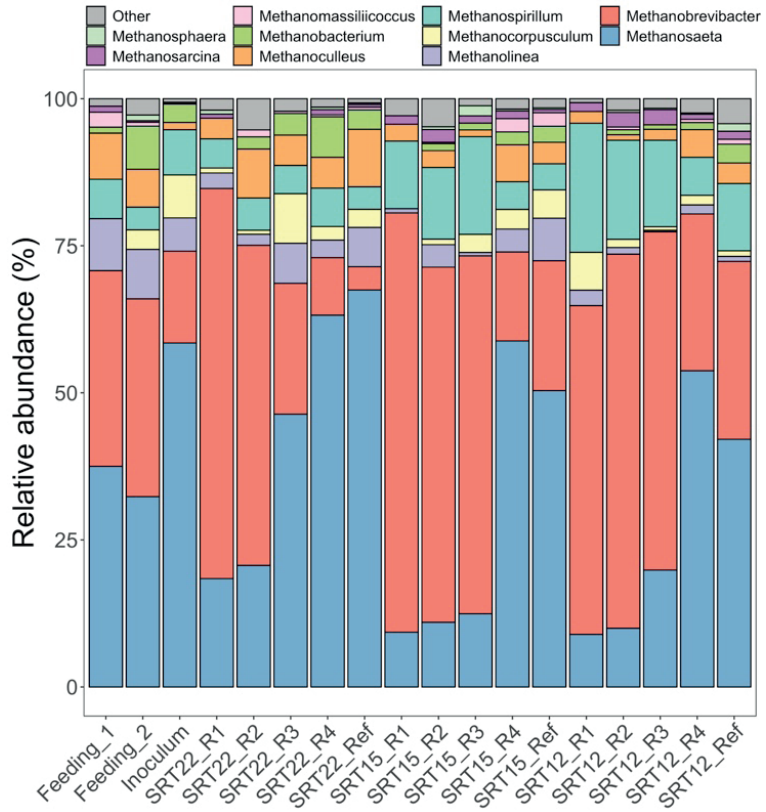

Figure 2.9 Species taxonomy of methanogenic communities at the genus level. The species, whose sums of percentage in all the samples are less than 0.5%, are classified as "the others"

It is noteworthy that sequences affiliated with *Methanospirillum* had promoted relative abundance in all digesters from the Phase-II to Phase-IV, which implies the importance of this methanogen in AD under high loading conditions. Recently, *Methanospirillum* has been found to play an important role in syntrophic propionate oxidation in phased anaerobic digestion (Maspolim et al. 2015c). As an increase in relative abundance was also observed for propionate oxidisers such as *Smithella*, the applied CAD apparently provides proper conditions for attaining efficient syntrophic propionate conversion (de Bok et al. 2001).

2.4 Conclusions

The conclusions drawn from the current work can be summarized as follows:

1. AD in the CAD led to 8% more tCOD reduction than the single stage CSTR digester, both operated at a total SRT of 22 days. Stepwise reduction of the total SRT from 22 to 12 days did not affect the tCOD removal efficiency for the CAD, but showed a 29% decrease in the tCOD removal in the reference-CSTR. Maintaining stability at high organic loading rates in a CAD denotes an enhanced sludge treatment capacity of 30-35%, compared to a conventional sludge digester of the same volume.
2. Normalised specific hydrolysis rates, resembling the first-order hydrolysis rate constant, differed per reactor and increased with decreasing SRTs. The highest increase by a factor 2 was found in the individual reactors of the CAD. Normalised hydrolysis increased by a factor 1.52 in the reference-CSTR.
3. Clear higher enzyme activities were found in the CAD compared to the reference-CSTR, especially under short SRTs, which explains the overall accelerated specific hydrolysis rate in the CAD system. The overall hydrolytic enzyme activities increased with a factor up to 3 or even more, while this was a factor less than 2 for the specific hydrolysis rate, indicating that hydrolysis was limited by the solids-surface availability.
4. Several enzymes that target hydrolysis of SEPS-related organic compounds displayed reversed distribution and higher activity in the CAD than in the reference-CSTR, indicating an additional degradation capacity of refractory compounds in the CAD.
5. The increased relative abundance of key hydrolytic bacteria found in the first 3 reactors of the CAD and the structural shift from hydrogenotrophic methanogens to acetoclastic methanogens alongside the cascade under low SRTs, demonstrated that cascading CSTRs possibly imposed selective pressures on the microbial population, which contributed in achieving the enhanced enzymatic hydrolysis and sludge reduction.

Supplementary data

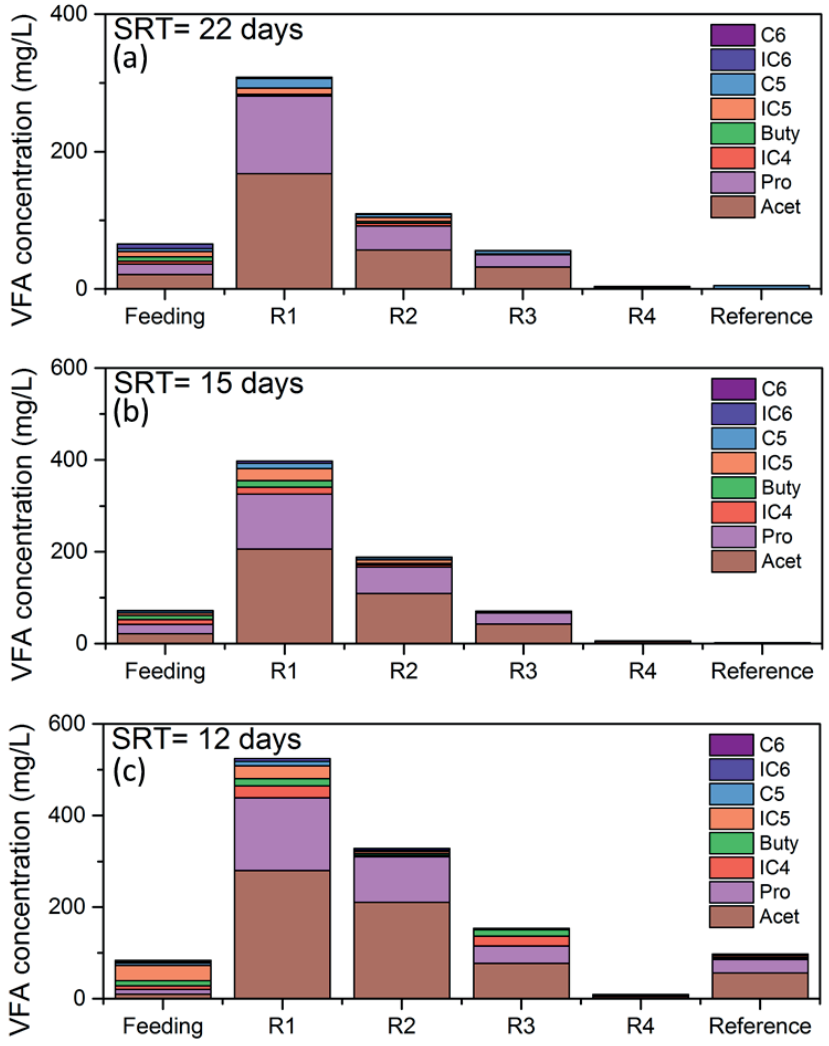

Figure S2.1 Distribution of average (n = 30) individual VFA concentration in the CAD and the reference CSTR

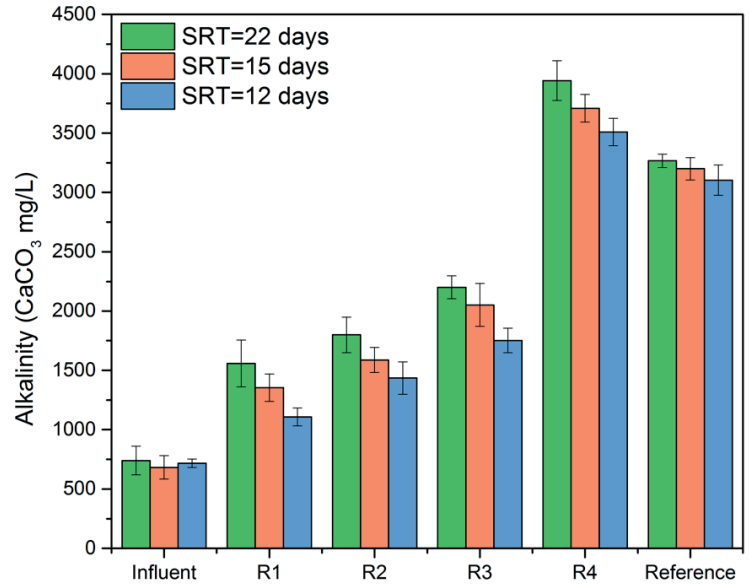

Figure S2.2 Alkalinity (n = 12) in the CAD and the reference CSTR

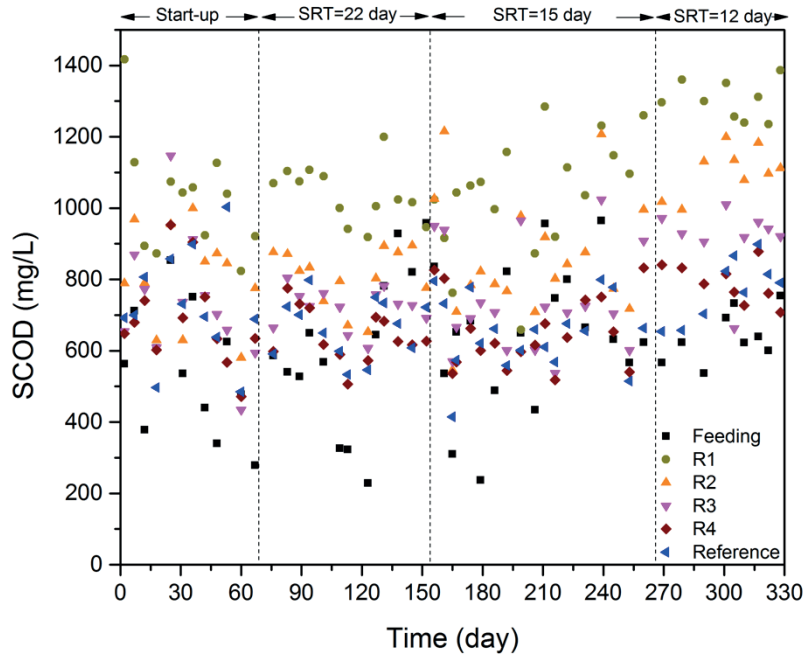

Figure S2.3 SCOD concentration in the CAD and the reference CSTR

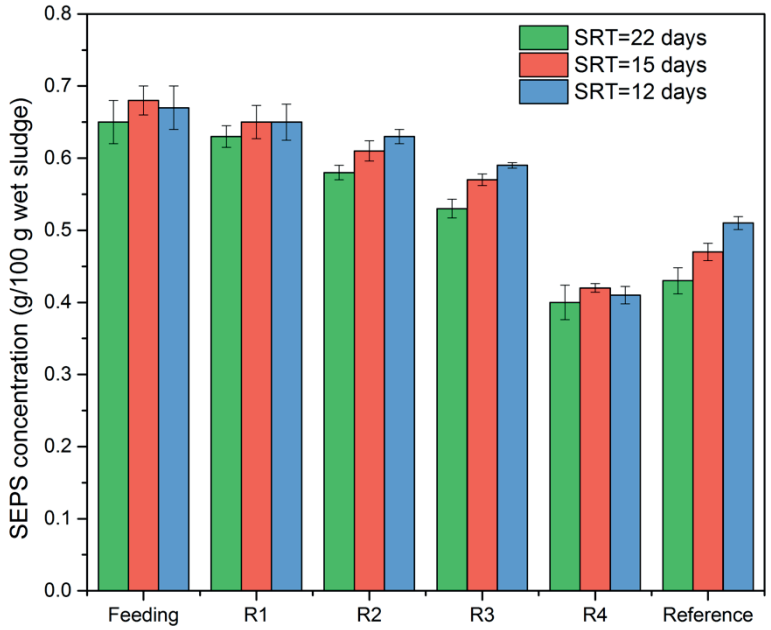

Figure S2.4 Distribution of structural EPS (SEPS) concentration (n = 6). The extraction method of SEPS was according to Guo et al. (2020a)Table S2.1Shannon diversity index of microorganism obtained from pyrosequencing data

Table S2.1 Shannon diversity index of microorganism obtained from pyrosequencing data

Sample	SRT=22 days	SRT=15 days	SRT=12 days
Feeding1	8.282		
Feeding2	8.375		
Inoculum	7.792		
R1	8.004	8.141	8.207
R2	7.983	8.044	8.278
R3	7.550	7.736	7.858
R4	7.406	7.348	7.723
Reference	7.819	8.050	8.108

References

Agabo-Garcia, C., Perez, M., Rodriguez-Morgado, B., Parrado, J. and Solera, R. (2019) Biomethane production improvement by enzymatic pre-treatments and enhancers of sewage sludge anaerobic digestion. Fuel 255, 115713.

APHA, 2005. Standard Methods for the Examination of Water and Wastewater, twenty-first ed. American Public Health Association, Washington, DC. USA.

Appels, L., Baeyens, J., Degreve, J. and Dewil, R. (2008) Principles and potential of the anaerobic digestion of waste-activated sludge. Progress in Energy and Combustion Science 34(6), 755-781.

Athanasoulia, E., Melidis, P. and Aivasidis, A. (2012) Optimization of biogas production from waste activated sludge through serial digestion. Renewable Energy 47, 147-151.

Batstone, D.J., Keller, J., Angelidaki, I., Kalyuzhnyi, S.V., Pavlostathis, S.G., Rozzi, A., Sanders, W.T.M., Siegrist, H. and Vavilin, V.A. (2002) The IWA Anaerobic Digestion Model No 1 (ADM1). Water Science and Technology 45(10), 65-73.

Blumensaat, F. and Keller, J. (2005) Modelling of two-stage anaerobic digestion using the IWA Anaerobic Digestion Model No. 1 (ADM1). Water Research 39(1), 171-183.

Bonilla, S., Choolaei, Z., Meyer, T., Edwards, E.A., Yakunin, A.F. and Allen, D.G. (2018) Evaluating the effect of enzymatic pretreatment on the anaerobic digestibility of pulp and paper biosludge. Biotechnology reports 17, 77-85.

de Bok, F.A., Stams, A.J., Dijkema, C. and Boone, D.R. (2001) Pathway of propionate oxidation by a syntrophic culture of Smithella propionica and Methanospirillum hungatei. Applied Environmental Microbiology 67(4), 1800-1804.

De la Rubia, M.A., Riau, V., Raposo, F. and Borja, R. (2013) Thermophilic anaerobic digestion of sewage sludge: focus on the influence of the start-up. A review. Critical Reviews in Biotechnology 33(4), 448-460.

Franke-Whittle, I.H., Walter, A., Ebner, C. and Insam, H. (2014) Investigation into the effect of high concentrations of volatile fatty acids in anaerobic digestion on methanogenic communities. Waste Management 34(11), 2080-2089.

Ge, H., Jensen, P.D. and Batstone, D.J. (2011a) Relative kinetics of anaerobic digestion under thermophilic and mesophilic conditions. Water Science and Technology 64(4), 848-853.

Ge, H.Q., Jensen, P.D. and Batstone, D.J. (2011b) Temperature phased anaerobic digestion increases apparent hydrolysis rate for waste activated sludge. Water Research 45(4), 1597-1606.

Gonzalez, A., Hendriks, A., van Lier, J.B. and de Kreuk, M. (2018) Pre-treatments to enhance the biodegradability of waste activated sludge: Elucidating the rate limiting step. Biotechnology Advances 36(5), 1434-1469.

Guo, H., Felz, S., Lin, Y., van Lier, J.B. and de Kreuk, M. (2020a) Structural extracellular polymeric substances determine the difference in digestibility between waste activated sludge and aerobic granules. Water Research, 115924.

Guo, H., van Lier, J.B. and de Kreuk, M.J.W.r. (2020b) Digestibility of waste aerobic granular sludge from a full-scale municipal wastewater treatment system. Water Research 173, 115617.

Huang, W.H., Wang, Z.Y., Zhou, Y. and Ng, W.J. (2015) The role of hydrogenotrophic methanogens in an acidogenic reactor. Chemosphere 140, 40-46.

Karthikeyan, O.P., Selvam, A. and Wong, J.W.C. (2016) Hydrolysis-acidogenesis of food waste in solid-liquid-separating continuous stirred tank reactor (SLS-CSTR) for volatile organic acid production. Bioresource Technology 200, 366-373.

Kim, H.W., Nam, J.Y., Kang, S.T., Kim, D.H., Jung, K.W. and Shin, H.S. (2012) Hydrolytic activities of extracellular enzymes in thermophilic and mesophilic anaerobic sequencing-batch reactors treating organic fractions of municipal solid wastes. Bioresource Technology 110, 130-134.

Kim, M., Gomec, C.Y., Ahn, Y. and Speece, R. (2003) Hydrolysis and acidogenesis of particulate organic material in mesophilic and thermophilic anaerobic digestion. Journal of Environmental Technology 24(9), 1183-1190.

Kim, M. and Speece, R.E. (2002) Aerobic waste activated sludge (WAS) for start-up seed of mesophilic and thermophilic anaerobic digestion. Water Research 36(15), 3860-3866.

Kirkegaard, R.H., McIlroy, S.J., Kristensen, J.M., Nierychlo, M., Karst, S.M., Dueholm, M.S., Albertsen, M. and Nielsen, P.H. (2017) The impact of immigration on microbial community composition in full-scale anaerobic digesters. Scientific Reports 7(1), 9343.

Klocke, M., Nettmann, E., Bergmann, I., Mundt, K., Souidi, K., Mumme, J. and Linke, B. (2008) Characterization of the methanogenic Archaea within two-phase biogas reactor systems operated with plant biomass. Systematic and Applied Microbiology 31(3), 190-205.

Levenspiel, O. (2006) CHEMICAL REACTION ENGINEERING, 3RD ED, Wiley India Pvt. Limited.

Liu, H.B., Wang, Y.Y., Yin, B., Zhu, Y.F., Fu, B. and Liu, H. (2016) Improving volatile fatty acid yield from sludge anaerobic fermentation through self-forming dynamic membrane separation. Bioresource Technology 218, 92-100.

Liu, X.Y., Li, R.Y., Ji, M. and Han, L. (2013) Hydrogen and methane production by co-digestion of waste activated sludge and food waste in the two-stage fermentation process: Substrate conversion and energy yield. Bioresource Technology 146, 317-323.

Liu, Y., Wachemo, A.C., Yuan, H.R. and Li, X.J. (2019) Anaerobic digestion performance and microbial community structure of corn stover in three-stage continuously stirred tank reactors. Bioresource Technology 287, 121339.

Luo, K., Xie, X., Yang, Q., Chen, F., Zhong, Y., Xie, P. and Wang, G. (2020) Multi-hydrolytic enzyme accumulation and microbial community structure of anaerobic co-digestion of food waste and waste-activated sludge. Environmental Technology 41(4), 478-487.

Maspolim, Y., Zhou, Y., Guo, C., Xiao, K. and Ng, W.J. (2015a) The effect of pH on solubilization of organic matter and microbial community structures in sludge fermentation. Bioresource Technology 190, 289-298.

Maspolim, Y., Zhou, Y., Guo, C.H., Xiao, K.K. and Ng, W.J. (2015b) Comparison of single-stage and two-phase anaerobic sludge digestion systems - Performance and microbial community dynamics. Chemosphere 140, 54-62.

Maspolim, Y., Zhou, Y., Guo, C.H., Xiao, K.K. and Ng, W.J. (2015c) Determination of the archaeal and bacterial communities in two-phase and single-stage anaerobic systems by 454 pyrosequencing. Journal of Environmental Sciences-China 36, 121-129.

Menzel, T., Neubauer, P. and Junne, S. (2020) Role of Microbial Hydrolysis in Anaerobic Digestion. Energies 13(21), 5555.

Miron, Y., Zeeman, G., Van Lier, J.B. and Lettinga, G. (2000) The role of sludge retention time in the hydrolysis and acidification of lipids, carbohydrates and proteins during digestion of primary sludge in CSTR systems. Water Research 34(5), 1705-1713.

Miyawaki, A., Taira, S. and Shiraishi, F. (2016) Performance of continuous stirred-tank reactors connected in series as a photocatalytic reactor system. Chemical Engineering Journal 286, 594-601.

Parawira, W., Murto, M., Read, J.S. and Mattiasson, B. (2005) Profile of hydrolases and biogas production during two-stage mesophilic anaerobic digestion of solid potato waste. Process Biochemistry 40(9), 2945-2952.

Qin, Y., Wu, J., Xiao, B.Y., Cong, M., Hojo, T., Cheng, J. and Li, Y.Y. (2019) Strategy of adjusting recirculation ratio for biohythane production via recirculated temperature-phased anaerobic digestion of food waste. Energy 179, 1235-1245.

Rorat, A., Courtois, P., Vandenbulcke, F. and Lemiere, S. (2019) Industrial and Municipal Sludge, pp. 155-180, Elsevier.

Shimada, T., Morgenroth, E., Tandukar, M., Pavlostathis, S.G., Smith, A., Raskin, L. and Kilian, R.E. (2011) Syntrophic acetate oxidation in two-phase (acid-methane) anaerobic digesters. Water Science and Technology 64(9), 1812-1820.

Stolze, Y., Zakrzewski, M., Maus, I., Eikmeyer, F., Jaenicke, S., Rottmann, N., Siebner, C., Puhler, A. and Schluter, A. (2015) Comparative metagenomics of biogas-producing microbial communities from production-scale biogas plants operating under wet or dry fermentation conditions. Biotechnology for Biofuels 8(1), 1-18.

Van Lier, J.B., Mahmoud, N. and Zeeman, G. (2020) Anaerobic Wastewater Treatment Biological Wastewater Treatment: Principles, Modelling and Design, Second Edition, Chapter 16, IWA Publishing, London, UK, 701-756.

Vavilin, V.A., Fernandez, B., Palatsi, J. and Flotats, X. (2008) Hydrolysis kinetics in anaerobic degradation of particulate organic material: An overview. Waste Management 28(6), 939-951.

Wang, H., Li, J., Zhao, Y., Xu, C., Zhang, K., Li, J., Yan, L., Gu, J.D., Wei, D. and Wang, W. (2020) Establishing practical strategies to run high loading corn stover anaerobic digestion: Methane production performance and microbial responses. Bioresource Technology 310, 123364.

Wang, Y., Zhang, Y., Wang, J. and Meng, L. (2009) Effects of volatile fatty acid concentrations on methane yield and methanogenic bacteria. Biomass and bioenergy 33(5), 848-853.

Westerholm, M., Crauwels, S., Van Geel, M., Dewil, R., Lievens, B. and Appels, L. (2016) Microwave and ultrasound pre-treatments influence microbial community structure and digester performance in anaerobic digestion of waste activated sludge. Applied Microbiology and Biotechnology 100(12), 5339-5352.

Wu, L.J., Higashimori, A., Qin, Y., Hojo, T., Kubota, K. and Li, Y.Y. (2016) Upgrading of mesophilic anaerobic digestion of waste activated sludge by thermophilic pre-fermentation and recycle: Process performance and microbial community analysis. Fuel 169, 7-14.

Wu, L.J., Qin, Y., Hojo, T. and Li, Y.Y. (2015) Upgrading of anaerobic digestion of waste activated sludge by temperature-phased process with recycle. Energy 87, 381-389.

Xiao, X., Shi, W., Huang, Z., Ruan, W., Miao, H., Ren, H., Zhao, M.J.I.B. (2017) Process stability and microbial response of anaerobic membrane bioreactor treating high-strength kitchen waste slurry under different organic loading rates. Biodegradation 121, 35-43.

Yasui, H., Goel, R., Li, Y. and Noike, T. (2008) Modified ADM1 structure for modelling municipal primary sludge hydrolysis. Water Research 42(1-2), 249-259.

Zamanzadeh, M., Parker, W.J., Verastegui, Y. and Neufeld, J.D. (2013) Biokinetics and bacterial communities of propionate oxidizing bacteria in phased anaerobic sludge digestion systems. Water Research 47(4), 1558-1569.

Zhang, B., He, P.J., Lu, F., Shao, L.M. and Wang, P. (2007) Extracellular enzyme activities during regulated hydrolysis of high-solid organic wastes. Water Research 41(19), 4468-4478.

Zhang, L., Loh, K.C., Zhang, J.X., Mao, L.W., Tong, Y.W., Wang, C.H. and Dai, Y.J. (2019) Three-stage anaerobic co-digestion of food waste and waste activated sludge: Identifying bacterial and methanogenic archaeal communities and their correlations with performance parameters. Bioresource Technology 285.

Zhen, G.Y., Lu, X.Q., Kato, H., Zhao, Y.C. and Li, Y.Y. (2017) Overview of pretreatment strategies for enhancing sewage sludge disintegration and subsequent anaerobic digestion: Current advances, full-scale application and future perspectives. Renewable & Sustainable Energy Reviews 69, 559-577.

Zhou, H.D., Lv, S.F., Ying, Z.X., Wang, Y.Y., Liu, J.C. and Liu, W.D. (2019) Characteristics of two-phase mesophilic anaerobic digestion of co-substrates consisting of waste activated sludge and corn silage based on modified ADM1. Waste Management 91, 168-178.

Chapter 3

ENHANCED BIOCONVERSION OF WASTE ACTIVATED SLUDGE IN A MESOPHILIC CASCADE ANAEROBIC DIGESTER APPLYING LOW-RATIO DIGESTATE RECIRCULATION

This chapter is based on:
Guo, H., Oosterkamp, M. J., Zhou, T., van Lier, J. B., & de Kreuk, M. (2023). Enhanced bioconversion of waste activated sludge in a mesophilic cascade anaerobic digester applying low-ratio digestate recirculation. Submission to Journal of Waste Management.

Abstract

A cascade anaerobic digester (CAD) consists of a series of completely stirred tank reactors (CSTRs) and is applied for enhanced bioconversion of waste activated sludge (WAS). CAD process performance can be optimized applying digestate recirculation. In our present study, we investigated the effects of low recirculation ratios, varying between 2% and 10% of the influent flow, on the hydrolysis and bioconversion of WAS in a four-stage mesophilic CAD process. The CAD was operated under mesophilic conditions (35 °C) and a total solids retention time of only 12 days. The results showed 40% overall total chemical oxygen demand (tCOD) removal efficiency, applying a recirculation ratio of 10%. Reducing the recirculation ratio from 10% to 2% resulted in a 14% decrease in the tCOD removal efficiency, which was attributed to the decreased hydrolysis activity. Results showed that the specific methanogenic activities of the sludge were hardly affected, meanwhile the hydrolytic enzyme activities severely decreased. When the liquid fraction of the recycled digestate was replaced by demi-water, and a recirculation ratio of 10% of the digestate, containing the solid fraction of the recycled digestate and demi water, was applied, the hydrolysis efficiency, as well as the tCOD removal efficiency recovered. Analysis of trace elements concentrations and the sludge microbial community composition of each CAD-stage revealed that the solid fraction of the digestate contained most of the trace elements and a high abundancy of hydrolytic bacteria. The relatively low recycle ratio of 10% was apparently large enough to effectively seed the first CAD-stages with active hydrolytic bacteria, while simultaneously provide the required trace elements for enzyme production and growth. Overall, results evidenced the advantage of using a small digestate recirculation flow in CAD systems. However, too low recirculation ratios will negatively affect the treatment performance.

3.1 Introduction

Conventional activated sludge-based wastewater treatment plants (WWTPs) produce waste activated sludge (WAS) as a by-product of the process. In the European Union alone, over 44 million tons of WAS is produced annually (Zhang et al., 2017) WAS handling usually accounts for approximately one third of the WWTP capital costs and half of the operating costs (Tomei et al., 2016). To reduce these costs, treatment technologies such as anaerobic digestion (AD) are often applied, to stabilize WAS, reduce organic residues, and to produce biochemical energy in the form of biogas. Hydrolysis of WAS is the first step in the anaerobic degradation of complex organics and is often seen as the rate limiting step of AD (Hassard et al., 2018). Slow hydrolysis rates of WAS form the bottleneck of conventional AD processes using a single continuous stirred tank reactor (CSTR), leading to a need for long solids retention times (SRTs) to reach acceptable WAS degradation efficiencies and its corresponding biogas production (Appels et al., 2008).

Several hydrolysis enhancement processes including thermal, chemical, and enzymatic methods can be applied to disrupt the complex microbial sludge floc structures, and therefore increase the accessibility of both the extra-cellular and intra-cellular substrates during AD. Hydrolysis enhancement by increased enzyme activities is conceived a promising method in recent years, as it avoids extreme conditions during sludge pre-treatment and thus, high investment costs (Chen et al., 2018). Moreover, there is no production of recalcitrant compounds, like in the case of thermal pretreatment (Zhang et al., 2020). Up to now, most of the concept-proven methods to achieve hydrolysis enhancement by increased enzyme activities are difficult to apply at industrial scale. For example, addition of highly active hydrolytic enzymes into an anerobic digester requires a continuous purchase of large amounts of expensive enzymes (Li et al., 2021). Another example is pre-fermentation prior to AD, making use of specific hydrolytic bacteria. However, under full-scale conditions, the preservation of specific biomass is barely possible while working with complex non-sterile substrates (Agabo-Garcia et al., 2019). Instead, transforming the reactor configuration from one single large reactor into several small reactors in a cascade configuration, was proven to effectively increase the hydrolytic enzyme activity and thus, the biosolids degradation (Guo et al., 2021). Guo et al. (2021) proved that the total SRT could be shortened to 12 - 15 days, corresponding to a 25-45% reduction in the total reactor size or higher throughput of WAS in the digester. Compared to other strategies for hydrolysis enhancement, the cascade anaerobic digester (CAD) process is technically and economically attractive, since it creates a relatively easy way to upgrade present AD installations, e.g., via retrofitting and compartmentalizing existing large-scale CSTR-based sludge digesters.

So far, most CAD studies for WAS digestion focused on understanding the feasibility of the process under different operational parameters, such as organic loading rate (Zhang et al., 2019), operational temperature (Riau et al., 2015) and reactor pH (Maspolim et al., 2016). In recent years, digestate recirculation from a later stage to the front stage of the cascades has been introduced to improve the performance of a CAD system treating manure, kitchen waste or thermal-pretreated WAS (Nabaterega et al., 2021). Recirculation can tackle the negative effects of volatile fatty acids (VFAs) accumulation in the first acidogenic reactor, which results from high hydrolysis/ acidogenesis rates (Giuliano et al., 2014; Hussain et al., 2017; Wu et al., 2015). Recycling the alkalinity-rich digestate increases the buffer capacity in the acidogenic/first reactor and stabilizes the process (Xu et al., 2014). To our best knowledge, application of digestate recirculation in mesophilic CAD systems for raw, untreated WAS has been not specifically reported so far. Unlike food waste and thermal-pretreated WAS, raw WAS largely consists of extracellular polymeric substances (EPS) that are difficult to hydrolyze and microbial cells (Gonzalez et al., 2018). Therefore, the VFA production rate and alkalinity generated in the acidogenic/ first reactor of a mesophilic CAD treating raw WAS might be different from reported feedstocks. Besides alkalinity, also microorganisms and nutrients are recycled due to digestate recirculation, which may influence the nutrient availability to the microorganisms in the first reactor (Zuo et al., 2015). Therefore, our present study focused on a possible improvement of the mesophilic CAD process performance by recycling digestate during raw WAS treatment, applying different recirculation ratios, i.e., the ratio of the recycle flow rate to the feeding flow rate (Qin et al., 2019). Most studies and applications apply high recirculation ratios, usually over 50%, with the aim to supplement sufficient buffer capacity (Wu et al., 2015; Zuo et al., 2015). However, too high ratios dilute substrate concentrations and lower the hydrolysis rate in the first reactor, which will reduce the process efficiency (Levenspiel, 2006; (Li et al., 2023). In our previous study, we investigated the performance of a CAD system, operated with a recycling ratio of 10% (Guo et al., 2021). Applying an SRT of only 12 days resulted in stable operational performance, while the observed WAS conversion efficiency was 30 - 35% higher than the conventional CSTR with the same total volume. Although these results clearly showed the potentials of applying a low-ratio recirculation strategy in CAD for WAS treatment, the exact mechanism determining a minimum recycle ratio remains unclear.

In our present study, we operated a CAD with four CSTRs in series for mesophilic WAS digestion. The objectives of the present study were (a) to compare the performance of the CAD system applying two recirculation ratios: 2% and 10%; (b) to determine the hydrolytic enzyme activity, as well as the specific methanogenic activity applying these two recirculation ratios, (c) to elucidate possible shifts in the microbial communities under the applied recirculation ratios.

3.2 Materials and methods

3.2.1 Sludge sources

All reactors were seeded with anaerobic sludge collected from a full-scale mesophilic anaerobic digester at the municipal WWTP Harnaschpolder, treating primary sludge and centrifuge-thickened WAS from an enhanced biological phosphorus removal (EBPR) process (Den Hoorn, The Netherlands). The full-scale digester was operated with an SRT of 20 days in average. The inoculum characteristics were pH 8.1 ± 0.4, total solids (TS) 33.0 ± 0.9 g/L and volatile solids (VS) 23.2 ± 0.3 g/L. WAS from the same plant was collected weekly to be used as substrate for the CAD, and was characterized by a total chemical oxygen demand (tCOD) concentration between 40 - 70 g/L. The tCOD concentration of the feeding sludge was adjusted to approximately 53 g/L by centrifugation or dilution with freshly centrifuged supernatant obtained from WAS of the same WWTP. Sludge was stored at 4 °C before use.

3.2.2 Experimental set-up and operational parameters

The experiments were carried out using a CAD system comprised of 3 x 2.2 L CSTRs (R1, R2, R3) and a 15.4 L CSTR (R4). More detailed information can be found elsewhere (Guo et al., 2021).

The total SRT was maintained at 12 days, while R1-3 accounted for 10% of the total SRT (1.2 days) each, and the SRT for R4 was set to 8.4 days. The entire experiment was divided into four phases based on the applied different recirculation ratios. The operational conditions during the 4 phases are shown in Table 3.1. Briefly, during the first 41 days, the recirculation ratio was set to 10% of the influent flow, while at Phase 2, the recirculation ratio was changed to 2% for 57 days. In Phase 3, the recirculation ratio of 10% was again applied. However, it must be noted that in Phase 3, the solid fraction of the recycled digestate was firstly separated from the liquid fraction prior to recycling; the liquid fraction was discarded and replaced by demi-water. Solids separation was obtained by digestate centrifugation at 14,000 rpm for 5 min. Hereafter, the solid pellet was washed three times in demi-water and finally, the pellet was resuspended in demi-water to reach to the same volume of the original digestate. In Phase 4 the same conditions as in Phase 1 were again applied, with a recirculation ratio of 10%.

Table 3.1 Digestate recirculation ratio of the CAD system during the 4 phases. The SRT throughout the experimental period was 12 days in total: R1-R3, 1.2 days each and R4 8.4 days

Phase	Experimental time (day)	Recirculation ratio (% of influent flow)
1	1-41	10%
2	42-99	2%
3	100-136	10% Note: only the solid fraction, the liquid fraction was replaced by demi-water
4	137-174	10%

3.2.3 Hydrolytic enzymatic activity test

Activity of protease and cellulase of the digestate from each CSTR was measured according to the method previously described (Guo et al. (2021). The activities of protease and cellulase were individually analyzed by Pierce fluorescent protease assay kit (Thermo Fisher, USA) and MarkerGene fluorescent cellulase assay kit (MarkerGene, USA), using a 96-well microplate spectrophotometer (Synergy HTX, BioTek, USA).

3.2.4 Analytical methods

The tCOD and soluble COD (sCOD) were measured using a spectrophotometer (DR3900, Hach Lange, Germany). pH was checked with a multi-functional meter (InoLab, Multi 720, WTW). VFAs and methane content of the biogas were measured based on the method reported by Guo et al. (2021). Specific methanogenic activity (SMA) tests were performed based on the method of Tian et al. (2017), using 2 different substrates, i.e., acetate and H_2/CO_2. Sludge samples for SMA tests were taken from each reactor at the end of each phase. The tests were conducted in batch serum vials of 118 mL total volume and 40 mL working volume. About 25% of the working volume consisted of active biomass, and 75% was basal anaerobic medium (Ghasimi et al., 2015) in all SMA tests. All the vials (liquid phase and headspace) were flushed with a N_2/CO_2 gas mixture (80/20%, v/v) to create anaerobic conditions. Acetate (20 mM) and H_2/CO_2 (80/20%, v/v, under 1 bar) were individually used, as carbon and energy sources (Luo et al., 2011). The measured SMA, therefore, were named as acetate SMA (ASMA) and H_2/CO_2 SMA (HSMA), respectively. Finally, vials with only inoculum and basal medium were used as blanks and all the tests were performed in triplicates. Trace elements concentrations, including Mn and Zn, were measured by inductively coupled plasma mass spectrometry (ICP-MS, model PlasmaQuant MS, Analytik Jena, Germany).

3.2.5 Microbial population analysis

Duplicate biomass samples were analyzed during the experiment to evaluate the microbial community dynamics. The biomass samples were taken from one feeding

sample and 12 digestate samples from the CAD system. The feeding samples were taken individually on day 101 and the digestates were sampled at the end of each phase. The method for extraction of DNA was according to the procedure reported in our previous study (Guo et al. 2021). Briefly, the FastDNA® SPIN Kit for Soil (MP Biomedicals, USA) was used to extract DNA according to the manufacturer's instructions. The quality and quantity of the DNA obtained was checked by Qubit3.0 DNA detection (Qubit® dsDNA HS Assay Kit, Life Technologies, USA). High throughput sequencing was performed using the HiSeq Illumina platform and a universal primer 515F/806R (5'-GTGCCAGCMGCCGCGGTAA-3'/ 5'-GGACTACHVGGGTWTCTAAT-3') for bacterial and archaeal 16S rRNA genes (Novogene, Cambridge, UK). Raw reads were deposited in the European Nucleotide Archive under accession number PRJEB40450. Sequences was analyzed by the QIIME pipelines (Version 1.7.0) to pair forward and reverse sequences (Caporaso et al., 2010), and removal of chimeras sequences was performed by UCHIME algorithm.

Sequences with ≥ 97% similarity were clustered into one operational taxonomic unit (OTUs) by UCLUST algorithm (Edgar et al., 2011). Singletons were removed, and OTUs with an occurrence less than three times in at least one sample were excluded. Taxonomic assignment was performed in Mothur software against the SILVA Database. The detection processes including DNA extraction, barcode attachment, 16S rRNA sequencing analysis, and resulting data analysis were previously reported by Chen et al. (2018).

3.2.6 Statistical analysis

Student's *t*-test was used for general variance analysis by SPSS Statistics 25 (IBM, USA), with the threshold for significance set at a *P-value* < 0.05. The STMAP software was applied to determine the significantly changed OTUs between different samples (Parks & Beiko, 2010).

3.3 Results and discussion

3.3.1 Performance of the CAD system under different digestate recirculation strategies

Figure 3.1 shows the pH and the tCOD and VFA concentrations of the feed and the digestate in the individual reactors, as well as the methane production in each reactor. Each experimental phase covered at least three times the system SRT, i.e., 36 days, to ensure biomass acclimation to the varying conditions.

The CAD system was started-up and operated for 70 days prior to the start of the here described experiment. During that period, the SRT was stepwise reduced from 20 to 12 days and results are described in (Guo et al., 2021). The recirculation ratio of 10% during Phase 1, resulted in a tCOD reduction efficiency that stabilized around 40%, corresponding to an average daily methane production of 12.4L. Considering that the effluent tCOD of R3 was 43 g/L on average, the first three reactors with a total volume of 6.6 L and SRT of 3.6 days, accounted for approximately half of the tCOD reduction in the CAD system.

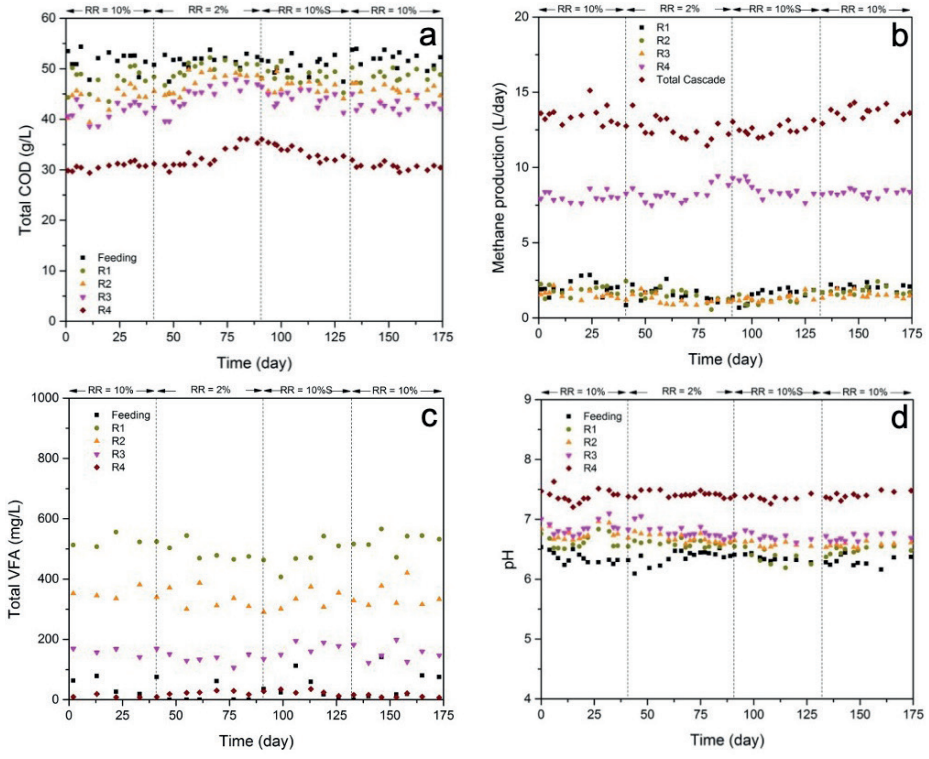

Figure 3.1 (a) Total COD (tCOD) concentration, (b) methane production, (c) total VFA concentration and (d) pH, during the different phases using recirculation ratios (RR) of 10%, 2% or 10% with demi water + solid fraction (10%S)

In Phase 2, the recycle ratio was decreased from 10% to 2%, which caused a remarkable decrease in tCOD reduction efficiency of 14%. This drop was primarily caused by the decreased tCOD reduction efficiency in R1, R2 and R3, accompanied by the significant increment of average tCOD effluent concentrations to 50, 48 and 46 g/L, respectively (Figure 3.1a). As a consequence, the organic loading rate to R4 distinctly increased, resulting in a decreased methane production in the first 3 reactors, and an increased methane production in the final large reactor. Because of the relatively low SRT of 8.4 days in R4, and the limited degradation in R1-3, the total efficiency of the CAD process during Phase 2 did not exceed 34.6% on average.

When the recirculation ratio was increased to 10% again, during Phase 4, both tCOD reduction efficiency and methane production rate recovered to the same level as during Phase 1. Previous studies also reported a decreased tCOD removal efficiency and methane production in staged AD systems when recirculation ratios were reduced (Chen et al., 2021; Wu et al., 2016; Zuo et al., 2015). These authors attributed the observed reduction to a substantial accumulation of VFA in the first reactors that likely hindered methanogenesis in the rest of their CAD system. However, in our study, we observed a relatively stable VFA concentration in R1, R2 and R3, not exceeding 600 mg COD/L in R1 and independent from the recycle ratio (Figure 3.1c). Furthermore, the VFA/alkalinity ratio and pH, two important indicators that evaluate the process stability of AD, stayed within the appropriate range, respectively, i.e., between 0.35 - 0.41 (according to Figure 3.1c, and Figure S3.1 in the supplementary data) and 6.3 - 6.5 (Figure 3.1d) during all experimental phases. Contrary to the reported declined methanogenic activity at a decreased recycle ratio, we found no statistically relevant difference (*p-value* > 0.05) between the SMA test results at different recycle ratios (Figure 3.2). In general, the SMA for hydrogenotrophic methanogens was highest in R1 and gradually decreased along the CAD system, while the trend of SMA for acetogenic methanogens was the opposite. Unlike the cases reported in literature, all our present results revealed that the methanogenic activity remained stable in the mesophilic CAD system treating WAS at a low recirculation ratio.

Interestingly, a 10% recycle of only the digestate solid phase in Phase 3, resulted in very similar (*p-value* > 0.05) tCOD conversion efficiencies as during full digestate recycling: efficiencies of 12.5%, 15.8% and 23.3% were reached in R1, R2 and R3, resulting in a total tCOD conversion efficiency of 38.7% on average. This finding indicated that the solid fraction likely played a more important role in process stability than the liquid fraction of the recycled digestate. Also these results contrasted to literature, in which the liquid fraction of the digestate is indicated as the key factor in enhancing the organics conversion during staged AD processes treating other feedstocks such as food waste or manure (Stowe et al., 2015; Zuo et al., 2014). The liquid fraction of digestate in later stages of staged AD systems is characterized by a relatively high alkalinity, explaining an increased buffer capacity of the first reactor via digestate recirculation (Qin et al., 2019). Considering the fact that the VFA concentration in the first reactor remained low in our experiment, digestate recirculation for alkalinity supply was apparently less important than for reported CAD processes treating food waste and manure (Zuo et al., 2014).

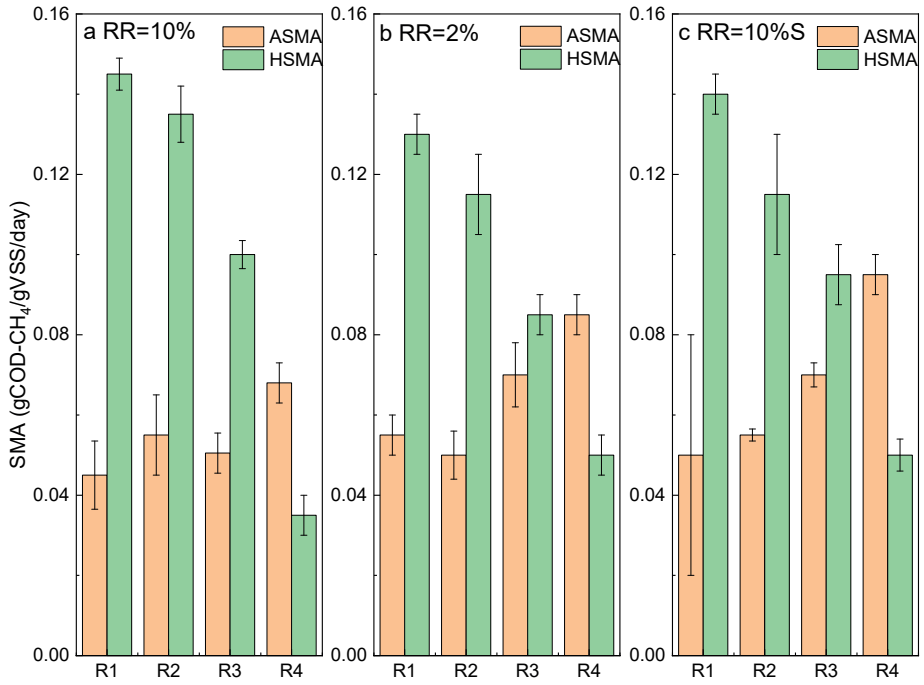

Figure 3.2 SMA test results in the reactors of the CAD system at different recirculation strategies using (a) RR of 10%, (b) 2% and (c) 10% demi water + the solid fraction of sludge (10%S)

3.3.2 Hydrolytic enzymatic activity

Since hydrolysis is regarded as the rate-limiting step in AD of WAS, a decreased hydrolysis rate might be indicative for an overall decreased tCOD removal efficiency at a decreased recirculation ratio. To study a possible change in hydrolytic activity in the different reactors of the CAD system, cellulase and protease activities were analyzed as representative hydrolytic enzyme activities for WAS degradation (Lu et al., 2016).

Figure 3.3 depicts the variation in free and sludge attached cellulase and protease activity under different recirculation ratios. Both cellulase and protease activities showed a downward trend from R1 to R4 at the recirculation ratio of 10%, which was in line with our earlier findings (Guo et al. (2021). The decreased recirculation ratio to 2% in Phase 2 significantly lowered the enzyme activities of R1 and R2 by approximately 25% and 20%, respectively. The distribution between cell attached and free enzyme activity remained similar compared to Phase 1. The activities of both enzymes in R4 increased in Phase 2, compared to Phase 1, which may explain the observed increased methane production in R4 (Figure 3.1b). The results clearly indicate that the lower tCOD conversion efficiency

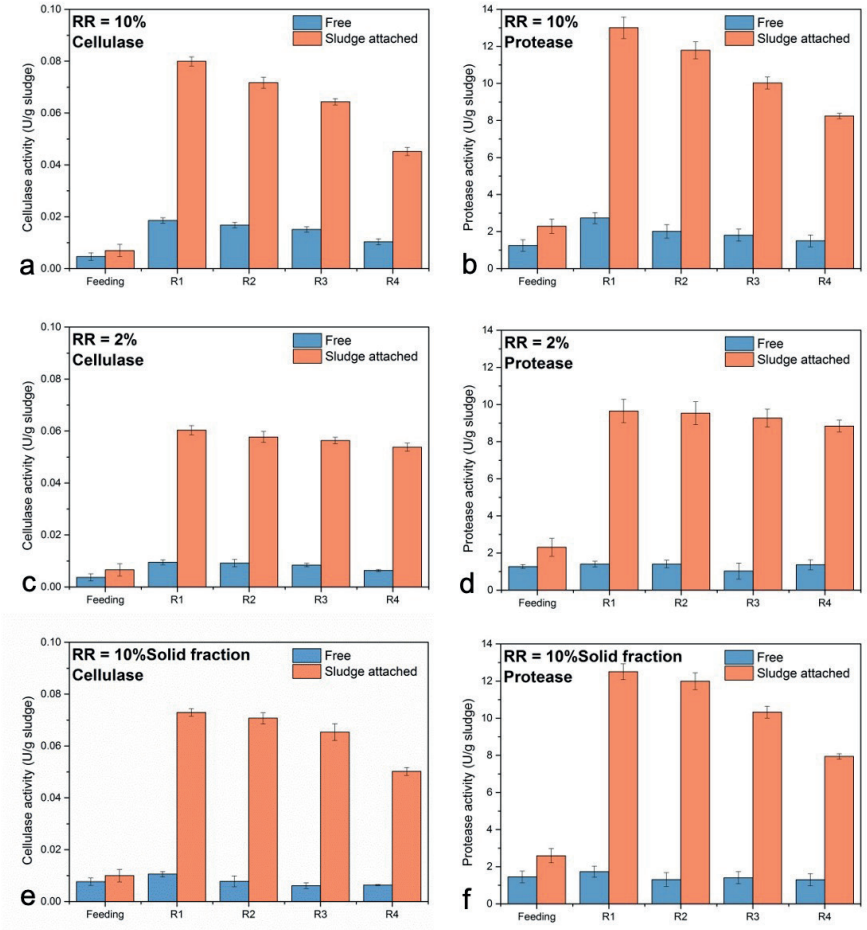

Figure 3.3 Cellulase and protease activities in the feeding and the different reactors of the CAD system: (a and b) enzyme activities at RR of 10%, (c and d) enzyme activities at RR of 2%, and (e and f) enzyme activities at RR of 10% demi water + solid fraction of sludge

in Phase 2 followed from a decreased hydrolytic capacity, rather than an inhibition of methanogenesis. A similar observation on hydrolytic enzyme activities was reported by Zhang et al. (2007) in their study, who reduced recirculation ratios in a staged AD system for municipal solid waste. The authors interpreted their observation by a slower synthesis and reduced refreshment of cell-free extracellular enzymes under decreased recirculation ratios. Nevertheless, in our study it is shown that the activity of sludge-attached enzymes, rather than that of cell-free enzymes, accounted for the majority of the total enzyme activity (Figure 3.3). Results indicated that the enzymatic catalysis predominantly took place on/within the solid fraction of the sludge matrix. This hypothesis was evidenced by the observations during Phase 3, in which only the solid fraction of the digestate was

recirculated from R3 to R1: both protease and cellulase activity in R1 and R2 were roughly restored to the values observed during Phase 1. Apparently, recycled sludge-attached hydrolytic enzymes in the solid fraction of the digestate played a key role in regulating the process performance at the different applied recirculation ratios.

3.3.3 Micronutrients analysis

Enzymatic reactions in anaerobic processes depend on the bioavailability of trace elements, which are either incorporated in enzyme structures or in enzyme cofactors (Pasalari et al., 2021). To further investigate the effects of changes in the recirculation ratio on the trace element concentration in the CAD system, we explored the distribution of Mn and Zn, which are important key trace elements for the activity and production of hydrolytic enzymes (Hendriks et al., 2018). Considering the importance of solids-bound hydrolytic enzymes, the two trace elements were analyzed from the sludge-attached enzyme extract through membranes with different cut-offs. In this study, two cut-offs, 10 kDa and 100 kDa were applied, since the molecular weights of most proteases (Razzaq et al., 2019; Zhang et al., 2015) and cellulases (Libardi et al., 2019; Qi et al., 2012) fall within the 10-100 kDa range. Some other key enzymes that are highly active in AD, such as hydrogenase and methyl-coenzyme M reductase, are also grouped with Zn or even Mn (Hendriks et al., 2018), but their molecure weights are usually much higher than the applied cut-offs (Fiebig & Friedrich, 1989; Scheller et al., 2013). Therefore, we assumed that trace elements captured between the indicated two cut-offs ($metals_{10\text{-}100\ kDa}$) will be hydrolytic enzymes-related. Results showed that during all operational conditions both Mn and Zn concentrations in the range of 10 kDa-100 kDa decreased from R1-R3, and their concentrations were significantly higher at both the 10% recirculation ratios. The element concentration in the feeding was remarkably lower than that in digesters (Figure 3.4). These results show a similar trend as the observed distribution of enzyme activities (Figure 3.3).

Also, Zn and Mn concentrations passing a 10kDa membrane ($metals_{<10\ kDa}$) were analyzed, displaying an increasing concentration over the subsequent reactors of the CAD system. Trace elements like Zn and Mn are often bound to, or originated from, small organic residuals in the sludge matrix that are not completely anaerobically biodegraded (Fermoso et al., 2019). At the recirculation ratio of 10%, the Mn and Zn concentrations in both the size-fractions were approximately double in each reactor compared to the 2% recirculation ratio. Possibly, enhanced digestate recirculation ensured the presence of more bioavailable trace elements for enzyme production, resulting from accelerated hydrolysis of the sludge matrix. Also, the 5 times higher recirculation of enzymes and bioavailable trace elements, respectively produced and released, has led to increased concentrations in all subsequent reactors.

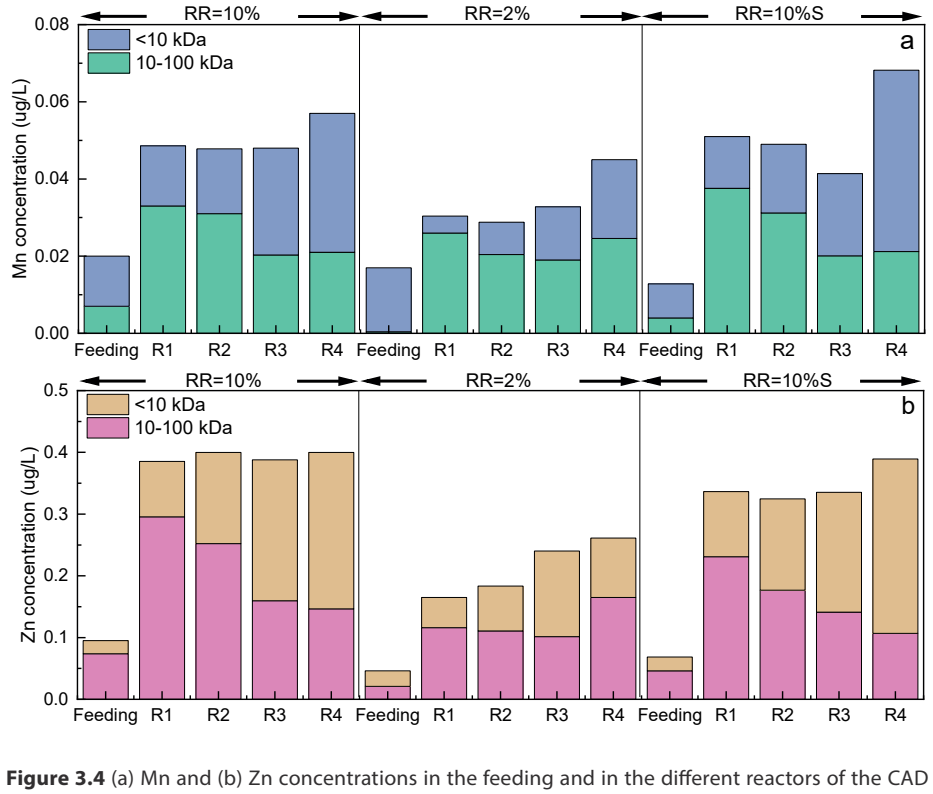

Figure 3.4 (a) Mn and (b) Zn concentrations in the feeding and in the different reactors of the CAD system during the different recirculation ratios: RR = 10% at phase 1, RR = 2% at phase 2, and RR = 10% of demi water + the solids fraction of sludge at phase 3 (10%S)

3.3.4 Microbial population structure

Above presented results revealed that digestate recirculation ratio of 10% resulted in an increase in solids-bound hydrolytic enzymes and enzyme-related trace elements in the first reactors of the CAD system. Since changes in stability and efficiency of enzymatic hydrolysis also might be related to changes in the microbial community, the sludge microbial composition in each reactor of the CAD system was analyzed. In all reactors, the bacterial communities at the Class level were dominantly composed of *Alpha/Beta/Gamma Proteobacteria, Bacteroidia, Clostridia, Acidimicrobiia* and *Actinobacteria* (Figure 3.5a), with a relative abundance of each individual class ≥ 4%. Among them, *Bacteroidia* and *Clostridia* include species that have been indicated as important species involved in hydrolysis and acidification of WAS in AD (Chen et al., 2017). Notably, their relative abundance distinctly increased in the subsequent reactors of the CAD system, independent of the recirculation strategy. These results are in accordance with the observed increased hydrolytic activity as a results of the applied high loading rates in the first reactors, as explained by Guo et al.

(2021). Statistical analysis using STAMP (Figure 3.5c), showed that the decrease in the recirculation ratio from 10% to 2% caused a significant decrease (*p-value* < 0.05) in the relative abundance of both *Bacteroidia* and *Clostridia* in each reactor of the CAD system. These results confirmed the importance of applying a sufficiently high recirculation ratio for preserving the growth of required hydrolytic bacteria. Interestingly, also the recirculation of only the solid fraction sorted the same effect on the abundance of *Bacteroidia* and *Clostridia,* since the consortia in Phase 1 and 3 were highly comparable on class level.

Some minor fermenters within the Class level showed statistically relevant differences in relative abundance between Phase 3 and 1 (Figure 3.5d). These species included the glucose degrading *unidentified_Spirochaetes* (Lee et al., 2013) and *Bacill* that are assumed to decompose both lipids and carbohydrates (Carballa et al., 2015). These differences imply that the liquid fraction of the recycled digestate could be crucial for the metabolism of these functional bacteria, which needs further research.

The analysis of the archaeal community (Figure 3.5b) revealed that *Methanobrevibacter,* a common hydrogenotrophic methanogen, was the most abundant methanogen in R1 during all phases. Their abundance decreased further downstream in the CAD system, while *Methanosaeta* that utilize acetate as the sole substrate, became more dominant from R2 to R4. The shift in relative abundance from hydrogenotrophic to acetoclastic methanogens was generally consistent with the SMA results. This shift was possibly attributable to higher maximum specific growth rates (μ_{max}) of hydrogenotrophic methanogens (2.00 - 2.85 d^{-1}) compared to that of *Methanosaeta* species (0.33 - 0.71 d^{-1}) (Van Lier et al., 2020), which resulted in the predominance of hydrogenotrophic methanogenic species in R1-3 applying very short SRTs (Huang et al., 2015). Although the transition of the major methanogenic pathways along the CAD system remained unchanged under the different experimental phases, some specific methanogens seemed to be influenced by the changed recirculation ratios. For example, the relative abundance of the sequences affiliated with genus *Methanosprillum* in R1-3 was significantly lower (*p-value* < 0.05) in Phase 2, applying 2% recirculation ratio, than during the other phases. *Methanospirillum* is identified to regulate syntrophic propionate oxidation in phased anaerobic digestion (Maspolim et al., 2015). The decrease in their relative abundance at 2% recirculation ratio suggests that the reduced recirculation ratio was likely unfavorable for attaining efficient syntrophic propionate conversion, which will be systematically investigated in future studies.

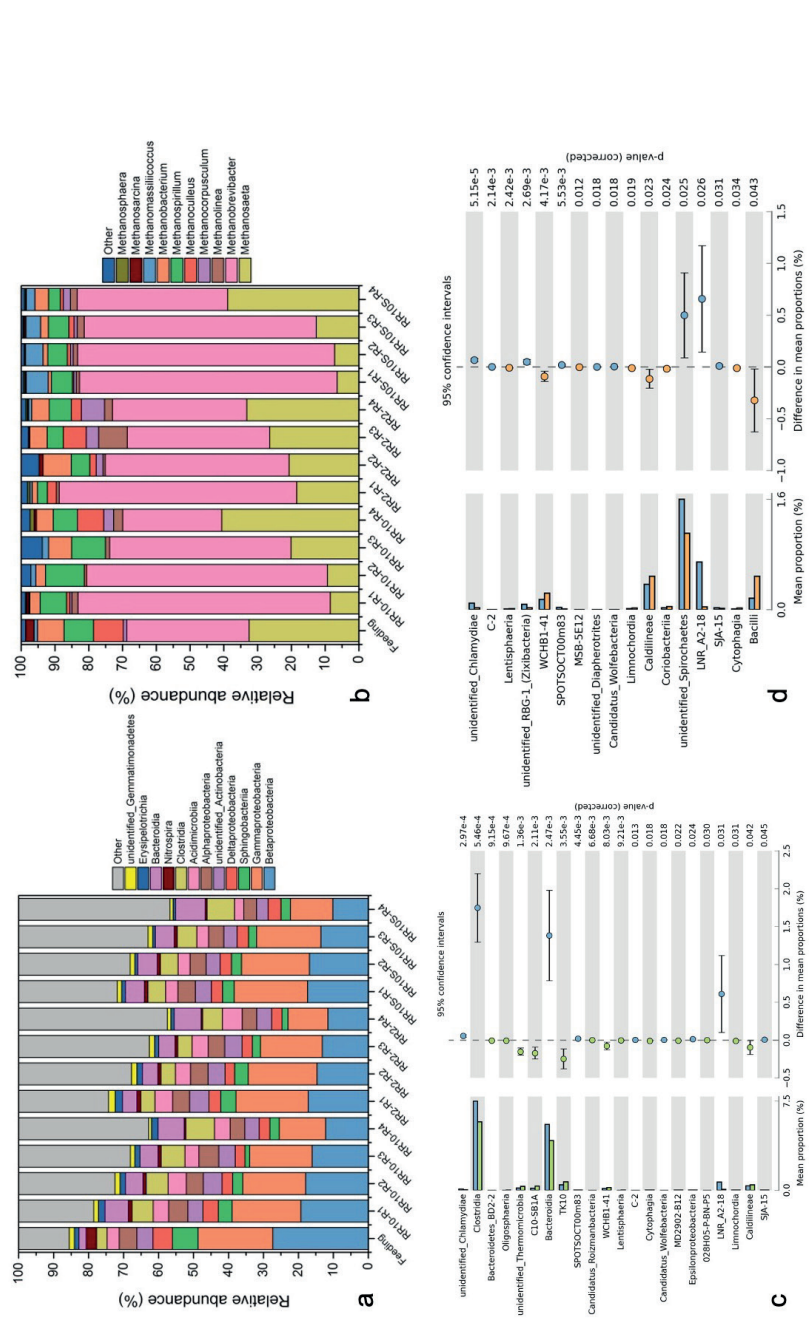

Figure 3.5 Analysis of microbial community structure of the CAD process. (a) Species taxonomy of bacteria at the class level, and (b) species taxonomy of methanogens at the genus level. Meanwhile, species (at the class level) that changed significantly (p-value<0.05) were shown between the group (c) RR=10% vs. RR=2%, and (d) RR=10% vs. RR=10%S

4 Conclusions

The conclusions drawn from the current work can be summarized as follows:

1) WAS treatment in the short-SRTs CAD system operated with 10% recirculation ratio resulted in a stable tCOD reduction efficiency of 40% on average. Reducing the digestate recirculation ratio from 10% to 2% led to a decreased tCOD reduction efficiency by 14%. Based on the results of SMA and hydrolytic enzyme activity tests, we concluded that this decrease in sludge removal efficiency was due to lower hydrolysis rates, rather than methanogenesis inhibition.
2) Recycling solely the solid fraction of the digestate at a ratio of 10% (Phase 3) recovered the tCOD conversion efficiency approximately to that of Phase 1 when both the solid and liquid fraction of the digestate was recycled, revealing the crucial role of the solid fraction in the efficiency of WAS digestion in a CAD system.
3) Both Mn and Zn concentrations related to the molecular size fractions in the range of 10 kDa-100 kDa cut-offs, which were extracted from the solid fraction of the sludge, revealed a decreasing trend over the subsequent reactors of the CAD system. Zn and Mn in the fraction below 10kDa showed an increased concentration in the subsequent reactors of the CAD system.
4) Comparative analysis of the microbial composition of the sludge applying different recirculation ratios indicated that the solid fraction of the digestate supplemented active hydrolytic microorganisms from R3 to R1.

Supplementary data

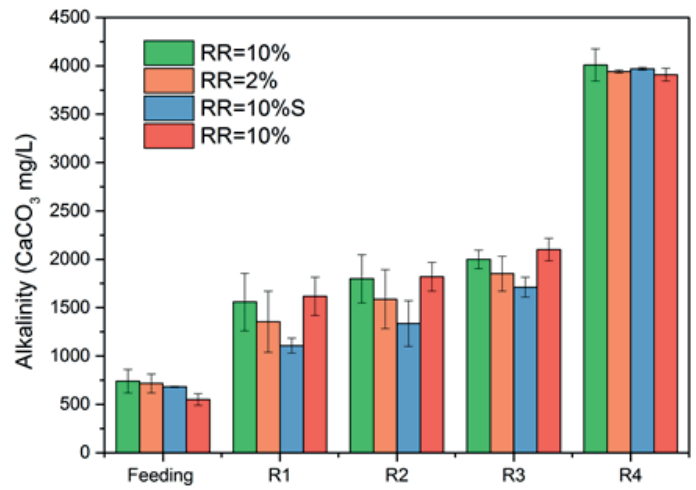

Figure S3.1 Alkalinity profiles in the cascade AD system

References

CFD investigation of the flow characteristics of a plug flow anaerobic digester for lignocellulosic biomass methanisation.

Agabo-Garcia, C., Perez, M., Rodriguez-Morgado, B., Parrado, J., Solera, R. 2019. Biomethane production improvement by enzymatic pre-treatments and enhancers of sewage sludge anaerobic digestion. Fuel, 255.

Appels, L., Baeyens, J., Degreve, J., Dewil, R. 2008. Principles and potential of the anaerobic digestion of waste-activated sludge. Progress in Energy and Combustion Science, 34(6), 755-781.

Caporaso, J.G., Kuczynski, J., Stombaugh, J., Bittinger, K., Bushman, F.D., Costello, E.K., Fierer, N., Pena, A.G., Goodrich, J.K., Gordon, J.I. 2010. QIIME allows analysis of high-throughput community sequencing data. Nature methods, 7(5), 335.

Carballa, M., Regueiro, L., Lema, J.M. 2015. Microbial management of anaerobic digestion: exploiting the microbiome-functionality nexus. Curr Opin Biotechnol, 33, 103-11.

Chen, H., Zhang, W., Wu, J., Chen, X., Liu, R., Han, Y., Xiao, B., Yu, Z., Peng, Y. 2021. Improving two-stage thermophilic-mesophilic anaerobic co-digestion of swine manure and rice straw by digestate recirculation. Chemosphere, 274, 129787.

Chen, J.H., Liu, S.H., Wang, Y.M., Huang, W., Zhou, J. 2018. Effect of different hydrolytic enzymes pretreatment for improving the hydrolysis and biodegradability of waste activated sludge. Water Science and Technology, 592-602.

Chen, Y., Jiang, X., Xiao, K., Shen, N., Zeng, R.J., Zhou, Y. 2017. Enhanced volatile fatty acids (VFAs) production in a thermophilic fermenter with stepwise pH increase - Investigation on dissolved organic matter transformation and microbial community shift. Water Res, 112, 261-268.

Edgar, R.C., Haas, B.J., Clemente, J.C., Quince, C., Knight, R. 2011. UCHIME improves sensitivity and speed of chimera detection. Bioinformatics, 27(16), 2194-2200.

Fermoso, F.G., van Hullebusch, E., Collins, G., Roussel, J., Mucha, A.P., Esposito, G. 2019. Trace Elements in Anaerobic Biotechnologies. IWA Publishing, London, UK.

Fiebig, K., Friedrich, B. 1989. Purification of the F420-reducing hydrogenase from Methanosarcina barkeri (strain Fusaro). J European journal of biochemistry, 184(1), 79-88.

Ghasimi, D.S.M., Tao, Y., de Kreuk, M., Zandvoort, M.H., van Lier, J.B. 2015. Microbial population dynamics during long-term sludge adaptation of thermophilic and mesophilic sequencing batch digesters treating sewage fine sieved fraction at varying organic loading rates. Biotechnology for Biofuels, 8.

Giuliano, A., Zanetti, L., Micolucci, F., Cavinato, C. 2014. Thermophilic two-phase anaerobic digestion of source-sorted organic fraction of municipal solid waste for bio-hythane production: effect of recirculation sludge on process stability and microbiology over a long-term pilot-scale experience. Water Science and Technology, 69(11), 2200-2209.

Gonzalez, A., Hendriks, A., van Lier, J.B., de Kreuk, M. 2018. Pre-treatments to enhance the biodegradability of waste activated sludge: Elucidating the rate limiting step. Biotechnol Adv, 36(5), 1434-1469.

Guo, H., Oosterkamp, M.J., Tonin, F., Hendriks, A., Nair, R., van Lier, J.B., de Kreuk, M. 2021. Reconsidering hydrolysis kinetics for anaerobic digestion of waste activated sludge applying cascade reactors with ultra-short residence times. Water Res, 202, 117398.

Hassard, F., Biddle, J., Harnett, R., Stephenson, T. 2018. Microbial extracellular enzyme activity affects performance in a full-scale modified activated sludge process. Sci Total Environ, 625, 1527-1534.

Hendriks, A.T.W.M., van Lier, J.B., de Kreuk, M.K. 2018. Growth media in anaerobic fermentative processes: The underestimated potential of thermophilic fermentation and anaerobic digestion. Biotechnology Advances, 36(1), 1-13.

Huang, W.H., Wang, Z.Y., Zhou, Y., Ng, W.J. 2015. The role of hydrogenotrophic methanogens in an acidogenic reactor. Chemosphere, 140, 40-46.

Hussain, A., Filiatrault, M., Guiot, S.R. 2017. Acidogenic digestion of food waste in a thermophilic leach bed reactor: Effect of pH and leachate recirculation rate on hydrolysis and volatile fatty acid production. Bioresource Technology, 245, 1-9.

Lee, S.H., Park, J.H., Kang, H.J., Lee, Y.H., Lee, T.J., Park, H.D. 2013. Distribution and abundance of Spirochaetes in full-scale anaerobic digesters. Bioresour Technol, 145, 25-32.

Li, W.J., Cai, T., Lu, X.Q., Han, Y.L., Kudisi, D., Chang, G.H., Dong, K., Zhen, G.Y. 2023. Two-Phase improves Bio-hydrogen and Bio-methane production of anaerobic membrane bioreactor from waste activated sludge with digestate recirculation. Chemical Engineering Journal, 452.

Li, X., Xie, H., Liu, G., Zhang, R., Ma, X., Chen, H. 2021. Optimizing temperature for enhancing waste activated sludge decomposition in lysozyme and rhamnolipid pretreatment system. Bioresour Technol, 341, 125868.

Libardi, N., Soccol, C.R., de Carvalho, J.C., de Souza Vandenberghe, L.P.J.B.t. 2019. Simultaneous cellulase production using domestic wastewater and bioprocess effluent treatment–A biorefinery approach. 276, 42-50.

Lu, F., Wang, J.W., Shao, L.M., He, P.J. 2016. Enzyme disintegration with spatial resolution reveals different distributions of sludge extracellular polymer substances. Biotechnology for Biofuels, 9.

Maspolim, Y., Guo, C.H., Xiao, K.K., Zhou, Y., Ng, W.J. 2016. Performance and microbial community analysis in alkaline two-stage enhanced anaerobic sludge digestion system. Biochemical Engineering Journal, 105, 296-305.

Maspolim, Y., Zhou, Y., Guo, C.H., Xiao, K.K., Ng, W.J. 2015. Determination of the archaeal and bacterial communities in two-phase and single-stage anaerobic systems by 454 pyrosequencing. Journal of Environmental Sciences-China, 36, 121-129.

Nabaterega, R., Kumar, V., Khoei, S., Eskicioglu, C.J.J.o.E.C.E. 2021. A review on two-stage anaerobic digestion options for optimizing municipal wastewater sludge treatment process. 105502.

Parks, D.H., Beiko, R.G. 2010. Identifying biologically relevant differences between metagenomic communities. Bioinformatics, 26(6), 715-721.

Pasalari, H., Gholami, M., Rezaee, A., Esrafili, A., Farzadkia, M. 2021. Perspectives on microbial community in anaerobic digestion with emphasis on environmental parameters: A systematic review. Chemosphere, 270, 128618.

Qi, B., Luo, J., Chen, G., Chen, X., Wan, Y.J.B.t. 2012. Application of ultrafiltration and nanofiltration for recycling cellulase and concentrating glucose from enzymatic hydrolyzate of steam exploded wheat straw. 104, 466-472.

Qin, Y., Wu, J., Xiao, B.Y., Cong, M., Hojo, T., Cheng, J., Li, Y.Y. 2019. Strategy of adjusting recirculation ratio for biohythane production via recirculated temperature-phased anaerobic digestion of food waste. Energy, 179, 1235-1245.

Razzaq, A., Shamsi, S., Ali, A., Ali, Q., Sajjad, M., Malik, A., Ashraf, M. 2019. Microbial proteases applications. J Frontiers in Bioengineering

Biotechnology Advances, 7, 110.

Riau, V., De la Rubia, M.A., Perez, M. 2015. Upgrading the temperature-phased anaerobic digestion of waste activated sludge by ultrasonic pretreatment. Chemical Engineering Journal, 259, 672-681.

Scheller, S., Goenrich, M., Thauer, R.K., Jaun, B. 2013. Methyl-coenzyme M reductase from methanogenic archaea: Isotope effects on the formation and anaerobic oxidation of methane. J Journal of the American Chemical Society, 135(40), 14975-14984.

Stowe, E.J., Coats, E.R., Brinkman, C.K. 2015. Dairy manure resource recovery utilizing two-stage anaerobic digestion - Implications of solids fractionation. Bioresource Technology, 198, 237-245.

Tian, H., Fotidis, I.A., Mancini, E., Angelidaki, I. 2017. Different cultivation methods to acclimatise ammonia-tolerant methanogenic consortia. Bioresour Technol, 232, 1-9.

Tomei, M.C., Bertanza, G., Canato, M., Heimersson, S., Laera, G., Svanström, M.J.J.o.c.p. 2016. Techno-economic and environmental assessment of upgrading alternatives for sludge stabilization in municipal wastewater treatment plants. 112, 3106-3115.

Van Lier, J.B., Mahmoud, N., Zeeman, G. 2020. Anaerobic Wastewater Treatment Biological Wastewater Treatment: Principles, Modelling and Design, Second Edition, Chapter 16, IWA Publishing, London, UK, 701-756.

Wu, L.J., Higashimori, A., Qin, Y., Hojo, T., Kubota, K., Li, Y.Y. 2016. Upgrading of mesophilic anaerobic digestion of waste activated sludge by thermophilic pre-fermentation and recycle: Process performance and microbial community analysis. Fuel, 169, 7-14.

Wu, L.J., Qin, Y., Hojo, T., Li, Y.Y. 2015. Upgrading of anaerobic digestion of waste activated sludge by temperature-phased process with recycle. Energy, 87, 381-389.

Xu, S.Y., Karthikeyan, O.P., Selvam, A., Wong, J.W.C. 2014. Microbial community distribution and extracellular enzyme activities in leach bed reactor treating food waste: Effect of different leachate recirculation practices. Bioresource Technology, 168, 41-48.

Zhang, B., He, P.J., Lu, F., Shao, L.M., Wang, P. 2007. Extracellular enzyme activities during regulated hydrolysis of high-solid organic wastes. Water Research, 41(19), 4468-4478.

Zhang, D., Feng, Y., Huang, H., Khunjar, W., Wang, Z.W. 2020. Recalcitrant dissolved organic nitrogen formation in thermal hydrolysis pretreatment of municipal sludge. Environ Int, 138, 105629.

Zhang, L., Loh, K.C., Zhang, J.X., Mao, L.W., Tong, Y.W., Wang, C.H., Dai, Y.J. 2019. Three-stage anaerobic co-digestion of food waste and waste activated sludge: Identifying bacterial and methanogenic archaeal communities and their correlations with performance parameters. Bioresource Technology, 285.

Zhang, P., Shen, Y., Guo, J.-S., Li, C., Wang, H., Chen, Y.-P., Yan, P., Yang, J.-X., Fang, F. 2015. Extracellular protein analysis of activated sludge and their functions in wastewater treatment plant by shotgun proteomics. J Scientific reports, 5(1), 1-11.

Zhang, Q., Hu, J., Lee, D.J., Chang, Y., Lee, Y.J. 2017. Sludge treatment: Current research trends. Bioresour Technol, 243, 1159-1172.

Zuo, Z., Wu, S.B., Qi, X.Y., Dong, R.J. 2015. Performance enhancement of leaf vegetable waste in two-stage anaerobic systems under high organic loading rate: Role of recirculation and hydraulic retention time. Applied Energy, 147, 279-286.

Zuo, Z., Wu, S.B., Zhang, W.Q., Dong, R.J. 2014. Performance of two-stage vegetable waste anaerobic digestion depending on varying recirculation rates. Bioresource Technology, 162, 266-272.

Chapter 4

PROCESS PERFORMANCE AND MICROBIAL COMMUNITY COMPOSITION OF FULL-SCALE HIGH-RATE CASCADE SLUDGE DIGESTER

This chapter will be submitted for publication:
Guo, H., McIntyre, M., Visser, A., Kuipers, H., van Lier, J. B., & de Kreuk, M. Process performance and microbial community composition of full-scale high-rate cascade sludge digester.

Abstract

A full-scale cascade anaerobic digester (CAD) system consisting of four conventional continuous stirred thank reactors (CSTRs) in series and equipped with a low-ratio digestate recirculation was operated and monitored to evaluate its performance. The CAD system was built at wastewater treatment plant (WWTP) Tollebeek in the Netherlands. The newly build digester was vertically divided into 3 smaller pie-shaped segments, which were connected in series and were subsequently followed by the second already existing sludge digester. Long-term operation of the CAD system fed with a mixture of waste activated sludge (WAS) and primary sludge (PS) showed an efficient and stable tCOD reduction of 56.1 ± 6.8%, and an enhanced enzymatic sludge hydrolysis rate at 14.5 days total solids retention time (SRT). High-throughput sequencing analysis revealed that all reactors shared a similar microbial community structure dominated by consortia that govern hydrolysis and acidogenesis. Despite the relatively short SRTs in the first 3 reactors of the CAD system, acetoclastic methanogens belonging to *Methanosaeta spp.* became the most abundant Archaea. Overall, we strongly believe that the results obtained in this study pave a way for the industrialization of the novel CAD process in the treatment of municipal waste sewage sludge.

4.1 Introduction

The conventional activated sludge (CAS) process is currently the most common biological wastewater treatment technology worldwide, extensively applied in wastewater treatment plants (WWTPs). CAS systems usually produce a high amount of waste sewage sludge, consisting of waste activated sludge (WAS) and primary sludge (PS) (Cao & Pawlowski, 2012). In the European Union alone, approximately 9-12 million tons of waste sewage sludge is produced annually (Eurostat, European Commission, 2022, link: https://ec.europa.eu/eurostat). Inappropriate use and poor treatment of waste sewage sludge may lead to odor nuisance, and greenhouse gas emissions, leading to public health and environmental health hazards. Therefore, proper sludge processing and adequate disposal are essential parts of wastewater treatment systems (Raheem et al., 2018).

Anaerobic digestion (AD) is one of the most well-established processes applied to stabilize waste sewage sludge, achieving volume reduction and recovery of biochemical energy via biogas production. Unlike PS, which contains easily biodegradable cellulosic fibers, proteins and fats, WAS contains more persistent extracellular polymeric substances and bacterial cells (Guo et al., 2020). Therefore, compared to PS digestion, WAS digestion often experiences lower hydrolysis rates and longer sludge retention times. This typically results in larger reactor volumes, which in turn leads to increased capital costs and lower solids biodegradation rates (Gonzalez et al., 2018). To overcome these drawbacks, several hydrolysis enhancement pre-treatment strategies for WAS have been developed, with thermal and acid/base treatments being the most commonly reported (Zhen et al., 2017). While these strategies accelerate WAS hydrolysis rates, they also reveal the constraints related to excessive utilization of chemicals and/or energy inputs (Xu et al., 2020), and generation of refractory byproducts (Zhang et al., 2020). Compared to heating or chemically disrupting the sludge structure, enzymatic hydrolysis enhancement strategies have gained popularity in recent years. This is due to the mild process conditions and absence of the production of byproducts that may negatively affect downstream processing of the digestate (Jiang et al., 2021). Enzymatic hydrolysis enhancement can be realized by either additionally dosing active hydrolytic enzymes, or by stimulating hydrolytic reaction/enzyme activities in-situ. To date, most enzymatic WAS hydrolysis enhancement studies have been limited to lab-scale investigations for concept verification, with a pressing need for practical applications (Agabo-Garcia et al., 2019).

Recently, a very promising enzymatic hydrolysis enhancement strategy has been developed, which makes use of high substrate concentration and thus accelerated

first order conversion rates. This novel digestion process makes use of cascading three or more small conventional completed stirred tank reactors (CSTRs) and is currently marketed under the tradename Ephyra®. The CAD (CAD) system effectively accelerates the hydrolytic enzyme activity during WAS digestion (Guo et al., 2021). The system maintains stable WAS digestion efficiencies of 40 - 47% and consistent biomethane production, with a notably short total SRTs of 12 days. Under the same conditions, the conventional anaerobic CSTR operated was unstable at a 12 days SRT and showed a 13% lower conversion efficiency at a 15 days SRT compared to the CAD process at a 12 days SRT.

Full-scale sludge AD processes are typically operated to co-digest WAS and PS, rather than the treatment of WAS alone (Ozgun, 2019). Previous studies reported that hydrolysis enhancement strategies, which were shown to be effective for WAS digestion, could have a negative effect on PS digestion, or not an effect at all (Zhang et al., 2016). CAD systems fed with WAS alone have been studied at lab scale, because the most significant effect of enzyme enhancement was expected on the typically slow-to-biodegrade WAS fraction. The impact on PS digestion, or on a mixture of PS and WAS remains unexplored.

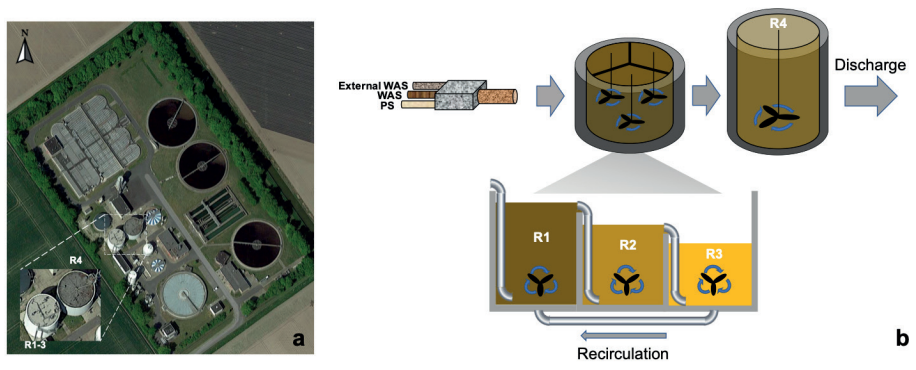

Figure 4.1 (a) The location of the full-scale CAD system in WWTP Tollebeek, the Netherlands, (b) Schematic illustration of the CAD process (Royal Haskoning DHV)

A CAD process at full scale can be feasibly transformed from two CSTR sludge digesters by dividing one of the two digesters into three vertically divided smaller segments, or by adding a new compartmentalized digester in front of an existing digester. The three so-called pie shaped segments were connected in series to achieve the cascading effect, and were subsequently followed by the second digester in series (see also Figure 4.1). The full-scale CAD system was fed with a PS/WAS mixture with a fluctuating composition, resulting from a fishing industry

discharging wastewater to this WWTP and the high ratio between storm and dry weather flows. Degradation of the PS/WAS mixture was individually assessed for each reactor compartment of the process by determining the organic solids reduction and volatile fatty acids production efficiencies, as well as methane production rate. Additionally, the microbial community composition throughout the CAD process was analyzed using high-throughput sequencing methods.

4.2 Materials and methods

4.2.1 Description of the WWTP and the CAD system

The WWTP at Tollebeek receives approximately 20,000 and 100,000 m^3/day of municipal wastewater, during dry weather flow and stormwater flow, respectively. This WWTP consists of a two-stage activated sludge plant, and a sludge digestion process with an annual treatment capacity of 4,600 tons of dry solids. The location of the CAD system in the WWTP and its detailed process configuration are presented in Figure 4.1a and 1b, respectively. As it is shown, the CAD system was composed of two digesters both with working volume of 1500 m^3. One of the digesters was vertically divided into three mechanically mixed pie-shaped compartments of 500 m^3 each. A mixture of thickened PS (making up 40 - 45% of the total flow, 15 - 48 g total solids (TS)/L) and WAS (making up 30 - 35% of the total flow, 66 - 72 g TS/L) from the same WWTP, as well as a portion of external WAS (ES, making up 25 - 30% of the total flow, 58 - 78 g TS/L) from WWTP Lelystad and Zeewolde, was fed to the first compartment R1. Hereafter, the sludge mixture flowed to R2 and R3 via a pipe overflow. From there, the mixture flowed to the second 2,000 m^3 digester, denominated as R4, which was mixed via biogas recirculation. A controlled recycle flow with a low flow rate from R3 to R1 was used, based on our previous study (Guo et al., 2021). The level difference between the compartments was limited by the use of equalization holes in the lower part of the vertical partitions. Finally, the digested sludge exiting R4 was dewatered in screw presses and transported to the final sludge disposal. The average retention time of each pie-shape compartment was 2 days. During peak loadings the SRT dropped to 1.7 days. The SRT of R4 was 8.5 days, resulting in a total system SRT of between 13.6 and 14.5 days. The operating temperature of the entire CAD process was maintained at 38 ± 0.5 °C.

4.2.2 Sampling and analytic methods

Influent and effluent TS of the CAD system, as well as the total methane production of the entire process were measured daily. PS, WAS, external WAS and effluent from each digester (R1 - R4) were sampled bi-weekly, and an additional six batch samples were collected between days 79 and 160. The six sampling batches (B1 - B6) were

used to determine the physicochemical characteristics of the sludge, i.e. chemical oxygen demand (COD) concentration, ammonium (NH_4-N) and ortho-phosphate (PO_4-P) , using standard test kits: LCK014 for COD, LCK303 for NH_4-N and LCK350 for PO_4-P (Hach Lange, Germany). Volatile fatty acids (VFAs) were measured by gas chromatography (GC) with a flame ionization detector (FID) (Agilent 7890A, USA). A column of 25 m × 320 µm × 0.5 µm (Agilent 19091F-112) was used and Helium was used as carrier gas with a flow rate of 1.8 mL/min. The injection and oven temperature were 240°C and 80°C, respectively. The hydrolytic enzyme activities, including protease and cellulase, of all sludge samples were analyzed to investigate the hydrolysis step in the CAD system. The activity of protease was determined using Pierce fluorescent protease assay kit (Thermo Fisher, USA) and the activity of cellulase was determined using MarkerGene fluorescent cellulase assay kit (MarkerGene, USA). All measurements were conducted with a 96-well microplate spectrophotometer (BioTek Synergy-HTX, USA). Triplicate sludge samples, including influent and the effluent from each digester of the CAD system, were collected for enzyme extraction on day 131. The hydrolytic enzymes were separated into free and sludge-attached fractions. The detailed information of these two enzyme fractions have been reported in elsewhere (Guo et al., 2021).

During the experiment, the feed samples were sampled on days 100 and 145, and the digestates from R1, R2, R3, R4 sampled on days 110, 141 and 155 were analyzed to evaluate the microbial community dynamics based on the procedure previously published (Guo et al., 2021). In principal, FastDNA® SPIN-Kit-for-Soil (MP Biomedicals, USA) was used to extract DNA according to the manufacturer's instructions, and the obtained DNA's quality was verified by Qubit3.0 DNA detection (Qubit® dsDNA-HS-Assay-Kit, Life Technologies, USA). High throughput sequencing and taxonomic assignment of the extracted DNA samples were performed at Novogene, UK. Raw sequence reads of the extracted DNA were placed in the European Nucleotide Archive with the accession number of PRJEB66492.

One-way ANOVA was applied with SPSS Statistics 25 (IBM, USA) to evaluate the level of significance between the differences in chemical characteristics between the sludge samples. The significance level of probability (p-value) was determined to be 0.05 in this study.

4.3 Results and discussion

4.3.1 Performance of the full-scale CAD process

The daily monitored total solids and methane production rate of the CAD system are shown in Fig 2a and 2b, respectively. During the entire experimental period of 214 days, the total solids concentration of the influent sludge highly fluctuated between 28.4 and 68.2 g/L. Nevertheless, a stable effluent total solids concentration of approximately 30 g/L was assessed during the entire study. The sludge reduction efficiency by the CAD system was 43.7 ± 10.9% in TS, resulting in a total methane production of around 3,000 m^3/d. These results indicated that the CAD system could satisfactorily handle strong fluctuations in the influent solids concentration.

To better understand the different processes in the four compartments of the CAD system, influent and effluent of each reactor compartment were sampled six times between days 79 and 160. The values of the measured TS, tCOD, sCOD, total VFAs, NH_4-N and PO_4-P concentrations are presented in Fig 3. The TS reduction determined from these six samples showed a similar trend as in the daily measurements, revealing that the highest TS reduction was obtained in R1 and R4, i.e, 25.5 ± 5.9% and 16.5 ± 2.1%, respectively. The results revealed a tCOD conversion of 56.1 ± 6.8 %, a declining percentage throughout the cascade process from 70.2 ± 11.6 in R1 to 30.1 ± 0.9 g/L in R4 (Figure 4.3a and b). In line with the TS reduction, the largest decrease in tCOD concentration occurred in R1, where more than 70% of the tCOD conversion took place. R2 and R3 only contributed to a tCOD reduction of approximately 4% each. This observation was in line with the ammonia profile that followed a reciprocal trend (Figure 4.3a and e). Observed results indicate that R1 had the highest conversion rate for protein compounds. The phosphate concentration also increased sharply in R1, but stabilized in subsequent reactors and even slightly decreased in R4 (Fig 3f). Possible explanations for the observed dynamics are the release of phosphate by phosphate accumulating organisms in the first compartment, which coincided with high VFA concentrations in the influent and sludge in R1 (Figure 4.3d), whilst phosphate precipitation likely occurred in R4.

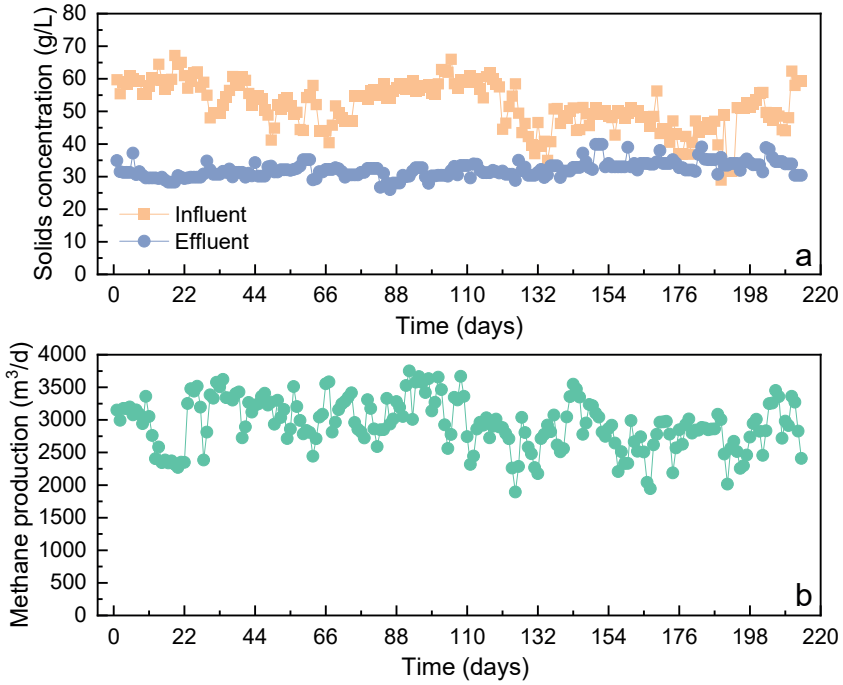

Figure 4.2 (a) Total influent and effluent solids concentration and (b) total methane production rate of the CAD system

The results obtained in this full-scale measuring campaign were compared with the results obtained in our laboratory scale CAD system (Guo et al., 2021). In the latter work, the CAD system was operated at a similar total SRT of 12-15 days, while only 8.1% of the tCOD was converted in R1, and 9.0, 7.7, and 14.3% of tCOD was converted in R2, R3, and the larger digester R4. A major difference between the two systems is that the full-scale installation was fed with a mixture of PS and WAS, while the laboratory scale system was fed solely with WAS from a nearby WWTP. The influent of the full-scale system contained a high fraction of readily biodegradable COD; 4.9 g/L of which on average 2.1 g/L were VFAs (Figure 4.3c and d). This readily biodegradable COD is very likely converted immediately in the first compartment (R1). As mentioned, it must be noted that PS was absent in the feed of the laboratory-scale system. Typically, the conversion rate of PS is 1.4 times higher than that of WAS during AD, due to the high content of cellulose fibers and lipids that are easily biodegradable (Guo et al., 2020). Unfortunately, the methane production of the individual compartments could not be determined in the full-scale installation; the produced biogas of all compartments was collected and the total volume was measured with a single device. Therefore, it was not possible to determine the specific hydrolytic activity per compartment in the full-scale

CAD system. However, the hydrolytic activity can be estimated from the tCOD removal efficiencies, which was the highest in R1, followed by R4, while the hydrolytic activity in R2 and R3 was the lowest.

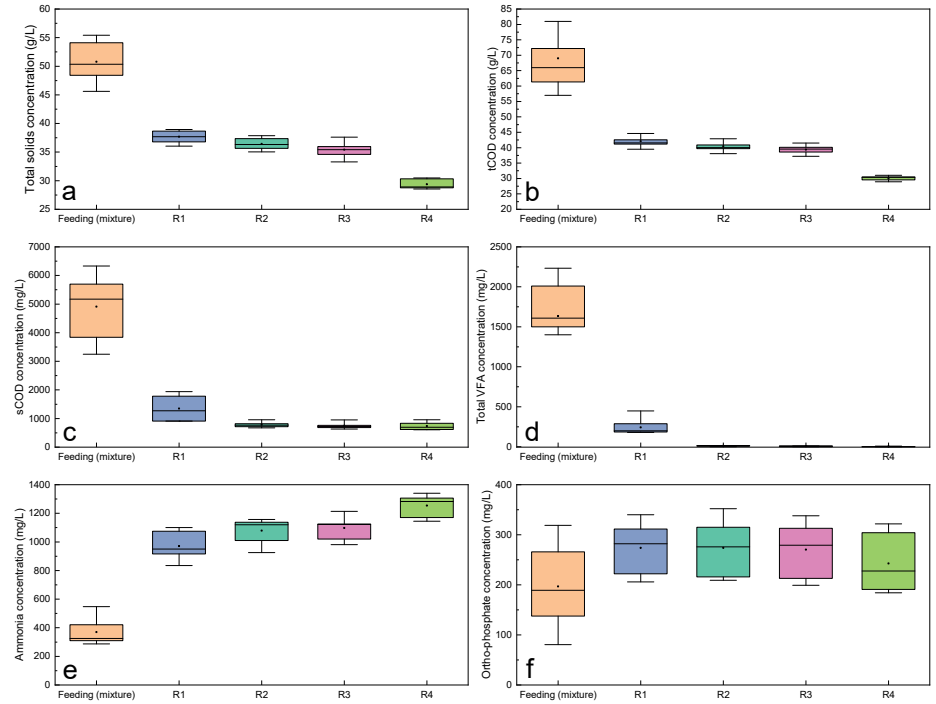

Figure 4.3 Chemical characteristics of each reactor (a) total solids concentration, (b) tCOD concentration, (c) sCOD concentration, (d) total VFA concentration, (e) ammonia concentration, and (f) ortho-phosphate (n = 6, with triplicates for each sample)

Instead of the specific hydrolytic activity, the activity of two types of hydrolytic enzymes, protease and cellulase, were analyzed (Figure 4.4). R1 presented the highest activity of both enzymes with the values of 10.00 ± 0.76 U/mL for protease and 0.078 ± 0.003 U/mL for cellulase, followed by R2 and R3, and R4 possessed the lowest enzyme activity. Compared to the lab-scale CAD system (Guo et al., 2021), the protease and cellulose enzyme activity was comparable in the first compartment, R1. The trend along the cascades was somewhat different, with higher enzyme activities in R2 and R3 from the lab-scale reactor compared to the full-scale CAD system. The tCOD loading rate of R1 in the full-scale CAD, was similar to the lab scale R1 at 15 days of system SRT (1.5 days SRT specifically in R1), indicating similar hydrolytic enzyme activities in R1 of both full-scale and lab-scale CAD processes. The results successfully prove the accelerated enzymatic hydrolysis of sludge using the cascade digestion configuration at full-scale.

4.3.2 Microbial community composition and dynamics

In the laboratory scale CAD system, a clear differentiation of the microbial population between the different compartments was observed (Guo et al., 2021). To determine whether this was the case at full-scale, the microbial community structure of the different compartments of the CAD system was analyzed, and compared with the influent sludge. Three sampling batches (day 110, 141 and 155) were analyzed by high-throughput gene sequencing. Around 2.2 million high quality sequences were generated from all sludge samples and were assigned to OTUs. The duplicates of each sludge sample were clustered in a PCA plot (Figure 4.5). The results show that R1, R2 and R3 samples of each batch shared a similar microbial structure. A distinct difference in microbial structure was expected between R4 and R1-3, owing to the relatively long SRT applied in R4 (Baldi et al., 2019; Wang et al., 2018). However, there was no remarkable difference observed in the microbial composition between R4 and the other compartments.

A detailed examination of the microbial composition of all sludge samples at genus level revealed that the three types of feed sludge contained different dominant groups. The WAS possessed high relative abundances of nitrifiers and phosphate accumulating organisms, such as *Nitrospira* and *Candidatus_Accumulibacter* (Rubio-Rincon et al., 2017; Zhang et al., 2015), as is expected from activated sludge from a modified UCT system. PS was dominated by facultative *Ottowia*, *Trichococcus* and Arcobacter as well as strictly anaerobic *Macellibacteroides* (Mei et al., 2016). The ES that is initally (anaerobically) stored until transport to WWTP Tollebeek, showed species commonly associated with denitrification: *Kouleothrix* and *Pseudomonas* (De Sotto & Bae, 2020), and *Clostridium_sensu_stricto_1* that are known as anaerobic sugar and protein fermenters (Luo et al., 2020). Obviously, the mixing of three sludge types and the solids hold-up in the first step of the cascade (R1) significantly reduced the relative abundances of the predominated genus of the individual sludge types (p-value < 0.05). The most abundant bacteria on genus level in R1, ranked by relative abundance, were *Candidatus_Cloacimonas*, *DMER64*, *Sedimentibacter*, *Christensenellaceae_R-7_group* and *Syntrophomonas* , which are reported to regulate the hydrolysis and acidogenesis of sludge in sludge digesters (Lee et al., 2018; Shakeri Yekta et al., 2021). Despite a slightly higher relative abundances of indicated genera in R1 and R2 compared to R3 and R4, no clear changes in the bacterial fingerprints of the digestate from R1 - R4 was observed, irrespective of samples from different batches. This finding supports the results of PCA.

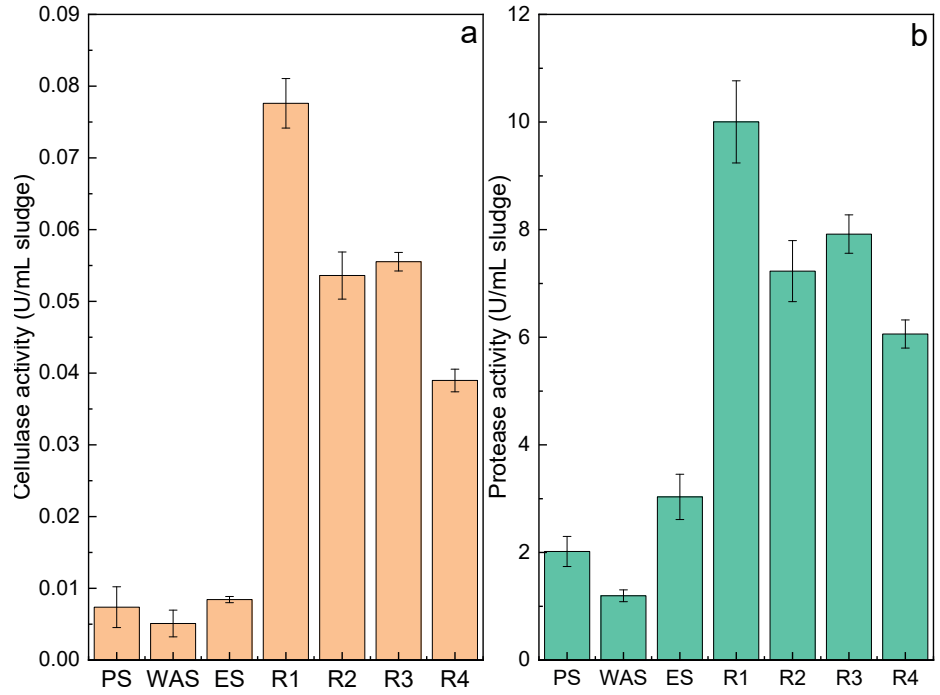

Figure 4.4 Enzyme activity in U per mL of sludge from the feeding and each reactor compartment. (a) Sludge-attached cellulase, and (b) sludge-attached protease. Error bars refer to the standard deviation (n = 6)

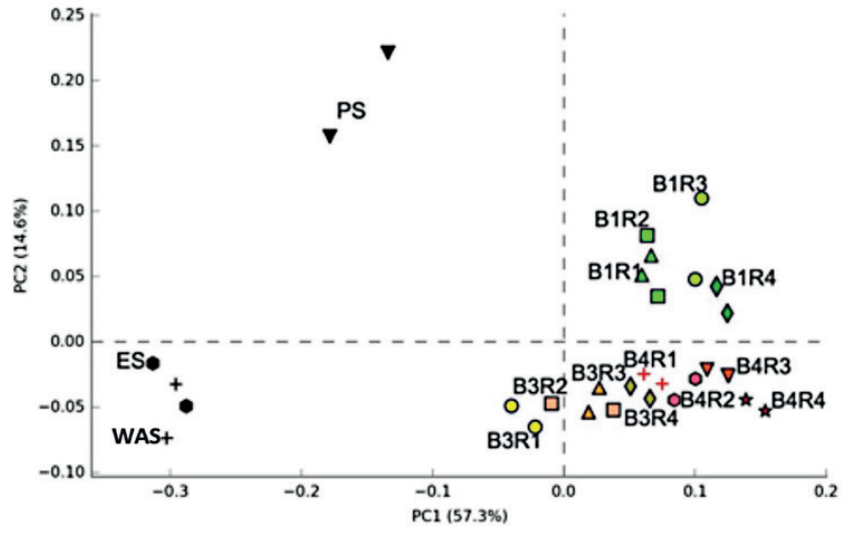

Figure 4.5 Principle component analysis (PCA). All samples were measured in duplicate

Two genera affiliated to Phylum Euryarchaeota, i.e., *Methanosaeta* and *Candidatus Methanofastidiosum*, were substantially enriched in all digesters at the different sampling rounds (Figure 4.6). Figure 4.7 shows that *Methanosaeta* and *Candidatus Methanofastidiosum* accounted for approximately 60% and 15% in abundance of the Archaea in R1-R3, and 50% and 20% in R4, respectively. *Methanosaeta* spp. are typical acetoclastic methanogens that strictly metabolize acetate as their sole source of energy. Members of the genus *Candidatus Methanofastidiosum* have been reported to produce methane through methylated thiol reduction that plays an important role in bridging the carbon and sulfur cycles in a stable anaerobic digestion environment (Nobu et al., 2016). In multi-stage digesters and cascading AD systems, usually hydrogenotrophic methanogens normally proliferate in the first high loaded reactor (Shimada et al., 2011; Guo et al., 2021). *Methanosaeta* has a weaker tolerance to extreme conditions, and has a maximum growth rate (u_{max}) 3 - 9 times lower than that of hydrogenotrophic methanogens (Van Lier et al., 2020). Considering the high acetate concentrations in the influent and in R1, *Methanosaeta* would be growing at its maximum rate, despite the fact that the SRT in each reactor is too low to maintain them. Therefore, the high relative abundance of *Methanosaeta* might be related to low digestate recirculation from R3 to R1. The applied recirculation continuously inoculated R1 and simultaneously supplied key micro-nutrients that are liberated during the sludge degradation process (Guo et al., 2023, chapter 3, submitted). The obtained results were possibly also affected by the design of the full-scale CAD system: the equalization holes in the partitioning walls could have led to additional biomass exchange between R1-R3. Furthermore, the pie-shaped reactors R1-R3 were possibly characterized by inefficient mixing and poorly mixed zones, affecting the actual SRT in the reactors (Angelidaki et al., 2005). Though it is not fully clear how *Methanosaeta* could become dominant in the first compartment of the full-scale CAD system, sludge degradation remained at a high level. This was also the case when applying a high solid loading rate and short SRT. Future research should focus on the mixing patterns in the different compartments, while having provisions for measuring methane production in each separate compartment, to further characterize the different stages of a full-scale CAD.

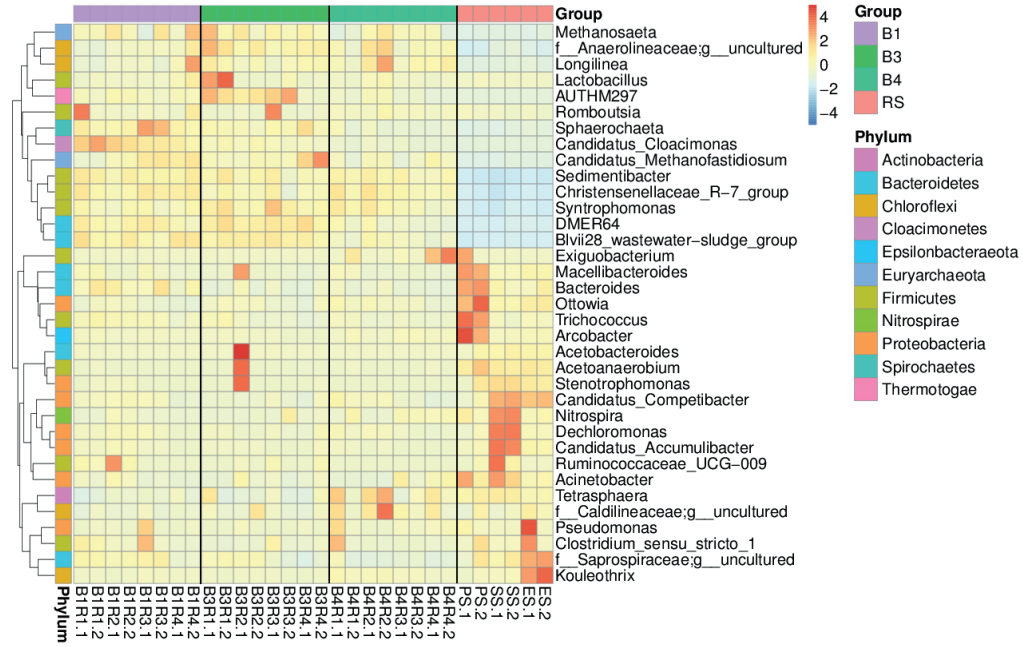

Figure 4.6 Normalized relative abundance of taxa related to the dominated microbes of interest (top 35 species that presented in both feeding and reactors) at the genus level

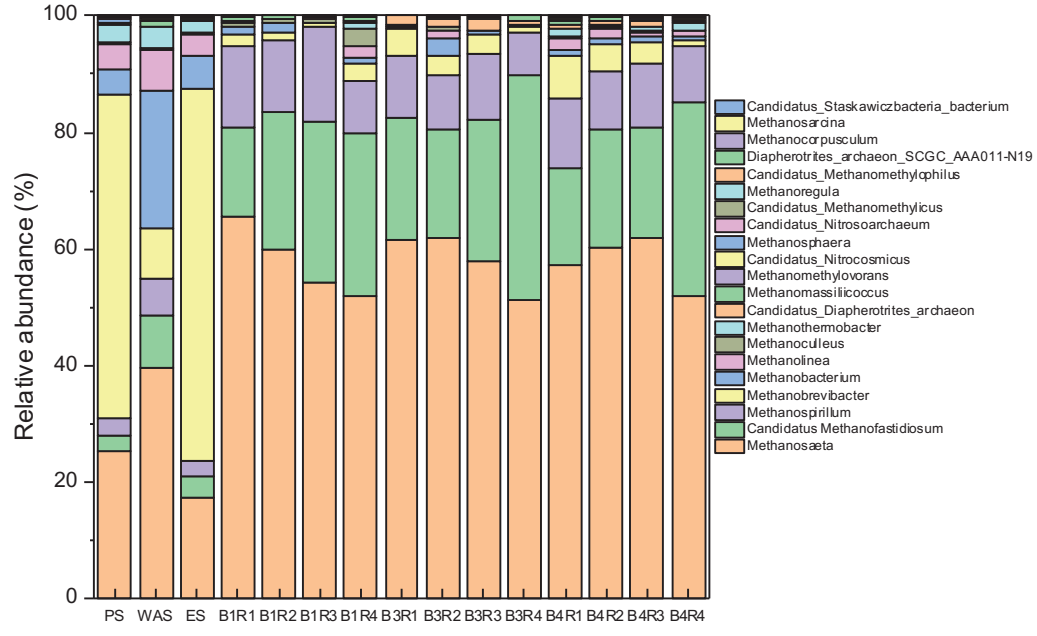

Figure 4.7 Species taxonomy of methanogenic communities at the genus level

4.4 Conclusion

A full-scale CAD system treating a mixture of WAS and PS was built in WWTP Tollebeek, the Netherlands. One newly build CSTR was divided into three small pie-shaped CSTR compartments operated in series at low SRT, with a low recycle flow between R3 and R1. These were followed by a large existing CSTR in series (R4). During long-term operation, the feed consisted of PS, WAS and ES in average ratios of 40-45%:30-35%:25-30% with highly fluctuating loading rates. Nevertheless, results showed a stable sludge reduction efficiency of approximately 56%, and an enhanced enzymatic activity of protease and cellulase in the first compartments of the CAD system. Microbial population analysis revealed a dominance of fermentative bacteria in the first 3 compartments, and a high abundance of *Methanosaeta* in all reactors. The expected distinct separation of microbial population and related conversion processes, such as has been observed during laboratory experiments, was less pronounced in the full-scale CAD system.

References

Agabo-Garcia, C., Perez, M., Rodriguez-Morgado, B., Parrado, J., Solera, R. 2019. Biomethane production improvement by enzymatic pre-treatments and enhancers of sewage sludge anaerobic digestion. Fuel, 255.

Angelidaki, I., Boe, K., Ellegaard, L. 2005. Effect of operating conditions and reactor configuration on efficiency of full-scale biogas plants. Water Sci Technol, 52(1-2), 189-94.

Baldi, F., Pecorini, I., Lannelli, R. 2019. Comparison of single-stage and two-stage anaerobic co-digestion of food waste and activated sludge for hydrogen and methane production. Renewable Energy, 143, 1755-1765.

Cao, Y.C., Pawlowski, A. 2012. Sewage sludge-to-energy approaches based on anaerobic digestion and pyrolysis: Brief overview and energy efficiency assessment. Renewable & Sustainable Energy Reviews, 16(3), 1657-1665.

De Sotto, R., Bae, S. 2020. Nutrient removal performance and microbiome of an energy-efficient reciprocation MLE-MBR operated under hypoxic conditions. Water Res, 182, 115991.

Gonzalez, A., Hendriks, A., van Lier, J.B., de Kreuk, M. 2018. Pre-treatments to enhance the biodegradability of waste activated sludge: Elucidating the rate limiting step. Biotechnol Adv, 36(5), 1434-1469.

Guo, H., Oosterkamp, M.J., Tonin, F., Hendriks, A., Nair, R., van Lier, J.B., de Kreuk, M. 2021. Reconsidering hydrolysis kinetics for anaerobic digestion of waste activated sludge applying cascade reactors with ultra-short residence times. Water Res, 202, 117398.

Guo, H., van Lier, J.B., de Kreuk, M.J.W.r. 2020. Digestibility of waste aerobic granular sludge from a full-scale municipal wastewater treatment system. Water Research, 173, 115617.

Jiang, J., Wang, Y., Yu, D., Yao, X., Han, J., Cheng, R., Cui, H., Yan, G., Zhang, X., Zhu, G. 2021. Garbage enzymes effectively regulated the succession of enzymatic activities and the bacterial community during sewage sludge composting. Bioresour Technol, 327, 124792.

Lee, J., Kim, E., Han, G., Tongco, J.V., Shin, S.G., Hwang, S. 2018. Microbial communities underpinning mesophilic anaerobic digesters treating food wastewater or sewage sludge: A full-scale study. Bioresour Technol, 259, 388-397.

Luo, K., Xie, X., Yang, Q., Chen, F., Zhong, Y., Xie, P., Wang, G. 2020. Multi-hydrolytic enzyme accumulation and microbial community structure of anaerobic co-digestion of food waste and waste-activated sludge. Environmental Technology, 41(4), 478-487.

Mei, R., Narihiro, T., Nobu, M.K., Kuroda, K., Liu, W.T. 2016. Evaluating digestion efficiency in full-scale anaerobic digesters by identifying active microbial populations through the lens of microbial activity. Sci Rep, 6, 34090.

Nobu, M.K., Narihiro, T., Kuroda, K., Mei, R., Liu, W.T. 2016. Chasing the elusive Euryarchaeota class WSA2: genomes reveal a uniquely fastidious methyl-reducing methanogen. ISME J, 10(10), 2478-87.

Ozgun, H. 2019. Anaerobic Digestion Model No. 1 (ADM1) for mathematical modeling of full-scale sludge digester performance in a municipal wastewater treatment plant. Biodegradation, 30(1), 27-36.

Raheem, A., Sikarwar, V.S., He, J., Dastyar, W., Dionysiou, D.D., Wang, W., Zhao, M. 2018. Opportunities and challenges in sustainable treatment and resource reuse of sewage sludge: A review. Chemical Engineering Journal, 337, 616-641.

Rubio-Rincon, F., Lopez-Vazquez, C., Welles, L., van Loosdrecht, M., Brdjanovic, D. 2017. Cooperation between Candidatus Competibacter and Candidatus Accumulibacter clade I, in denitrification and phosphate removal processes. Water research, 120, 156-164.

Shakeri Yekta, S., Liu, T., Mendes Anacleto, T., Axelsson Bjerg, M., Safaric, L., Goux, X., Karlsson, A., Bjorn, A., Schnurer, A. 2021. Effluent solids recirculation to municipal sludge digesters enhances long-chain fatty acids degradation capacity. Biotechnol Biofuels, 14(1), 56.

Shimada, T., Morgenroth, E., Tandukar, M., Pavlostathis, S.G., Smith, A., Raskin, L., Kilian, R.E. 2011. Syntrophic acetate oxidation in two-phase (acid-methane) anaerobic digesters. Water Science and Technology, 64(9), 1812-1820.

Van Lier, J.B., Mahmoud, N., Zeeman, G. 2020. Anaerobic Wastewater Treatment Biological Wastewater Treatment: Principles, Modelling and Design, Second Edition, Chapter 16, IWA Publishing, London, UK, 701-756.

Wang, G.P., Dai, X.H., Zhang, D., He, Q.B.A., Dong, B., Li, N., Ye, N. 2018. Two-phase high solid anaerobic digestion with dewatered sludge: Improved volatile solid degradation and specific methane generation by temperature and pH regulation. Bioresource Technology, 259, 253-258.

Xu, X.J., Wang, W.Q., Chen, C., Xie, P., Liu, W.Z., Zhou, X., Wang, X.T., Yuan, Y., Wang, A.J., Lee, D.J., Yuan, Y.X., Ren, N.Q. 2020. Bioelectrochemical system for the enhancement of methane production by anaerobic digestion of alkaline pretreated sludge. Bioresour Technol, 304, 123000.

Zhang, D., Feng, Y., Huang, H., Khunjar, W., Wang, Z.W. 2020. Recalcitrant dissolved organic nitrogen formation in thermal hydrolysis pretreatment of municipal sludge. Environ Int, 138, 105629.

Zhang, P., Shen, Y., Guo, J.S., Li, C., Wang, H., Chen, Y.P., Yan, P., Yang, J.X., Fang, F. 2015. Extracellular protein analysis of activated sludge and their functions in wastewater treatment plant by shotgun proteomics. Sci Rep, 5, 12041.

Zhang, T.T., Wang, Q.L., Ye, L., Yuan, Z.G. 2016. Effect of free nitrous acid pre-treatment on primary sludge biodegradability and its implications. Chemical Engineering Journal, 290, 31-36.

Zhen, G.Y., Lu, X.Q., Kato, H., Zhao, Y.C., Li, Y.Y. 2017. Overview of pretreatment strategies for enhancing sewage sludge disintegration and subsequent anaerobic digestion: Current advances, full-scale application and future perspectives. Renewable & Sustainable Energy Reviews, 69, 559-577.

Chapter 5

DIGESTIBILITY OF WASTE AEROBIC GRANULAR SLUDGE FROM A FULL-SCALE MUNICIPAL WASTEWATER TREATMENT SYSTEM

This chapter is based on:
Guo, H., van Lier, J. B., & de Kreuk, M. (2020). Digestibility of waste aerobic granular sludge from a full-scale municipal wastewater treatment system. Water research, 173, 115617.

Abstract

Full-scale aerobic granular sludge technology under the trade name Nereda® has been mainly implemented for municipal wastewater treatment. Owing to the operational reactor procedures, two types of waste aerobic granular sludge can be clearly distinguished: 1) aerobic granular sludge selection discharge (AGS-SD) and 2) aerobic granular sludge mixture (AGS-RTC). This study systematically compared the anaerobic biodegradability of AGS-SD and AGS-RTC under mesophilic conditions. Results were further compared with the anaerobic conversion of waste activated sludge (WAS) as well as primary sludge (PS) from full-scale municipal wastewater treatment plants. Analysis showed similar chemical characteristics for AGS-SD and PS, which were both characterized by a high carbohydrate content (429 ± 21 and 464 ± 15 mg glucose/g VS sludge, respectively), mainly cellulosic fibres. Concurrently, AGS-RTC exhibited chemical properties close to WAS, both characterized by a relatively high protein content, which were individually 498 ± 14 and 389 ± 15 mg/g VS sludge. AGS-SD was characterized by a high biochemical methane potential (BMP) (296 ± 15 mL CH_4/g VS substrate), which was similar to that of PS, and remarkably higher than that of AGS-RTC and WAS. Strikingly, the BMP of AGS-RTC (194 ± 10 mL CH_4/g VS substrate) was significantly lower than that of WAS (232 ± 11 mL CH_4/g VS substrate). Mechanically destroying the compact structure of AGS-RTC only accelerated the methane production rate but did not significantly affect the BMP value. Results indicated that compared to WAS, the proteins and carbohydrates in AGS-RTC were both more resistant to anaerobic bio-degradation, which might be related to the presence of refractory microbial metabolic products in AGS-RTC.

5.1 Introduction

Conventional activated sludge wastewater treatment systems (CAS) have been widely applied in the treatment of many types of wastewater for decades. However, large quantities of waste sludge, i.e. primary (PS) and waste activated sludge (WAS), are being produced during this process, which is regarded problematic owing to its environmental risk and high cost for treatment and disposal (Appels et al., 2008). A relatively new biological treatment for wastewater is the aerobic granular sludge (AGS) or Nereda® technology which is applied at full scale since 2005 (Giesen et al., 2013). Currently, there are over than 70 Nereda® wastewater treatment plants in operation or under construction worldwide (https://www.royalhaskoningdhv.com/nereda). It's main advantages, i.e. a smaller process footprint, quicker sludge settling and reduced energy demand, resulted in a rapid market acceptance from promising innovation to a mature technology, capable of competing with established conventional wastewater treatment technologies (de Kreuk et al., 2007, Pronk et al., 2015). The biomass yield, represented by the mass of sludge produced over the mass of organic matter (COD or BOD) consumed, appears to be similar for aerobic granules and activated sludge given the same conditions (Nancharaiah and Reddy, 2018). As granular sludge processes are typically operated at relatively long solid retention times, the sludge production of this process will typically be relatively lower than that of CAS in this sense. However, the waste sludge of AGS installationsis not yet separately processed. With the increasing number and size of Nereda® installations, strategies for the efficient management of generated waste sludge from AGS systems (WAGS) are required.

Anaerobic digestion (AD) has been commonly used in the treatment of PS and WAS with the purpose of organics reduction and energy recovery in the form of biogas. Similarly, AD is a potential option for WAGS treatment. However, to our best knowledge, the anaerobic digestion of WAGS has been limitedly studied (Bengtsson et al., 2018). The anaerobic biodegradability of WAGS with large granules (larger than 1.6 mm) has been investigated in batch and continuous AD systems (Bernat et al., 2017, del Rio et al., 2011, del Rio et al., 2014, Palmeiro-Sanchez et al., 2013). Most studies merely reported the biochemical methane potential (BMP) in mL CH_4 per g VS substrate of WAGS, but lack information on hydrolysis rate coefficients or degradation efficiencies of its key organic fractions. Therefore, a direct comparison of the biodegradation kinetics of WAGS with the better understood WAS degradation is not yet possible. Furthermore, the BMP results of WAGS are often inconsistent between studies, which can be attributed to the highly biodegradable, often synthetic or industrial, influent used to grow these granules in a well-controlled laboratory or pilot scale system. The operational conditions of AGS systems and its

feeding characteristics significantly influence the physiochemical and morphological properties of WAGS, and thus may affect their degradation behaviour in AD (Bernat et al., 2017, de Kreuk et al., 2010).

So far, the granular sludge based Nereda® technology has been mainly applied in municipal wastewater treatment (https://www.royalhaskoningdhv.com/nereda). Municipal wastewater typically has a much lower chemical oxygen demand (COD) concentration than industrial wastewater and has more complex substrates and a higher suspended solids concentration than synthetic influent used in laboratory experiments (Moy et al., 2002). Therefore, there is a great interest about the actual anaerobic biodegradability of the WAGS produced in full scale AGS systems treating municipal sewage. Two types of WAGS can be distinguished: (1) sludge that is removed every cycle, which we call the aerobic granular sludge selection discharge, or selection spill (AGS-SD). This is the more flocculent sludge with a lower settling velocity than the aerobic granules. By removing this sludge, a biological selection pressure is applied towards faster settling granules. Because it is removed every cycle, this waste aerobic granular sludge has had a lower retention time than the granules (Ali et al., 2019); (2) The excess granular sludge that originates from biomass growth and that is removed to avoid too high biomass concentrations in the reactor, the so called solid retention time control of the AGS. We refer to this fraction as waste aerobic granular sludge (AGS-RTC).

Therefore, this study systematically assessed (1) the characteristics and anaerobic biodegradability of AGS-SD and AGS-RTC as well as (2) the differences in physicochemical property and biodegradability of these fractions with PS and WAS. BMP tests were conducted under mesophilic conditions to compare solids reduction, methane yield, hydrolysis rate coefficient, as well as the biodegradability of carbohydrates, proteins, lipids and lignocelluloses in all types of sludge. These results lead to an improved understanding of the biodegradation of WAGS in AD and are helpful to design and effectively operate AD systems for WAGS treatment at full-scale implementations.

5.2 Materials and methods

5.2.1 Substrates and inoculum

AGS-SD and AGS-RTC were collected from a full-scale municipal wastewater-fed Nereda® system (Garmerwolde, The Netherlands), which has a treatment capacity of 91,583 population equivalents (p.e.). At the time when both types of sludge were sampled, the Nereda® reactor was operated with a process cycles of approximately

6 hours; 4 hours of aeration, 1 hour of settling, 1 hour of anaerobic feeding/ simultaneous effluent withdrawal, and 15 min of excess sludge discharge. The excess sludge was stored in a sludge buffer tank before being transported to the on-site sludge treatment facilities. AGS-RTC was withdrawn at the end of the aeration phase under fully mixed conditions, whereas AGS-SD was collected from the sludge buffer tank. Wastewater treatment plant (WWTP) Garmerwolde has 6 mm screens, followed by grit removal, where after the influent is stored for 3.4 hours in a mixed influent buffer. There is no primary settler (Pronk et al., 2015) and the influent from the buffer tank is directly fed to the Nereda® tanks. WAS and anaerobic inoculum were sampled from an enhanced biological phosphate removal (EBPR) activated sludge tank under fully aerated and mixed conditions and an anaerobic sludge digester at WWTP Harnaschpolder (Den Hoorn, The Netherlands), respectively. The latter WWTP is designed for a 1.3 million p.e., and is equipped with 6 mm screens, sand and grit removal, followed by a primary clarifier. Primary sludge (PS) was sampled from this primary clarifier. The inoculum characteristics were pH 8.1 ± 0.4, total solids (TS) 3.3 ± 0.09 wt % and volatile solids (VS) 2.32 ± 0.03 wt %. All types of sludge were stored at 4 °C for a maximum of 24 hours to prevent acidification. Cellulose (microcrystalline powder, Sigma Aldrich, USA) was used as model substrate for the positive control of the BMP tests. Wastewater characteristics and operational parameters of both WWTPs are shown in Table 5.1.

Batch BMP tests of sludge were conducted in quadruplicates by using an automated methane potential test system (AMPTS) (Bioprocess Control, Sweden) with 500 mL serum bottles. One of the serum bottles was sacrificed for VFA concentration measurements. The recipes and dosages for phosphorus buffer solution, macronutrients, and trace elements were according to Zhang et al. (2014). The volume of the mixture of inoculum and substrate was 300 mL. The ratio of VS (g) of inoculum to VS (g) of substrate was 2 in the batch bottles. VS concentrations of different types of sludge were manipulated by centrifugation (5 min at 3,500 × g). In order to explain whether the morphology of the sludge affect the biodegradability, the structures of AGS and WAS were destroyed by crushing the sludge with a household blender (HR2052/90, Philips, the Netherlands) for 5 min at 10,000 RPM and 450 W.

Table 5.1 Averaged influent characteristics and operational parameters of aerobic granular sludge plant and conventional activated sludge plant in Garmerwolde and Den Hoorn, The Netherlands, respectively

Parameter	Nereda® plant Garmerwolde [a]			Process parameter		AGS plant	Activated sludge plant Harnaschpolder [b]			
Unit	Influent mg/L	Effluent mg/L	Load kg/kg TSS/d		Unit		Influent mg/L	Effluent mg/L	Load kg/kg TSS/d	
TSS	247	8.9	0.09	Hydraulic retention time	d	0.7	279	2.4	0.07	2.5
BOD_5	232	9.3	0.08	Solids retention time	d	28[c]	275	3.5	0.07	24
COD	528	57	0.20	MLSS	g/L	8	599	35	0.16	3.5
TN	53	7.4	0.02	Volumetric load	$m^3/m^3/d$	1.5	58	2.8	0.02	0.4
TP	7.2	0.7	0.003	Sludge production	kg/kg $COD_{influent}$	0.23	7.7	0.6	0.002	0.25

[a] The data was obtained from WWTP Garmerwolde, The Netherlands.
[b] The data was obtained from WWTP Harnaschpolder, The Netherlands.
[c] This is an average solids retention time (SRT). The WAGS fraction can have SRT as low as 4 days, whilst the largest granules can be maintained over 150 days due to their settling capabilities (Ali *et al.*, 2019).

5.2.2 Biochemical methane potential tests modelling

The hydrolysis rate coefficient (k) and biochemical methane potential (B_0), two key parameters associated with methane production from the sludge (Gonzalez et al., 2018), were used to evaluate and compare methane production kinetics and BMP values between different types of sludge. To analyse the data, a two-substrate model, consisting of a rapidly biodegradable substrate and slowly biodegradable substrate, developed by Rao et al., (2000) was used:

$$B_t = B_{0,rapid}\left(1 - e^{-k_{rapid}t}\right) + B_{0,slow}\left(1 - e^{-k_{slow}t}\right) \quad \text{[Eq. 5.1]}$$

where $B_{0,rapid}$ = biochemical methane potential of the rapidly biodegradable substrates (mL CH_4/g VS substrate); k_{rapid} = hydrolysis rate coefficient of the rapidly biodegradable substrates (1/d); $B_{0,slow}$ = biochemical methane potential of the slowly biodegradable substrates (mL CH_4/g VS substrate); k_{slow} = hydrolysis rate coefficient of the slowly biodegradable substrates (1/d).

The simulation of accumulated methane production by the two-substrate model was implemented in MATLAB R2016b (MathWorks, USA).

5.2.3 Analytical methods

Total carbohydrate contents were estimated as a glucose-equivalent concentration using a phenol-sulfuric acid assay (Dubois et al., 1956). Total protein concentrations were determined by the Kjeldahl method (APHA, 2005) based on N_{kj} and NH_4^+–N measurements, assuming that 1 g protein (assumed as $C_4H_{6.1}O_{1.2}N_x$) is equivalent to 1 g amino acids, 0.16 g N_{kj} and 0.16 g NH_4^+–N. Total lipids were measured by chloroform-methanol extraction method (Bligh and Dyer, 1959). Volatile fatty acids (VFAs) were analysed by a gas chromatography (GC) with a flame ionization detector (FID) (Agilent 7890A, USA). The GC was equipped with an Agilent 19091F-112 column of 25 m × 320 µm × 0.5 µm and Helium was used as carrier gas with a flow rate of 1.8 mL/min. Injection temperature was 240 °C and oven temperature was 80 °C. The lignocellulosic fibres content in sludge samples was determined by Van Soest method (Van Soest, 1963). The particle size distribution (PSD) of AGS-RTC was analysed by a sieving method (Pronk et al., 2015), whereas the PSD of the other sludge types (including the crushed sludge) were measured with a particle size analyser (Bluewave, Microtrac, Germany). A digital microscope (VHX-6000, Keyence, Belgium) with a universal zoom lens from 20× to 200× (VH-Z20UR, Keyence, Belgium) was used to identify the morphology of the sludge. Principal component analysis (PCA) for investigating the difference in digestibility between sludges was performed by MATLAB R2016b (MathWorks, USA). For the statistical analysis, the student's t-test

(for two groups of samples) and one-way ANOVA (for multiple groups of samples) were both applied with SPSS Statistics 25 (IBM, USA) to evaluate the significance of differences in BMPs and chemical characteristics between sludges. The significance level of probability (p-value) was 0.05 in this study.

5.3 Results and discussion

5.3.1 Sludge characteristics

Particle size distribution of each type of sludge was measured to identify the physical difference between the types of sludge (Figure 5.1). It is found that the AGS-RTC sample was dominated by particle sizes larger than 500 µm, i.e. > 90% of the total particles, which was clearly different from the other sludge samples. On the contrary, AGS-SD was composed of particle sizes below 500 µm, and therefore showed great similarity with the particle size of WAS. This observed difference in morphology agrees with the results observed by Pronk et al. (2015). In addition, a small fraction of particles in the 500-2000 um range was observed in PS, likely resulting from settling in the primary sedimentation tank.

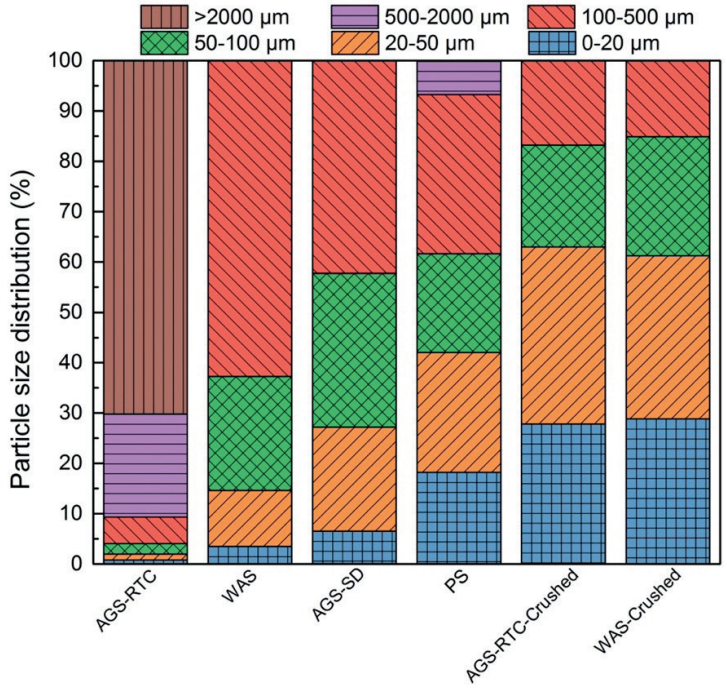

Figure 5.1 Particle size distribution of sludge

The distribution of biochemical components of each sludge sample is presented in Table 5.2. The VS concentrations of all sludge types were adjusted to about 5% by centrifugation, in order to minimize the effect of different substrate concentrations (in VS) on their methane potential (Wang et al., 2015). The used VS concentration is similar to the 3-6 wt % range that is usually fed to full-scale digesters (WWTP Harnaschpolder, The Netherlands). However, the original VS concentration of sludge extracted from the different flows were different, namely 0.9 ± 0.02, 0.4 ± 0.01, 0.6 ± 0.01 and 3.3 ± 0.03 wt % for AGS-RTC, AGS-SD, WAS and PS, respectively.

Table 5.2 Characteristics of different types of sludge

Parameters	Unit	AGS-RTC	AGS-SD	WAS	PS
Total COD	g/L	71.3 ± 0.4	79.1 ± 0.1	72.4 ± 0.2	77.8 ± 0.3
TS	wt %, g/100 g sludge	6.1 ± 0.2	6.6 ± 0.1	6.2 ± 0.1	6.4 ± 0.1
VS	wt %, g/100 g sludge	4.9 ± 0.1	5.1 ± 0.1	5.0 ± 0	5.0 ± 0.1
Carbohydrates	mg glucose/g VS	217 ± 11	429 ± 21	190 ± 10	464 ± 15
Proteins	mg/g VS	498 ± 14	301± 16	389 ± 15	248 ± 10
Protein/carbohydrates	(-)	2.3	0.7	2.0	0.5
Lipids	mg/g VS	37 ± 8	60 ± 5	35 ± 7	73 ± 6
VFAs	mg/g VS	4.6 ± 0.6	9.7 ± 1.0	5.6 ± 0.5	8.6 ± 0.2

Key organic fractions analysed were protein, carbohydrates, lipids and VFAs, since they are considered as the most pertinent indicators in assessing and predicting the anaerobic biodegradability of sewage sludge mixtures (del Rio et al., 2011, Mottet et al., 2010). Results showed that proteins and carbohydrates predominated in all types of sludge, representing in total 58%-73% of the organic matter (Table 5.2), which are within the typical range reported for sewage sludge (del Rio et al., 2011, Gonzalez et al., 2018). However, the ratio of proteins and carbohydrates differed. Both AGS-SD and PS showed a much lower protein/carbohydrates ratio than AGS-RTC and WAS. AGS-SD contained a similar carbohydrate content as PS, which was almost double the carbohydrate content in AGS-RTC and WAS. The protein content in AGS-SD was slightly higher than that in PS, but still about 30% lower than that in AGS-RTC and WAS. A large protein fraction in both AGS-RTC and WAS was expected, since these sludges are mainly composed of cells, (exo-) enzymes and microbial metabolic products (Adav et al., 2008, Gonzalez et al., 2018). Different studies also reported that the proteins/carbohydrates ratio of the extracellular polymeric structures for AGS was usually higher than that for activated sludge (AS) (McSwain et al., 2005, Zhu et al., 2015), which is in line with our findings (Table 5.2). The high content of carbohydrates and the deviating proteins/carbohydrates ratio of AGS-SD

indicates that this sludge fraction is considerably different from the AGS-RTC with big granules. It is known that, in contrast to AS, PS is rich in fibres and contains much less microbial related organics, resulting in the high carbohydrates' fraction in this type of sludge (Bernat et al., 2017). The high abundance of fibres in AGS-SD has been observed before (Pronk et al., 2015) and agrees with the analyses performed in this study (Figure 5.2 c and d).

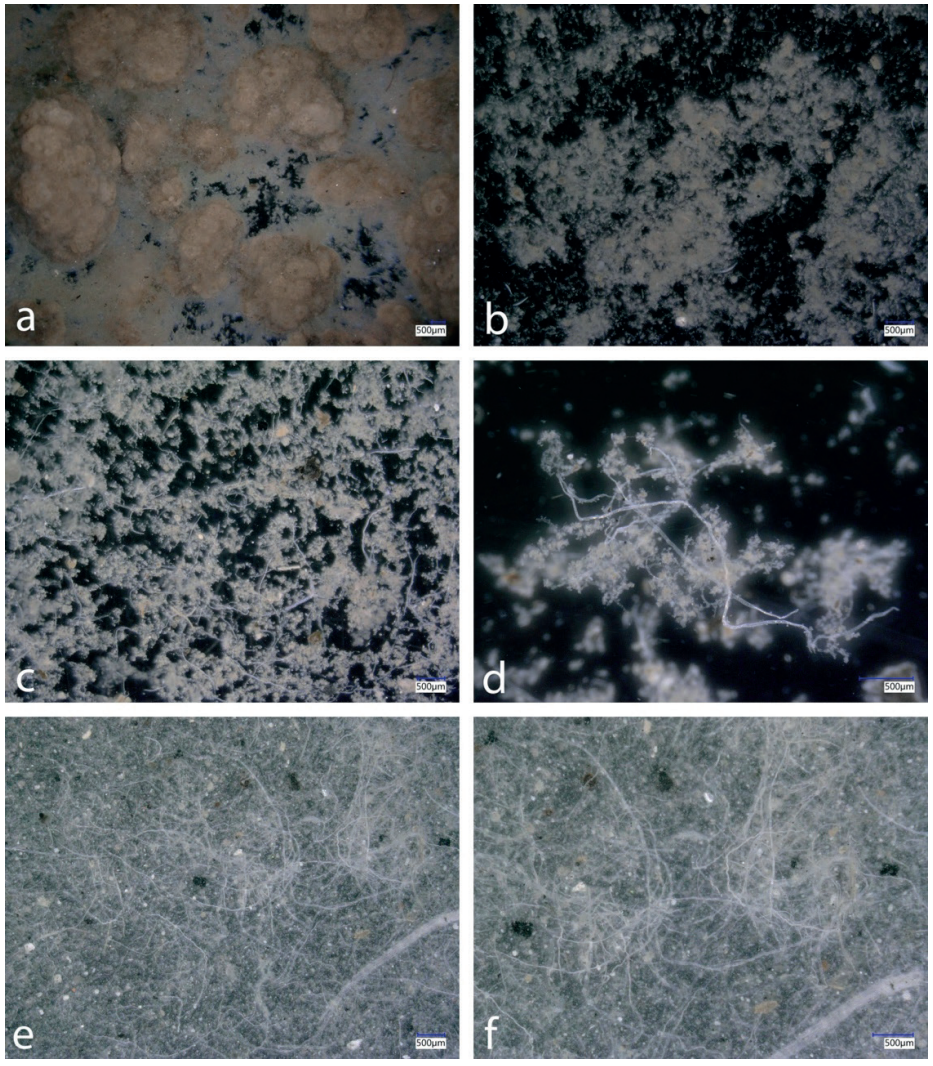

Figure 5.2 Morphology of different types of sludge: (a) AGS mixture obtained from the Nereda® reactor (AGS-RTC), (b) waste activated sludge sampled from the EBPR activated sludge tank, (c and d) AGS-SD fraction gathered from the buffer tank connected to the Nereda® reactor and (e and f) PS collected from the primary clarifier

To verify the fibrous content and composition, cellulose, hemicellulose, and lignin contents in all sludge samples were determined (Figure 5.3). The used Van Soest method was originally developed for the assessment of fibre-rich materials of plant origin. Therefore, when the Van Soest method is applied for sewage sludge characterization, the resulting fractions are commonly referred to as "like-" fractions (Mottet et al., 2010, Wu et al., 2015). Figure 5.3 shows that the content of lignin-like and hemicellulose-like fractions was approximately 9% and 15% of the VS on average, respectively, similar for all sludge samples. The concentration of the cellulose-like fibres in AGS-SD and PS was similar, i.e. 15% and 18% of the total VS on average, respectively. This was almost twice the value in AGS-RTC and WAS, which was 7% and 9% of the total VS on average, respectively. The result was supported by the microscopic examinations presented in Figure 5.2, confirming that this organic fraction is one of major components of carbohydrates in AGS-SD.

It needs to be mentioned that the sum of hemicellulose and cellulose in the WAS and AGS-RTC fractions was larger than the total carbohydrates measured (Figure 5.3 and Table 5.2), even though these two fractions are part of the total carbohydrate fraction. This could be caused by the interference of sludge components and the detergents used in the Van Soest method. For example, divalent cations from the sludge matrix could form complexes with the ethylenediaminetetraacetic acid (EDTA) used in the hemicellulose extraction step, resulting in an overestimation of the hemicellulose content. Mottet et al. (2010) indicated that the colorimetric method for direct carbohydrates determination, showed a higher reliability than the Van Soest fractionation. Therefore, the fibre fractionation in this study should only be used as an indicator of the differences between the sludge types, rather than a measure of the actual carbohydrate concentration.

Cellulose embodies between 30-50% of the suspended solids in the wastewater of western countries (STOWA, 2010). In conventional sewage treatment, cellulose is partly removed in the primary clarifier, being included in the PS (Champagne and Li, 2009), as is shown in this study as well. Cellulose entering the activated sludge tanks will be (partly) degraded (Ahmed et al., 2019). The Nereda® plant at Garmerwolde receives raw sewage without primary clarification. It is hypothesized that the large suspended solids, like the observed fibres, are not likely to interact with the fully developed compact granules and thus will stay part of the more flocculent fraction that is often observed with the AGS matrix (Pronk et al., 2015).As a result, sludge stratification takes place during settling phase. Together with the selection pressure applied in granular sludge systems to retain large granules, the non-granules fraction, including the mentioned cellulose fibers, can be washed out during the sludge selection discharge.

5.3.2 Methane production and degradation kinetics of sludges in BMP tests

The different biomass composition, as well as the different degree of stabilization, will likely lead to a different extent and rate of anaerobic digestion. This assumption was verified in a BMP test of which the results are presented in Figure 5.4. The BMP of the positive control was 357 mL CH_4/g VS on average, which fulfilled the criteria stated by Holliger et al. (2016). Low amounts of total VFAs were detected during the first 6 days of digestion of the four sludge samples, with a maximum concentration of 332, 355, 421 and 402 mg/L at day 3, for AGS-RTC, WAS, AGS-SD and PS, respectively.

The inoculum applied for all batch tests was obtained from the full-scale digester at Harnaschpolder WWTP, treating WAS and PS and was not specifically adapted to the WAGS fractions. del Rio et al. (2014) showed that after long-term acclimation with AGS as sole substrate, the main microbial populations present were still those commonly found in digesters treating waste municipal sewage sludge. Therefore, the inoculum used was considered similarly effective for all sludge samples tested.

Results clearly show the lowest BMP value for AGS-RTC, namely 194 mL CH_4/g VS substrate. This was significantly lower (p-value = 0.01) than the 243 mL CH_4/g VS substrate reported for AGS grown in a pilot scale reactor, fed with synthetic domestic wastewater (del Rio et al., 2011). It should be noted that the organic loading rate to the Nereda® in Garmerwolde was higher than that of the activated sludge plant, i.e. 0.20 and 0.16 g COD g/TSS/d, respectively, and the COD content of the AGS-RTC was somewhat higher than that of the WAS (Table 5.2). Nonetheless, the BMP value of AGS-RTC was remarkably lower (p-value = 0.02) than that of WAS. Our results agree with those of Bernat et al. (2017) and suggest an inherently lower anaerobic biodegradability of the aerobic granules compared to activated sludge flocs.

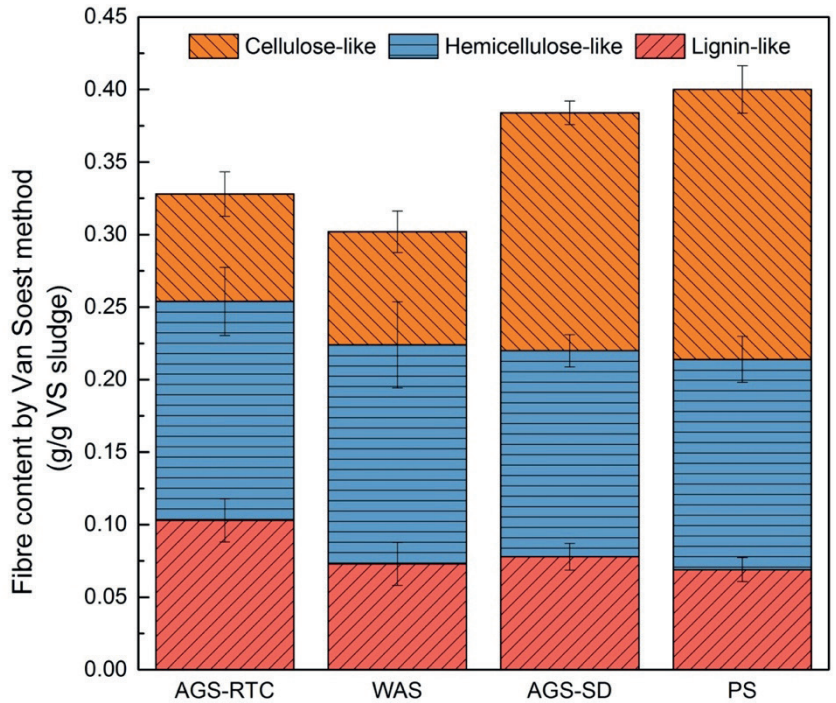

Figure 5.3 Fractionation of sludge volatile solids by Van Soest method

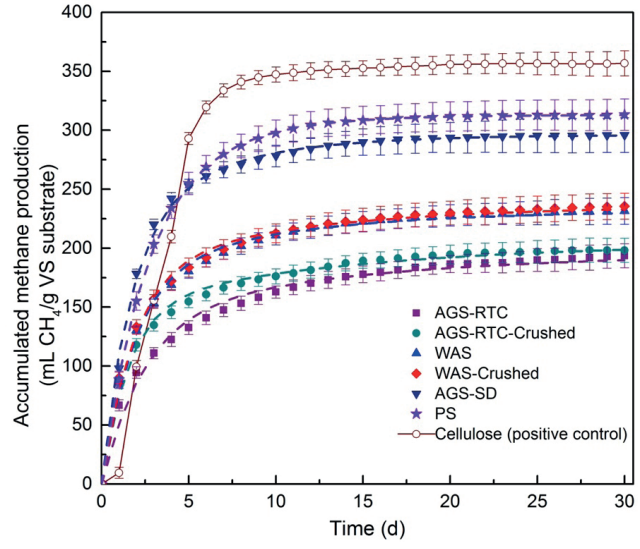

Figure 5.4 Measured and simulated methane production in the BMP tests (symbols represent experimental measurements and dotted lines represent model fit using two-substrate model)

Table 5.3 Estimated k_{rapid}, $B_{0, rapid}$, k_{slow}, $B_{0, slow}$ and $B_{0, total}$ of different types of sludge using Two-Substrate Model

Parameters	Unit	AGS-RTC	AGS-RTC-Crushed	WAS	WAS-Crushed	AGS-SD	PS
k_{rapid}	1/d	0.41 ± 0.02	0.51 ± 0.01	0.54 ± 0.01	0.54± 0.02	0.61 ± 0.01	0.56 ± 0.02
$B_{0, rapid}$	mL CH_4/g VS substrate	140 ± 6	152 ± 5	175 ± 6	179 ± 8	215 ± 4	208 ± 8
k_{slow}	1/d	0.07 ± 0.02	0.07 ± 0.01	0.11 ± 0.01	0.11± 0.01	0.17 ± 0.02	0.19 ± 0.02
$B_{0, slow}$	mL CH_4/g VS substrate	54 ± 6	46 ± 4	57 ± 5	56 ± 3	81± 8	105 ± 9
$B_{0, total}$	mL CH_4/g VS substrate	194 ± 10	198 ± 10	232 ± 11	235 ± 13	296 ± 15	313 ± 11

The methane production curves (Figure 5.4) could be well fitted with the two-substrate model (Eq. 5.1, Figure 5.4 - dotted line, $R^2 > 0.99$ in all studied cases). Results suggest that all biomass samples consisted of a specific fraction that was rapidly biodegradable and one that was more slowly biodegradable. The estimated values of k_{rapid}, $B_{0, rapid}$, and k_{slow}, $B_{0, slow}$ for all types of sludge are shown in Table 5.3 and demonstrate that AGS-RTC presented a significantly lower k_{rapid} (p-value = 0.002) and k_{slow} (p-value = 0.04) than WAS. This calculation was based on the methane production rate, whereas the VFA production was excluded. Since VFA was detected in the first 6 days, the k-values do not fully represent the hydrolysis rates. However, compared to WAS, the assessed VFA values in AGS-RTC were lower as well, so it can be concluded that the AGS-RTC's hydrolysis rate was lower than that of WAS. The AGS-RTC used in this study mainly consisted of large granules (Figure 5.1 and 2), which limits the surface area to volume ratio. Since the hydrolysis rate is surface proportional (Angelidaki and Sanders, 2004, Sanders et al., 2000), the overall AGS-RTC digestibility might be determined by the morphological structure of the granules.

To clarify the influence of morphology over sludge composition on anaerobic digestion, AGS-RTC and WAS were both mechanically crushed to destroy the physical structure and to achieve a similar particle size distribution (Figure 5.3). Results from Figure 5.4 clearly show that the shape of accumulated methane production curve of the crushed WAS was almost the same compared to the integrated ones, but the shape of the curve for AGS-RTC had a obvious change by crushing. This observation could be further evidenced by the variations in kinetics in Table 3: all parameters for WAS did not change remarkably ($p > 0.05$), reavling that the digestion of WAS was not affected by the sludge crushing; however, AGS-RTC showed a significant increase in methane production rate (p-value = 0.005) from the rapid convertible fraction (k_{rapid} and $B_{0, rapid}$). The values found after crushing of AGS-RTC even approached the values of the rapid digestible fraction of crushed WAS. Kinetics of the slowly biodegradable fraction did not statistically change, although a small shift from $B_{0, slow}$ to $B_{0, rapid}$ could

be seen (Table 3). This means that destroying the structure of the aerobic granules and increasing its surface area could indeed accelerate the degradation rate of rapidly degradable organics, which was in agreement with the observation found by del Rio et al. (2014) who applied thermal pretreatment to granules. In addition, crushing liberated a fraction of slowly degradable organics to be degraded more rapidly. It should be noted that the total BMP ($B_{0, total}$) of crushed granules was similar to that of the intact AGS-RTC (Figure 5.4 and Table 5.3), indicating that the sludge structure only limits digestion rate, but not the overall digestibility. Meanwhile, the results imply that in practical, sludge pre-treatment is recommended to apply to the AGS-RTC fraction prior to anaerobic digestion.

The BMP of AGS-SD, was just slightly lower than that of PS, and remarkably higher than those of AGS-RTC and WAS. Also, the methane production rate, i.e. both k_{rapid} and k_{slow}, of both AGS-SD and PS were distinctly higher (Table 5.3). Considering the differences in VFA production in combination with the methane production rate, it can be stated that also hydrolysis rates of the AGS-SD and PS are higher than the hydrolysis rates measured for AGS-RTC and WAS. Our present results confirm the high degree of stabilization of AGS-RTC and the low stabilization degree of the more flocculent AGS-SD fraction, supporting the speculations that reported by Pronk et al. (2015). Apparently, compared to AGS, AGS-SD is characterized by a much lower solids retention time (SRT) in the Nereda® tank (Ali et al., 2019), resulting in a much higher BMP.

It should be mentioned that in this study, the tested AGS-SD was taken from a Nereda® reactor with an operational cycle of 6 hours in total, which is a common process setting applied in full scale municipal wastewater-fed Nereda® systems (Stubbé, 2016). However, the schedule of the process cycle sometimes changes due to other factors, such as the weather condition (Pronk et al., 2015). It is worth to investigate in future studies if changes of operational parameters of the Nereda® reactor could affect the characteristics and the digestibility of the different WAGS fractions, and its overall digestibility.

5.3.3 Degradation of organic components in sludges during BMP tests

To further elucidate the differences in anaerobic biodegradation of the different sludge types, the main organic fractions in the wet sludge mixtures were analysed at the start and the end of the BMP tests (Table S5.1, Supplementary data). The converted fractions during the BMP test are shown in Figure 5.5. One should take into account that the fractions are presented per 100 g wet sludge mixture, with initial sludge mixture VS concentrations around 2.7 wt % (Table S5.1, supplementary data).

The sum of the fraction accounts for over 96% of the total measured COD reduction. Taking into account that the total COD reduction linked to the inoculum in each sludge mixture was 450 ± 60 mg COD/100 g wet sludge mixture, the observed COD reduction was indeed significantly different (p-value = 0.002) between the sludges. The result of PCA according to the degradation of major organic fractions on COD basis (Figure S5.1 in Supplementary data) shows that the first component (PC1) was related to protein, while the second component (PC2) referred to carbohydrates. These two fractions accounted for the majority of the organics that were anaerobically degraded in all four types of sludge. AGS-RTC and WAS, as well as PS and AGS-SD, respectively, were grouped closer together than the sludges sampled from the Nereda® reactor and the samples from the activated sludge installation. This indicates that the two types of waste AGS had distinctive characteristics in digestibility, which agrees with the BMP results.

Figure 5.6 presents the changes in the three fibre fractions in the different sludges during AD. More than 80% of the cellulose-like compounds was degraded, while the degradation efficiency for hemicellulose-like compounds approximated amounted only 30% in all sludge samples. This is in accordance to the degradability during AD found by Mottet et al. (2010), which were 83 % and 33%, respectively. It is reasonable to assume that the higher content of cellulose in the AGS-SD and PS was responsible for the additional methane production. Hemicellulose has a lower molecular weight than cellulose and branches with short lateral sugar chains, which are easily hydrolysable polymers (Perez et al., 2002). The low measured degradation of hemicellulose-like fraction could be due to the contaminants such as metal-EDTA complexes formed in the analysis as discussed previously.

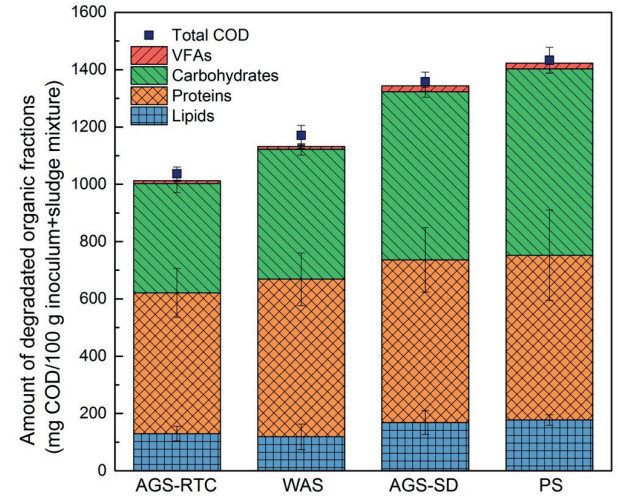

Figure 5.5 Calculated degradation of total carbohydrates, proteins, lipids and VFAs on COD basis and measured total COD reduction during the BMP tests in mg COD per 100g wet sludge mixture (I/S ratio = 2, initial VS concentration of the sludge mixture approximated 2.7 %; Table S5.1, supplementary data). The COD values used for the calculations were 1.5 g-COD/g proteins, 1.07 g-COD/g carbohydrates, 2.88 g-COD/g lipids, 1.08 g-COD/g acetate and 1.53 g-COD/g propionate (Sum of acetate and propionate represents the total VFAs in this study) (Filipe and Grady, 1998)

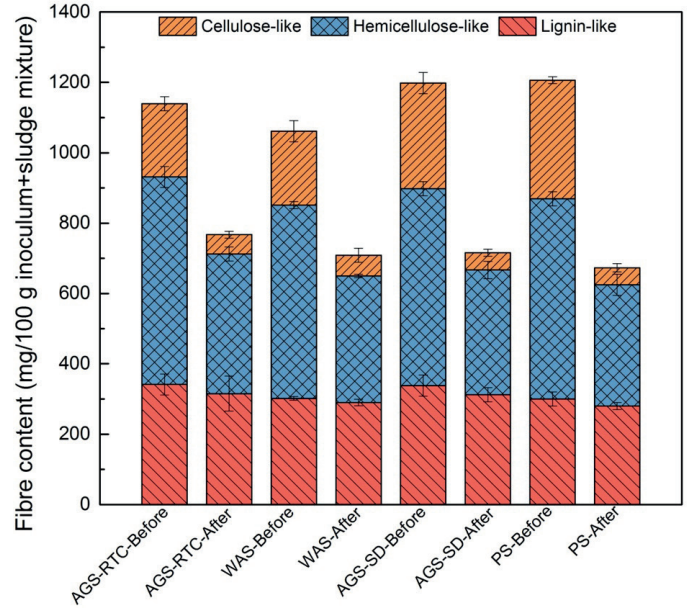

Figure 5.6 Characteristics of different fibre fractions in the wet sludge mixture (I/S ratio = 2, VS concentration of the sludge mixture approximated 2 w%; Table S5.1, supplementary data) by Van Soest method before and after BMP tests

Even though the amount of carbohydrates and proteins in AGS-RTC was higher than in WAS (Table 5.2), the methane production from WAS was larger than that of AGS-RTC per g VS (Figure 5.4). Bernat et al. (2017) hypothesized that the higher resistance-to-biodegradation lignin content could explain the observed lower BMP of AGS. However, in our case, the content of lignin fraction in AGS-RTC and WAS differed only 2%, which fall within the standard deviation (Figure 5.5). Besides, the anaerobic biodegradability of lignin in all samples were similar (Figure 5.6). The results hence suggest that the lower digestibility of aerobic granules should be ascribed to the inherent limited degradation efficiency of carbohydrates and proteins rather than the higher lignin content in AGS (Table 5.2 and Figure 5.3 and 5.6). The exact reason for the observed difference in biodegradation of carbohydrates and proteins between AGS-RTC and WAS remains unclear. An important fraction of carbohydrates and proteins in AGS-RTC and WAS originates from extra-cellular polymeric substances (EPS) (Chen et al., 2007, Yuan et al., 2014). Recent studies demonstrated that the distinguished sludge morphology between AGS and AS was determined by the chemical and mechanical properties of gel-forming EPS in the sludge of two (Felz et al., 2019, Lin et al., 2013). Possibly, the anaerobic conversion of such polymers in AGS-RTC differs from that in WAS. However, conformation of this hypothesis needs more study.

5.4 Conclusions

Based on the results of this research the following conclusions can be drawn:

- AGS-RTC revealed a significant lower BMP (194 ± 10 mL CH_4/g VS substrate) than WAS (232 ± 11 mL CH_4/g VS substrate). Mechanically destroying the compact structure of AGS did not affect its BMP, but accelerated the degradation rate of rapidly biodegradable organics and liberated a fraction of slowly biodegradable ones, resulting in higher methane production rate.
- The BMP of AGS-SD (296 ± 15 mL CH_4/g VS substrate) was similar to the BMP of PS (313 ± 11 mL CH_4/g VS substrate), and much higher than that of AGS-RTC, mainly due to the slow settle-ability of highly biodegradable cellulose-like fibres that end up in AGS-SD fraction of WAGS.
- Proteins and carbohydrates in AGS-RTC were more difficult to be degraded than those in WAS, even though the amount of these two fractions was higher in AGS-RTC. This difference was hypothesized to be related to the structural differences of EPS between these two biomass morphologies.

Supplementary data

Table S5.1 Characteristics of different types of sludge mixture before and after BMP tests

	Parameters	Unit	AGS-RTC	AGS-SD	WAS	PS
Sludge mixture (I/S ratio=2) Before BMP tests	COD	g/L	42.5 ± 0.3	44.0 ± 0.1	42.6 ± 0.2	43.7 ± 0.2
	TS	wt%, g/100 g sludge mixture	3.76 ± 0.02	3.85 ± 0.01	3.77 ± 0.01	3.81 ± 0.01
	VS	wt%, g/100 g sludge mixture	2.71 ± 0.03	2.77 ± 0.02	2.73 ± 0.03	2.78 ± 0.04
	Carbohydrates	wt%, g glucose/100 g sludge mixture	0.63 ± 0.01	0.84 ± 0.03	0.61 ± 0.01	0.87 ± 0.02
	Lipids	wt%, g/100 g sludge mixture	0.11 ± 0.01	0.14 ± 0.02	0.12 ± 0.01	0.15 ± 0.01
	Proteins	wt%, g/100 g sludge mixture	1.23 ± 0.08	1.10 ± 0.06	1.21 ± 0.07	1.04 ± 0.09
	VFAs	wt%, g/100 g sludge mixture	0.01 ± 0.002	0.02 ± 0.006	0.01 ± 0.004	0.02 ± 0.003
Sludge mixture (I/S ratio=2)After BMP tests	COD	g/L	32.1 ± 0.3	30.6 ± 0.6	30.9 ± 0.5	29.4 ± 0.2
	TS	wt%, g/100 g sludge mixture	3.22 ± 0.01	3.18 ± 0.03	3.24 ± 0.01	3.12 ± 0.03
	VS	wt%, g/100 g sludge mixture	2.02 ± 0.02	1.93 ± 0.03	2.00 ± 0.04	1.89 ± 0.03
	Carbohydrates	wt%, g glucose/100 g sludge mixture	0.28 ± 0.02	0.28 ± 0.01	0.19 ± 0.01	0.25 ± 0.03
	Lipids	wt%, g/100 g sludge mixture	0.07 ± 0.03	0.08 ± 0.02	0.08 ± 0.01	0.09 ± 0.02
	Proteins	wt%, g/100 g sludge mixture	0.90 ± 0.02	0.71 ± 0.01	0.84 ± 0.04	0.65 ± 0.05
	VFAs	wt%, g/100 g sludge mixture	0.00	0.00	0.00	0.00

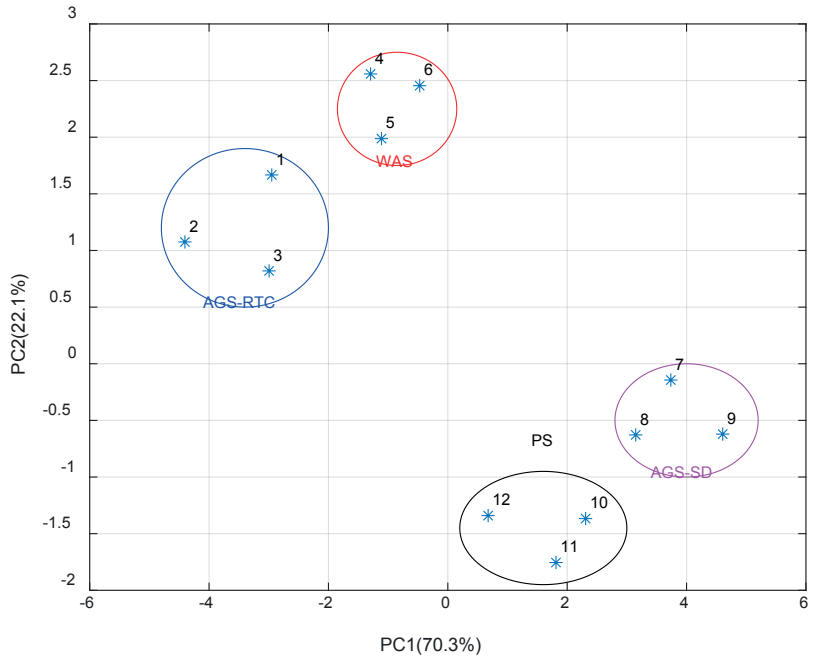

Figure S5.1 Principal component analysis (PCA) based on the converted organic fractions in different types of sludge (triplicate samples each) during the BMP tests. The principal component coefficient (PC) = [0.2565 0.0512 0.9588 -0.1105; 0.5265 0.7513 -0.2076 0.0010; 0.7348 -0.5579 -0.1637 -0.0204; 0.0430 -0.0086 0.1035 0.9937]

References

Adav, S.S., Lee, D.J. and Tay, J.H., 2008. Extracellular polymeric substances and structural stability of aerobic granule. Water Research 42(6-7), 1644-1650.

Ahmed, A.S., Bahreini, G., Ho, D., Sridhar, G., Gupta, M., Wessels, C., Marcelis, P., Elbeshbishy, E., Rosso, D. and Santoro, D., 2019. Fate of cellulose in primary and secondary treatment at municipal water resource recovery facilities. Water Environment Research 91(11), 1479-1489.

Ali, M., Wang, Z., Salam, K., Hari, A.R., Pronk, M., Van Loosdrecht, M.C. and Saikaly, P.E., 2019. Importance of species sorting and immigration on the bacterial assembly of different-sized aggregates in a full-scale aerobic granular sludge plant. Environmental science & technology 53(14), 8291-8301.

Angelidaki, I. and Sanders, W., 2004. Assessment of the anaerobic biodegradability of macropollutants. Reviews in Environmental Science & Bio/Technology 3(2), 117-129.

APHA, 2005. Standard methods for the examination of water and wastewater, 21st Edn. American Public Health Association, Washington, DC. USA

Appels, L., Baeyens, J., Degreve, J. and Dewil, R., 2008. Principles and potential of the anaerobic digestion of waste-activated sludge. Progress in Energy and Combustion Science 34(6), 755-781.

Bengtsson, S., de Blois, M., Wilen, B.M. and Gustavsson, D., 2018. Treatment of municipal wastewater with aerobic granular sludge. Critical Reviews in Environmental Science and Technology 48(2), 119-166.

Bernat, K., Cydzik-Kwiatkowska, A., Wojnowska-Baryla, I. and Karczewska, M., 2017. Physicochemical properties and biogas productivity of aerobic granular sludge and activated sludge. Biochemical Engineering Journal 117, 43-51.

Bligh, E.G. and Dyer, W.J., 1959. A Rapid Method of Total Lipid Extraction and Purification. Canadian Journal of Biochemistry and Physiology 37(8), 911-917.

Champagne, P. and Li, C., 2009. Enzymatic hydrolysis of cellulosic municipal wastewater treatment process residuals as feedstocks for the recovery of simple sugars. Bioresource Technology 100(23), 5700-5706.

Chen, M.Y., Lee, D.J. and Tay, J.H., 2007. Distribution of extracellular polymeric substances in aerobic granules. Applied Microbiology and Biotechnology 73(6), 1463-1469.

de Kreuk, M.K., Kishida, N., Tsuneda, S. and van Loosdrecht, M.C., 2010. Behavior of polymeric substrates in an aerobic granular sludge system. Water Research 44(20), 5929-5938.

de Kreuk, M.K., Kishida, N. and van Loosdrecht, M.C.M., 2007. Aerobic granular sludge - state of the art. Water Science and Technology 55(8-9), 75-81.

del Rio, A.V., Morales, N., Isanta, E., Mosquera-Corral, A., Campos, J.L., Steyer, J.P. and Carrere, H., 2011. Thermal pre-treatment of aerobic granular sludge: Impact on anaerobic biodegradability. Water Research 45(18), 6011-6020.

del Rio, A.V., Palmeiro-Sanchez, T., Figueroa, M., Mosquera-Corral, A., Campos, J.L. and Mendez, R., 2014. Anaerobic digestion of aerobic granular biomass: effects of thermal pre-treatment and addition of primary sludge. Journal of Chemical Technology and Biotechnology 89(5), 690-697.

Dubois, M., Gilles, K. A., Hamilton, J. K., Rebers, P. T., & Smith, F., 1956. Colorimetric method for determination of sugars and related substances. Analytical chemistry, 28(3), 350-356.

Felz, S., Vermeulen, P., van Loosdrecht, M.C. and Lin, Y.M., 2019. Chemical characterization methods for the analysis of structural extracellular polymeric substances (EPS). Water Research 157, 201-208.

Filipe, C.D.M. and Grady, C.P.L., 1998. Biological Wastewater Treatment, Revised and Expanded, CRC Press, USA.

Giesen, A., de Bruin, L.M.M., Niermans, R.P. and van der Roest, H.F., 2013. Advancements in the application of aerobic granular biomass technology for sustainable treatment of wastewater. Water Practice and Technology 8(1), 47-54.

Gonzalez, A., Hendriks, A.T.W.M., van Lier, J.B. and de Kreuk, M., 2018. Pre-treatments to enhance the biodegradability of waste activated sludge: Elucidating the rate limiting step. Biotechnology Advances 36(5), 1434-1469.

Holliger, C., Alves, M., Andrade, D., Angelidaki, I., Astals, S., Baier, U., Bougrier, C., Buffiere, P., Carballa, M., de Wilde, V., Ebertseder, F., Fernandez, B., Ficara, E., Fotidis, I., Frigon, J.C., de Laclos, H.F., Ghasimi, D.S., Hack, G., Hartel, M., Heerenklage, J., Horvath, I.S., Jenicek, P., Koch, K., Krautwald, J., Lizasoain, J., Liu, J., Mosberger, L., Nistor, M., Oechsner, H., Oliveira, J.V., Paterson, M., Pauss, A., Pommier, S., Porqueddu, I., Raposo, F., Ribeiro, T., Rusch Pfund, F., Stromberg, S., Torrijos, M., van Eekert, M., van Lier, J., Wedwitschka, H. and Wierinck, I., 2016. Towards a standardization of biomethane potential tests. Water Science and Technology 74(11), 2515-2522.

Lin, Y.M., Sharma, P.K. and van Loosdrecht, M.C.M., 2013. The chemical and mechanical differences between alginate-like exopolysaccharides isolated from aerobic flocculent sludge and aerobic granular sludge. Water Research 47(1), 57-65.

McSwain, B.S., Irvine, R.L., Hausner, M. and Wilderer, P.A., 2005. Composition and Distribution of Extracellular Polymeric Substances in Aerobic Flocs and Granular Sludge. Applied and Environmental Microbiology 71(2), 1051-1057.

Mottet, A., Francois, E., Latrille, E., Steyer, J.P., Deleris, S., Vedrenne, F. and Carrere, H., 2010. Estimating anaerobic biodegradability indicators for waste activated sludge. Chemical Engineering Journal 160(2), 488-496.

Moy, B. P., Tay, J. H., Toh, S. K., Liu, Y., & Tay, S. L., 2002. High organic loading influences the physical characteristics of aerobic sludge granules. Letters in Applied Microbiology, 34(6), 407-412.

Nancharaiah, Y.V. and Reddy, G.K.K., 2018. Aerobic granular sludge technology: Mechanisms of granulation and biotechnological applications. Bioresource Technology 247, 1128-1143.

Palmeiro-Sanchez, T., del Rio, A.V., Mosquera-Corral, A., Campos, J.L. and Mendez, R., 2013. Comparison of the anaerobic digestion of activated and aerobic granular sludges under brackish conditions. Chemical Engineering Journal 231, 449-454.

Perez, J., Munoz-Dorado, J., de la Rubia, T. and Martinez, J., 2002. Biodegradation and biological treatments of cellulose, hemicellulose and lignin: an overview. Int Microbiol 5(2), 53-63.

Pronk, M., de Kreuk, M.K., de Bruin, B., Kamminga, P., Kleerebezem, R. and van Loosdrecht, M.C., 2015. Full scale performance of the aerobic granular sludge process for sewage treatment. Water Research 84, 207-217.

Rao, M.S., Singh, S.P., Singh, A.K. and Sodha, M.S., 2000. Bioenergy conversion studies of the organic fraction of MSW: assessment of ultimate bioenergy production potential of municipal garbage. Applied Energy 66(1), 75-87.

Sanders, W.T., Geerink, M., Zeeman, G. and Lettinga, G., 2000. Anaerobic hydrolysis kinetics of particulate substrates. Water Science and Technology 41(3), 17-24.

STOWA, 2010. NEWs: The Dtuch Roadmap for the WWTP of 2030. Utrecht, The Netherlands.

Stubbé, S., 2016. The Fate of Phosphate in Full-Scale Aerobic Granular Sludge Systems. Delft University of Technology, Delft, The Netherlands.

Van Soest, P.J., 1963. Use of detergents in the analysis of fibrous feeds. 2. A rapid method for the determination of fiber and lignin. Journal of the Association of Official Agricultural Chemists 46, 829-835.

Wang, B., Stromberg, S., Li, C., Nges, I.A., Nistor, M., Deng, L. and Liu, J., 2015. Effects of substrate concentration on methane potential and degradation kinetics in batch anaerobic digestion. Bioresource Technology 194, 240-246.

Wu, C.D., Li, Y.B., Li, W.G. and Wang, K., 2015. Characterizing the distribution of organic matter during composting of sewage sludge using a chemical and spectroscopic approach. Rsc Advances 5(116), 95960-95966.

Yuan, D.Q., Wang, Y.L. and Feng, J., 2014. Contribution of stratified extracellular polymeric substances to the gel-like and fractal structures of activated sludge. Water Research 56, 56-65.

Zhang, X.D., Hu, J.M., Spanjers, H. and van Lier, J.B., 2014. Performance of inorganic coagulants in treatment of backwash waters from a brackish aquaculture recirculation system and digestibility of salty sludge. Aquacultural Engineering 61, 9-16.

Zhu, L., Zhou, J., Lv, M., Yu, H., Zhao, H. and Xu, X., 2015. Specific component comparison of extracellular polymeric substances (EPS) in flocs and granular sludge using EEM and SDS-PAGE. Chemosphere 121, 26-32.

Chapter 6

STRUCTURAL EXTRACELLULAR POLYMERIC SUBSTANCES DETERMINE THE DIFFERENCE IN DIGESTIBILITY BETWEEN WASTE ACTIVATED SLUDGE AND AEROBIC GRANULES

This chapter is based on:

Guo, H., Felz, S., Lin, Y., van Lier, J. B., & de Kreuk, M. (2020). Structural extracellular polymeric substances determine the difference in digestibility between waste activated sludge and aerobic granules. Water Research, 181, 115924.

Abstract

Aerobic granular sludge (AGS) technology is an alternative to conventional activated sludge to reduce the process footprint and energy consumption. Strategies for the efficient management of generated waste AGS (WAGS) need further development. Anaerobic digestion (AD) is commonly applied in waste activated sludge (WAS) treatment and is a potential option as well for WAGS treatment. In earlier studies, the biochemical methane potential of AGS (mainly granules, 70% particle size > 0.5 mm) was found lower than that of WAS, both grown in full-scale municipal wastewater treatment systems. In order to understand this difference, this study aimed to investigate the anaerobic conversion of structural extracellular polymeric substances (SEPS), which is a type of gel-forming biopolymer, being responsible for the aggregation of sludge. Using WAS and AGS as substrates, a comparative AD batch experiment was performed for 44 days during which the SEPS fraction was extracted from both types of sludge. The changes in their chemical composition was analysed by Fourier transformed infrared spectroscopy and three-dimensional excitation and emission matrix analysis. Meanwhile, the mechanical strength of hydrogels of extracted polymers cross-linked with Ca^{2+} ions was investigated by dynamic mechanical analysis. Results showed that the amount of SEPS was reduced by 26% in AGS ($SEPS_{AGS}$) and by 41% in WAS ($SEPS_{WAS}$), respectively. Particularly polysaccharides and, to a lesser extent, the proteins in the $SEPS_{AGS}$ were more refractory compared to those in $SEPS_{WAS}$. This resulted in a lower loss of the gel stiffness of $SEPS_{AGS}$ than that of $SEPS_{WAS}$ during the AD process. Moreover, the release of SEPS from tightly bound EPS to loosely bound EPS were observed in both types of sludge, but that in AGS exhibited a lower transition rate. The observed properties explain the distinct differences in anaerobic biodegradability, the slower decomposition of the sludge structure, as well as the better dewaterability of AGS as compared to WAS after the AD process.

6.1 Introduction

Conventional activated sludge (CAS) processes treating municipal wastewater create large quantities of waste activated sludge (WAS), resulting in high costs for sludge processing, such as stabilisation, incineration and discharge (Appels et al., 2008). The Nereda® technology (Nereda® is the registered trade name of the aerobic granular sludge technology owned by Royal HaskoningDHV) that is based on aerobic granular sludge (AGS) is gaining increasing popularity, due to its lower energy demand and compact reactor design; currently over 70 full-scale Nereda® plants are in operation or under construction worldwide (www.royalhaskoningdhv.com/nereda). Similar to the CAS process, also the AGS process results in the production of waste aerobic granular sludge (WAGS), which asks for proper processing and discharge.

Anaerobic digestion (AD) for WAS stabilisation is commonly applied and is proven to be a cost-effective solution, allowing energy and nutrient recovery (Appels et al., 2008, Luo et al., 2020). To date, the behaviour of WAGS during AD is largely unknown and only few studies have been reported in literature (del Rio et al., 2011; del Rio et al., 2014). More insight into the degradation of aerobic granules is needed to be able to design effective WAGS sludge processing reactors (Bernat et al., 2017; Palmeiro-Sanchez et al., 2013). In full-scale Nereda® systems, the WAGS can be two types: the AGS that can be periodically withdrawn from the reactor (mainly granules, 70% particle size > 0.5 mm), and the aerobic granular sludge selection spill (particle size ≤ 0.5 mm), a more flocculent biomass that is wasted every process cycle presenting lower settling velocity than big granules (Pronk et al., 2015). Very recent research has shown that the selection spill was easily biodegradable in AD (Guo et al., 2020) while the AGS showed a biochemical methane potential (BMP) that was significantly lower than WAS (Bernat et al., 2017; del Rio et al., 2011; del Rio et al., 2014). It was demonstrated that the high digestibility of the latter WAGS was due to the slow settle-ability of highly biodegradable cellulose-like fibres. However, the reason for the lower digestibility of AGS than that of WAS remained unclear. Guo et al. (2020) observed that proteins and carbohydrates in AGS were more difficult to be degraded than those in WAS, even though the amount of these two fractions was higher in AGS. Since AGS and WAS are mainly composed of cells, (exo-) enzymes and microbial metabolic products, very likely, this difference was related to the microbial organic polymeric matrix. Extracellular polymeric substances (EPS) account for the majority of microbial related carbohydrates and protein fractions in both AGS and WAS (Frolund et al., 1996; Liu & Fang, 2002; Salama et al., 2016). Therefore, analysing the biodegradability of the EPS present in AGS and WAS during AD will help to understand the differences in digestibility between the two sludge types.

Based on the ability to form hydrogels, EPS can be divided into gel-forming and non-gel-forming EPS (Felz et al., 2016; Seviour et al., 2009). The amount of gel-forming EPS or structural EPS (SEPS) can be considerable, i.e. 100-300 mg/g VS sludge, and unlike non-gel-forming EPS, SEPS contributes to the formation of a tertiary network structure within the sludge (Felz et al., 2016; Lin et al., 2010). It is hypothesized that the different concentration, organic composition and ionic gel-forming properties of SEPS extracted from AGS and activated sludge determine the sludge morphology differences of the two (Lin et al., 2013; Sam & Dulekgurgen, 2016). Anaerobic sludge digestion starts with breaking down the sludge structure,

resulting in the deterioration of sludge properties (Ye et al., 2014). This enlarges the surface area of the sludge making it more accessible for the hydrolytic enzymes and thus for conversion during AD. Considering the amount of SEPS in sludge and their importance to the sludge structure, the fate of these biopolymers in AD is very likely of crucial importance for the observed differences in digestion performance of AGS and WAS.

As a consequence, in this study, batch mesophilic anaerobic digestion tests were conducted for AGS and WAS under the same experimental conditions. SEPS from AGS ($SEPS_{AGS}$) and WAS ($SEPS_{WAS}$) were extracted during the experiment, and their conversion characteristics regarding overall biodegradability, chemical & gel-forming properties and spatial distribution were investigated and compared. Results led to a schematic representation of the SEPS degradation mechanism.

6.2 Materials and Methods

6.2.1 Inoculum and substrates

The inoculum for batch tests was taken from the sludge digester of the municipal wastewater treatment plant (WWTP) Harnaschpolder (Den Hoorn, The Netherlands). The WAS was collected from the low loaded, enhanced biological phosphate removal (EBPR) activated sludge tank at the same WWTP. AGS was collected from a full-scale Nereda® reactor treating municipal wastewater (Garmerwolde, The Netherlands). The influent characteristics and operational parameters of these two plants were reported elsewhere (Guo et al., 2020). The volatile solids (VS) concentrations of both types of sludge were manipulated by centrifugation (5 min at 3,500 × g) to reach to same sludge concentrations.

6.2.2 Experimental setup

The anaerobic digestion batch experiments were carried out at 35 ± 1 °C in 2-L flasks for 44 days in an incubator shaker at 120 rpm (Innova 44, Eppendorf AG, Germany). The total volume of the mixture of inoculum and substrate was 1.8 L with an inoculum/substrate ratio of 2 on a VS (g) basis. Phosphorus buffer solution, macronutrients and trace elements were dosed according to the recipes of Zhang et al. (2014). For each type of sludge, three flasks were connected to an Automatic Methane Potential Test System (AMPTS II, Bioprocess Control, Sweden) for real-time online monitoring of the accumulated methane production, while three other flasks were used for periodic collection of an 80 mL sample for further analysis. Prior to the start of the experiment, N_2 was purged into each reactor for 5 min to remove oxygen from the sludge and headspace.

6.2.3 Analytical methods

EPS extraction

The EPS was extracted from the sludge with a mild temperature-Na_2CO_3 extraction method developed by Felz et al. (2016). In brief: a sludge sample of 3 g (wet weight) was added into a 0.5% (w/v) Na_2CO_3 solution up to 50 mL and subsequently stirred at 400 rpm and 80 ˚C for 35 min, followed by centrifugation at 4,000 × g and 4 °C for 20 min. The organics in the supernatant comprised the total extractable EPS.

In addition, centrifugation and a mild-harsh heat method (Li & Yang, 2007) was applied to extract the stratified EPS: slime, loosely bound-EPS (LB-EPS) and tightly bound-EPS (TB-EPS); a sludge sample of 15 g (wet sludge) was centrifuged at 15,000 × g for 15 min at 4 °C. The produced supernatant was recovered as slime. The solid fraction after decanting the supernatant was re-suspended into a pre-heated 0.05% (w/v) NaCl solution restoring the original weight and reaching a final temperature of 50 °C. After centrifugation at 15,000 × g for 10 min at 4 °C, the organic matter in the supernatant was recovered as LB-EPS. The pellet was re-suspended in a 0.05% (w/v) NaCl solution, restoring the original weight. The mixture was heated to 60 °C in a water bath for 30 min, while steering it at 400 rpm. Hereafter it was centrifuged at 15,000 × g for 15 min at 4 °C. The collected supernatant was regarded as TB-EPS.

SEPS extraction

The SEPS was isolated according to Felz et al. (2016): the aforementioned extracted EPS were dialyzed with a dialysis membrane (3.5K MWCO, SnakeSkin, Thermo Fisher Scientific, USA) for 24 h against 1,000 ml MiliQ water. The pH of the dialyzed extracts was slowly adjusted to 2.2 ± 0.05 with 1 and 0.1 M hydrochloric acid. After these extracts were centrifuged at 4,000 × g and 4 °C for 20 min, the supernatant was discarded and the gel-like pellet was considered to be the SEPS. A certain amount of SEPS pellet obtained from the total extractable EPS (total extractable SEPS) and from the stratified EPS (stratified SEPS) was used for the VS analysis to measure the content of the SEPS fraction in the sludge (wt %, g/100 g sludge), and the rest was freeze-dried and stored for further analysis.

Physicochemical analyses

VS, total suspended solid (TSS) and volatile suspended solid (VSS) were analysed according to standard protocols (APHA, 2005). To measure the polysaccharides and proteins content of total extractable SEPS, the freeze-dried SEPS from a sludge sample of 3 g (wet weight) was solubilized in 1 M NaOH to 50 mL reaching final pH of 7.5. The polysaccharide concentration was determined by phenol-sulfuric

acid assay using glucose (Sigma, USA) as standard (Dubois et al., 1956) while the protein concentration was measured using a modified Lowry method with bovine serum albumin (Sigma, USA) as standard (Frolund et al., 1995). Although methods for quantification of polysaccharides and proteins in SEPS were not fully developed, the aforementioned methods are rapid and widely accepted and function as a relatively good estimator (Felz et al., 2019b). The polysaccharide and protein content in SEPS were then calculated based on the following equation:

$$\text{Content (wt \%, g/100 g sludge)} = \frac{C_{\text{photometric method}} \times V_{\text{solution}}}{W_{\text{sludge}}} \times 100\% \quad \text{(Eq.6.1)}$$

where $C_{photometric}$ method = concentration of polysaccharides or proteins determined by photometric methods (mg/L); $V_{solution}$ = volume of the solution (50 mL in this study); W_{sludge} = amount of the sludge sample (3 g in the current study).

Changes in dewaterability during AD of AGS and WAS (sludge-inoculum mixture) were detected by a capillary suction time (CST) apparatus (304M, Triton Electronics, England) with CST papers manufactured by the same company. A normalized CST (NCST) method was used to eliminate the influence of solid particles (Lu et al., 2015). Volatile fatty acids (VFAs) were measured by gas chromatography (GC), equipped with a flame ionization detector (FID) (Agilent 7890A, USA). Helium was used as carrier gas with a flow rate of 1.8 mL/min; the column (Agilent 19091F-112) was 25 m × 320 µm × 0.5 µm; injection port and oven temperatures were 240 °C and 80 °C, respectively. The particle size distribution (PSD) of AGS before and after AD process was analysed by a sieving method (Pronk et al., 2015), while that of WAS at Day 0 and 44 was measured by a particle size analyser (Bluewave, Microtrac, Germany).

FT-IR spectroscopy

The original and secondary derivative FT-IR spectra of total extractable SEPS (the freeze-dried solid) in KBr pellets were recorded in the 4,000-500 cm^{-1} region by a FT-IR spectrometer (Cary 630, Agilent, USA).

3D-EEM spectroscopy

The prepared solution for polysaccharide and protein measurements was also used to determine the 3D-EEM spectra of total extractable SEPS. These spectra were measured by a fluorescence spectrometer (Aqualog-UV-NIR-800-C, HORIBA, USA). Wavelength ranges for excitation and emission spectra were 280-550 nm and 240-400 nm, respectively. Both excitation and emission bandwidths were adjusted to 2 nm and the EEM signals were corrected by subtracting a blank (demineralized water). EEM fluorescence spectra were divided into four regions based on the differences of excitation-emission wavelengths of organic matters (Table S6.1 in Supplementary data) (Sun et al., 2016). The fluorescence regional integration (FRI) technique was utilized to calculate the fluorescent intensities of each region in all EEM spectra (Chen et al., 2003).

Table 6.1 Excitation and emission (Ex/Em) wavelengths of the different fluorescence regions that can be distinguished with 3D-FEEM

Region	Substance	Ex/Em wavelengths (nm)
Region I	Aromatic protein-like	240-250/280-380
Region II	Fulvic acid-like	240-250/380-550
Region III	Soluble microbial by-product-like region	250-340/280-380
Region IV	Humic acid-like	250-400/380-550

Gel formation property

To test total extractable SEPS's gel-forming property, 10% (w/v) freeze-dried SEPS-miliQ solution was extruded into a cylinder mould (1 cm^3) and sealed on both sides with a dialysis membrane (MWCO of 3.5kDa, Snakeskin, USA). The mould was then submersed into 3% (w/v) $CaCl_2$ solution for 24 h to produce a Ca^{2+}-SEPS hydrogel. The mechanical stiffness of the hydrogel was measured by dynamic mechanical analysis device (DMA7e, Perkin Elmer, USA) under the pressing force rate of 25 mN/min. The Young's modulus represented the mechanical strength of the hydrogel and was calculated by the slope of tensile stress and extensional strain obtaining from the test (Felz et al., 2019a).

6.2.4 Statistical analysis

Linear regression analysis for SEPS degradation was performed using R (R Core Team, Austria). Significant differences in biodegradability of SEPS, FT-IR spectrum and dewaterability between AGS and WAS were based on Student's t-test by means of SPSS Statistics 25 (IBM, USA). The significance level of probability (p-value) was 0.05.

6.3 Results and discussion

6.3.1 Batch anaerobic digestion of AGS and WAS

The difference in biodegradability of the sampled WAS and AGS was assessed. The characteristics of the substrate and inoculum are summarized in Table 6.2. The inoculum sludge was characterised by an anaerobic activity of 0.19 g CH_4-COD/g VS/day with acetate as the substrate.

To assess the degradation of the two sludge types accumulated methane production, VS and total VFAs were monitored during the anaerobic digestion. The results are presented in Table 6.3. The average accumulative methane production of AGS and WAS were both in line with prior researches (Guo et al., 2020; del Rio et al., 2014; Palmeiro-Sanchez et al., 2013). Besides, the average VS reduction of AGS and WAS was both in the typical range of 25-45% for sludge digestion (Bolzonella et al., 2005; Mottet et al., 2010). Specifically, the degraded VS was 0.69 ± 0.01 wt % for AGS, and was 0.77 ± 0.02 wt % for WAS, which obviously showed that WAS had a higher degradation extent in VS, approximately 0.08 ± 0.01 wt %, than AGS. VFAs were detected during day 0 and 6 of the digestion, peaking at day 3 (values shown in Table 6.3). The concentrations remained low enough to avoid inhibitory effects of the VFAs.

The differences in accumulated methane production and VS reduction of the two sludge types confirmed their dissimilarity in biodegradability (Table 6.3). To minimise the impact of surface area limitation of AGS compared to WAS, the biodegradability of crushed AGS and WAS were compared, revealing comparable differences in biodegradability extent (Guo et al., 2020).

Table 6.2 Characteristics of the substrate and inoculum

Parameters	Substrate		Inoculum
	WAS	AGS	Digestate
pH	7.1 ± 0.3	7.0 ± 0.2	8.1 ± 0.4
Median particle size (μm)	114 ± 9	1794 ± 121	50 ± 5
TS concentration (wt %, g/100 g sludge)	5.16 ± 0.08	5.41 ± 0.10	3.30 ± 0.09
VS concentration (wt %, g/100 g sludge)	4.14 ± 0.05	4.25 ± 0.07	2.32 ± 0.03
VS/TS (%)	80.0 ± 0.2	78.4 ± 0.7	70.5 ± 0.2

It should be mentioned that the inoculum selected in this study was taken from a full-scale anaerobic digester that treats both primary sludge and WAS. However, del Rio et al. (2014) have proved that, after long-term acclimation with AGS as the sole substrate, the main microbial populations present were still those commonly found in digesters treating waste municipal sewage sludge. Thus, to our understanding, also this type of inoculum should be highly active and effective for AGS digestion within a period of 44 days.

Table 6.3 Comparison of the performance of the batch anaerobic digestion of AGS and WAS

Sludge type (sludge-inoculum mixture)	Accumulated methane production (N-mL/g VSsubstrate)	VS concentration			Maximum total VFA concentration (mg/L)
		Before AD (wt %, g/100 g sludge)	After AD (wt %, g/100 g sludge)	Removal efficiency (%)	
AGS	197 ± 11	2.71 ± 0.02	2.02 ± 0.01	25.4 ± 1.3	329 ± 21
WAS	242 ± 18	2.74 ± 0.01	1.97 ± 0.03	28.1 ± 1.1	388 ± 15

6.3.2 Degradation kinetics of SEPS

Changes in the total extractable SEPS from AGS ($SEPS_{AGS}$) and WAS ($SEPS_{WAS}$) undergoing anaerobic digestion are shown in Figure 6.1. The initial average SEPS contents in AGS and WAS (sludge-inoculum mixture) were 0.53 ± 0.01 and 0.49 ± 0.01 wt % respectively or 196 ± 6 and 179 ± 5 mg/g $VS_{sludge\ mixture}$, respectively. These results are in accordance with previous studies where aerobic granules represented a higher SEPS concentration than activated sludge (Lin et al., 2013; Sam & Dulekgurgen, 2016). However, the total removal efficiency of $SEPS_{AGS}$ (26%, from 0.53 ± 0.01 to 0.39 ± 0.01 wt %) was significantly lower (p-value = 0.038) than that from $SEPS_{WAS}$ (41%, from 0.49 ± 0.02 to 0.29 ± 0.01 wt %). It could be calculated that the difference in degraded SEPS between AGS and WAS (sludge-inoculum mixture), was 0.06 ± 0.01 wt %. Comparing this value with the removed VS content (0.08 ± 0.01 wt %), the result clearly reveals that the SEPS is a major organic matter that differentiates the biodegradability of AGS and WAS. $SEPS_{AGS}$ degradation started with a low rate from day 0 to 3, followed by a rapid degradation phase from day 3 to 21, and a slow degradation after day 21. $SEPS_{WAS}$ degradation occurred with a higher rate from the start of the experiment, also followed by a slow degradation phase after 21 days. The degradation rate during the rapid degradation phase of $SEPS_{WAS}$ and $SEPS_{AGS}$ were similar (respectively 0.006 and 0.005 g SEPS/100g sludge/d). Additionally, during the slower degradation phase the SEPS degradation rates of WAS and AGS differed again, respectively 0.002 and 0.0003 g SEPS/100g sludge/d.

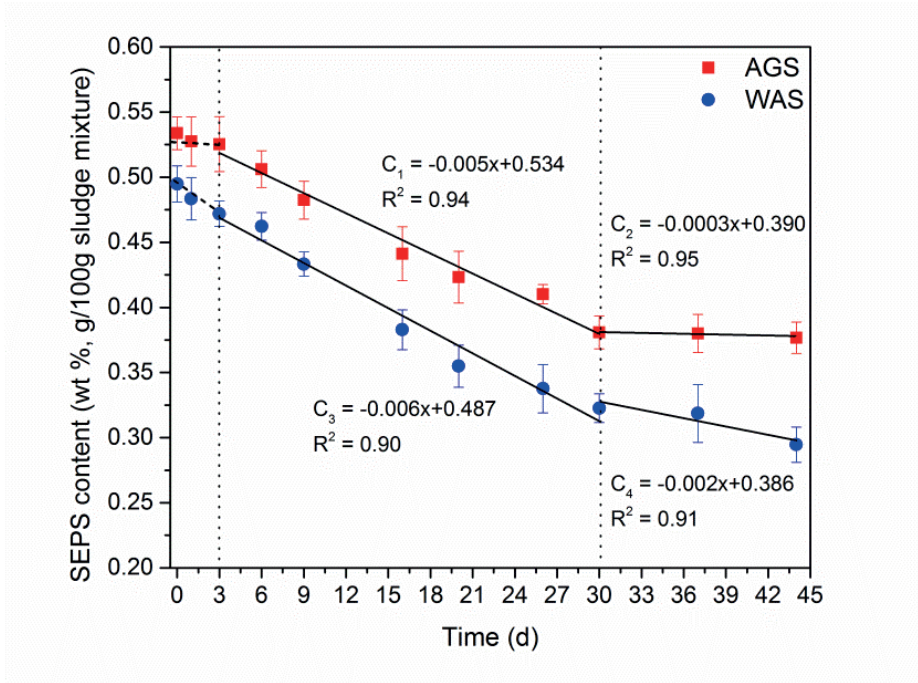

Figure 6.1 Degradation kinetics of SEPS during anaerobic digestion of AGS and WAS

6.3.3 Variation of chemical composition and gel-forming stiffness of SEPS

In order to explain the differences in degradation rate and extent of the SEPS in WAS and AGS, the chemical and gel-forming properties of the total extractable SEPS fractions were analysed on day 1, 3 and 44 of the AD experiments.

Chemical composition

The composition and degradation of polysaccharides and proteins, within the extracted SEPS, are presented in Figure 6.2. These two organic groups form the main constituents of SEPS (84% of $SEPS_{AGS}$ and 82% of $SEPS_{WAS}$). The removal efficiencies of the extracted polysaccharides and proteins in $SEPS_{WAS}$ were 62% and 33%, respectively, which were both higher than that of $SEPS_{AGS}$ (39% and 24%, respectively), during 44 days AD process. Specifically, polysaccharides and proteins in $SEPS_{WAS}$ presented remarkably faster biodegradation than that in $SEPS_{AGS}$ in the first three days. The results reveal that the extracted organic compounds, especially polysaccharides in $SEPS_{WAS}$ can be more easily biodegraded under anaerobic digestion as compared to that in $SEPS_{AGS}$ and thus leads to a higher degradation extent of $SEPS_{WAS}$ (Figure 6.1).

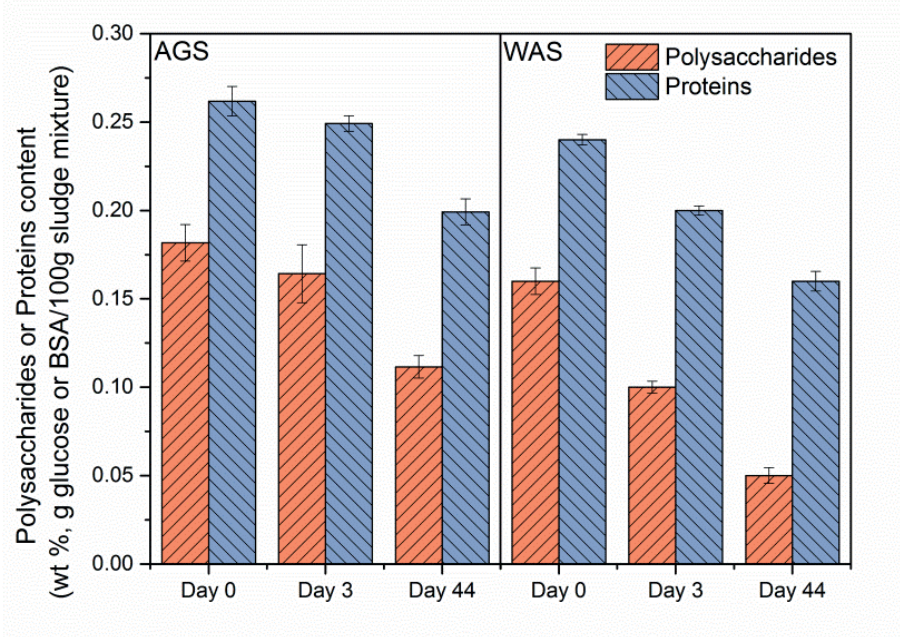

Figure 6.2 Polysaccharides and proteins degradation of $SEPS_{AGS}$ and $SEPS_{WAS}$ during anaerobic digestion of AGS and WAS

FT-IR analysis

To further investigate the changes in chemical structure of the SEPS during AD, FT-IR analysis was carried out (Figure 6.3). The FT-IR spectra for all SEPS samples were very similar, showing the same typical functional groups belonging to polysaccharides and proteins (Figure 6.3a and Table S6.2 in Supplementary data) (Badireddy et al., 2010; Guo et al., 2016; Zhang et al., 2015).

Research has shown that polysaccharides play a major role in the gel-forming characteristics of EPS, due to its binding capacity with divalent cations (Lin et al., 2013; Seviour et al., 2012). In FT-IR spectrum, the region at 950-700 cm^{-1} is the fingerprint (or anomeric) region of carbohydrates (Davis and Fairbanks, 2002). To enhance the carbohydrate signals, a second derivative spectrum of the extracted SEPS of AGS and WAS in this region was made (Figure 6.3b). In general, the change in position and number of the measured peaks of $SEPS_{AGS}$ after the first 3 days of anaerobic digestion was not statistically significant (p-value = 0.75), but a substantial difference (p-value = 0.034) was observed after 44 days of anaerobic digestion. However, for $SEPS_{WAS}$, the positions and number of peaks already changed during the first 3 days (p-value = 0.047). This result is consistent with the data indicating that the overall degradation of polysaccharides in $SEPS_{WAS}$ started before that in $SEPS_{AGS}$ (Figure 6.2).

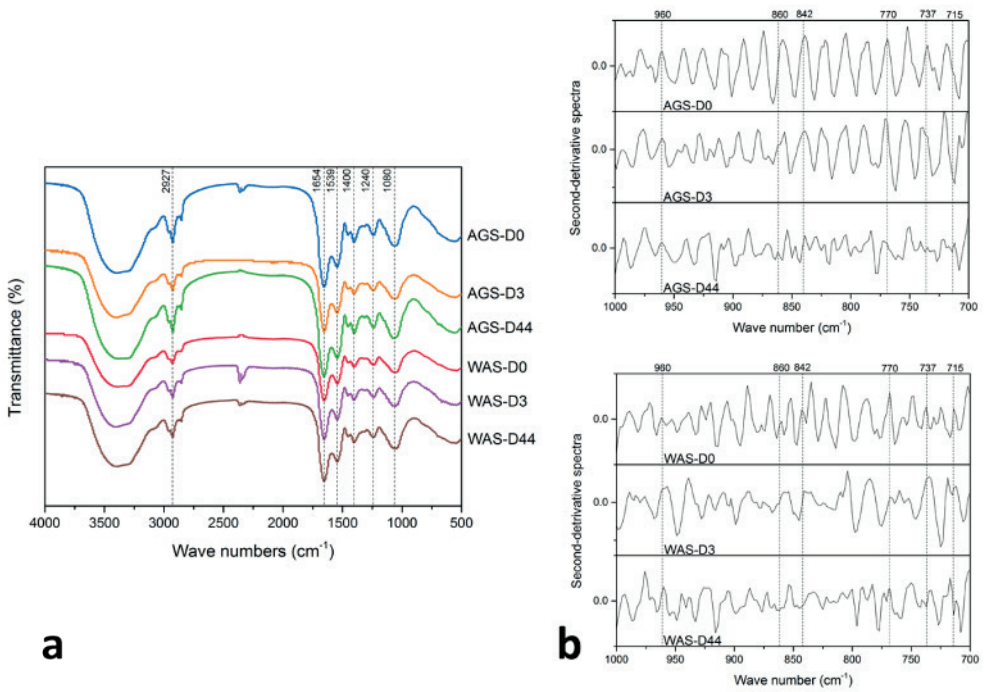

Figure 6.3 FT-IR spectra of $SEPS_{AGS}$ and $SEPS_{WAS}$ during anaerobic digestion of AGS and WAS: (a) full-wavelength FT-IR spectra, and (b) second-derivative FT-IR spectra at the fingerprint region of carbohydrate

Particularly, peaks at 960, 770, 737 and 715 cm^{-1} denoted to C-C-C, C-O-C, and O-C-O stretching vibrations of glucuronic acids (Tajmir-Riahi, 1984). For both types of SEPS, the position of these peaks remained unchanged during the anaerobic digestion. However, at the end of the digestion period (day 44), the 737 cm-1 peak of $SEPS_{AGS}$ was just lower, whereas the peak belonging to $SEPS_{WAS}$ disappeared completely, possibly indicating less biodegradation of glucuronic acid in AGS compared to WAS. Several researchers found that glucuronic acids are important monomers predominating in the polysaccharides (or glycoproteins) of gel-forming EPS (Seviour et al., 2010; Felz et al., 2019b). For example, they can act as the building blocks in the formation of hyaluronic-like acid, a type of extracellular substance that is capable of attracting cations and forming hydrogels (Felz et al., 2020). Although the characteristics of glucuronic acid-related polysaccharides in SEPS of activated sludge and aerobic granules are not fully understood, the observed result suggests that these polysaccharides in $SEPS_{AGS}$ were likely harder to anaerobic biodegradation than that in $SEPS_{WAS}$.

Table 6.4 FT-IR spectra band

Frequencies (cm^{-1})	Band assignment
Over 3000	O–H bond stretching vibrations of polysaccharides
2927	C-H bonds associated with polysaccharides
1654	C=O stretching (amide I) and C=N stretching associated with proteins
1539	N–H and C–N stretching in amide II associated with proteins
1400	Symmetric stretching of carboxylic O-C-O vibration for polysaccharides
1240	C-N stretch associated with secondary amides of proteins (amide III)
1080	C–O and C–O–C stretching vibration of hydroxyl in polysaccharides
700-950	Fingerprint (or anomeric) region of carbohydrate

Additionally, peaks at 860 and 842 cm^{-1} were observed in all SEPS samples. They are related to the glycosidic linkages of galactose and mannose (Das et al., 2011; Sardari et al., 2017). Recent researches reported by Seviour et al. (2010) and Felz et al. (2019b) proved the existence of galactose and mannose in the EPS of AGS and revealed that they may be also crucial carbohydrates that contribute to the gel-forming property of AGS. The substantial presence of these monomeric units in the EPS from activated sludge suggested their importance in the aggregation of sludge flocs (Dignac et al., 1998). The sugars form heteropolysaccharides by bonding with the repeated units of various monosaccharides such as glucose, fructose, etc. However, up to now, the similarity of the chemical structure of heteropolysaccharides formed by galactose and mannose in AGS and WAS is unclear in literature. Interestingly, in this study, the polysaccharide peaks for the $SEPS_{WAS}$ shifted to low wave numbers after 3 days, while that for the $SEPS_{AGS}$ samples remained unchanged even on day 44, indicating that $SEPS_{AGS}$ was slower degraded than $SEPS_{WAS}$, which implies that the composition of galactose and mannose-based heteropolysaccharides in $SEPS_{AGS}$ and $SEPS_{WAS}$ is different.

3D-EEM assays

3D-EEM spectroscopy was applied for characterizing the extracted SEPS at the different days of anaerobic digestion from AGS and WAS (Figure 6.4). Compared to conventional photometric methods, EEM provides more information about the presence and concentration of fluorescent organics. These organic matters, such as protein-like substances (i.e., aromatic and tryptophan-like substance), are shown to contribute to the formation of the sludge structure via surface charge adjustment (Zhu et al., 2015). The 3D-EEM plots of four different regions with their corresponding

possible substances are given in Table S6.1 in Supplementary data. Region III (soluble microbial by-products) had the highest fluorescence intensity, with its characteristic peak indicating the tryptophan & protein-like substances, identified at the excitation/emission wavelengths (Ex/Em) of 275-285/325-340 nm. Region IV (humic-like substances) revealed a signal with the characteristic humic-like substances peak observed at the Ex/Em of 345-355/425-440 nm. The results illustrate that irrespective of sludge type, tryptophan & protein-like, as well as humic acid-like substances were dominant among the organic matter with fluorescence characteristics in SEPS. These results were very similar as fluorescence spectra that were determined by Wang et al. (2009) for bound EPS extracted from activated sludge.

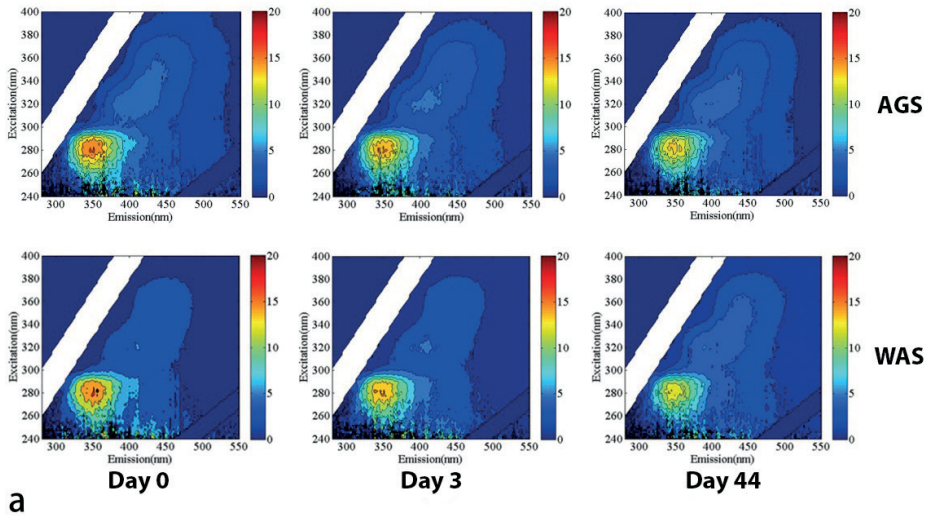

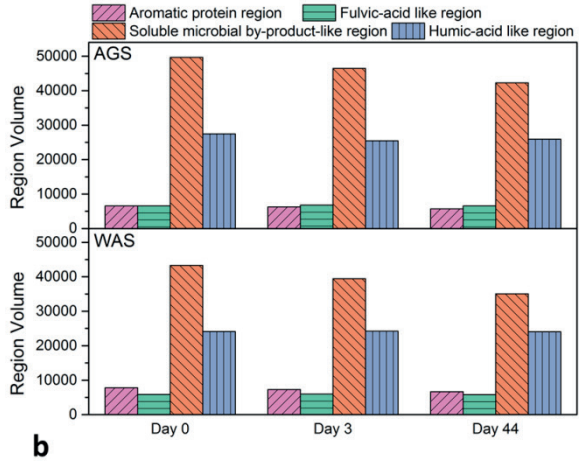

Figure 6.4 (a) 3D-EEM spectra and (b) fluorescence intensity of each fluorescence region of $SEPS_{AGS}$ and $SEPS_{WAS}$ during anaerobic digestion of AGS and WAS

During digestion, the characteristic peaks belonging to the protein-like substance regions (Region I and Region III) were reduced, demonstrating degradation of protein-like substances. However, the total calculated reduction ratio of the fluorescence intensity of the protein-like substance regions at day 3 and day 44 compared to day 0 was 6.2 and 14.7% for $SEPS_{AGS}$ and 8.6 and 18.5% for $SEPS_{WAS}$, respectively. This is in accordance with the results obtained by the photometric method (Figure 6.3). Reasons for the lower protein degradation efficiency in $SEPS_{AGS}$ can be two-fold. Firstly, the compact structure of AGS results in a lower specific surface area relative to activated sludge (Zheng et al., 2005). It is thus speculated that this may hinder the hydrolysis of structural extracellular proteins by protease. Secondly, as mentioned before, tryptophan & protein-like substances dominated among the protein-like substances. Li et al. (2014) reported that the tryptophan-like group was resistant to anaerobic digestion. In this study, the initial fluorescence intensity of the tryptophan-like substance region of $SEPS_{AGS}$ was higher than that of $SEPS_{WAS}$. The higher content of the tryptophan-like substance in $SEPS_{AGS}$ results in the lower overall degradation of proteins in $SEPS_{AGS}$, which is supported by the lower reduction in fluorescence intensity of Region III for $SEPS_{AGS}$ during AD process. In contrast to protein-like substance regions, the reduction of the fluorescence intensity of Region IV (humic-like substances) over time was not observed, suggesting that these substances were refractory to anaerobic biodegradation, which was in line with results reported by Ghasimi et al. (2016).

Gel-forming strength

SEPS is known to be capable of forming gels with multivalent cations in a broad range of temperature and pH. The viscous and elastic characteristics displayed by this biopolymer gel when undergoing deformation are regarded as a parameter to indicate the mechanical property of SEPS (Lin et al., 2013). Ca^{2+} is one of the most common cations in wastewater. Ca^{2+}-SEPS (ionic hydrogel) could play an important role in building up the gel matrix structure in both activated sludge and aerobic granules (Felz et al., 2016; Lin et al., 2013). Therefore, to understand the influence of SEPS degradation on the gel stiffness, hydrogels formed from $SEPS_{AGS}$ and $SEPS_{WAS}$ cross-linked with Ca^{2+} were made (Figure 6.5a) and subjected to a gel stiffness test. In Figure 6.5b the decreased Young's modulus is shown, indicating the loss of gel-forming property and increased susceptibility for destruction of the mechanical structure during the AD process. The Young's modulus of $SEPS_{AGS}$ decreased by 14.6 %, from 4126 ± 455 to 3522 ± 338 Pa in average, while the Young's modulus of $SEPS_{WAS}$ showed a much higher reduction of 30.1 % (2773 ± 78 to 1939 ± 133 Pa in average), which indicates that the stiffness reduction during AD is much higher for $SEPS_{WAS}$ than for $SEPS_{AGS}$. It has been demonstrated that some functional groups of

polysaccharides and proteins, such as carboxyl, hydroxyl, and amino acid groups, can be easily bridged with Ca^{2+} in the sludge matrix, resulting in the gel-forming ability of EPS (Felz et al., 2019b). In the present study, although strong peaks of these functional groups were found in all samples extracted during the AD process of SEPS (Figure 6.3), these key organic fractions, especially polysaccharides in $SEPS_{AGS}$, showed higher resistance to anaerobic degradation than that in $SEPS_{WAS}$, which eventually leads to the stronger gel-forming capacity in residue $SEPS_{AGS}$. This finding implies that the granular structure of AGS will likely sustain during digestion.

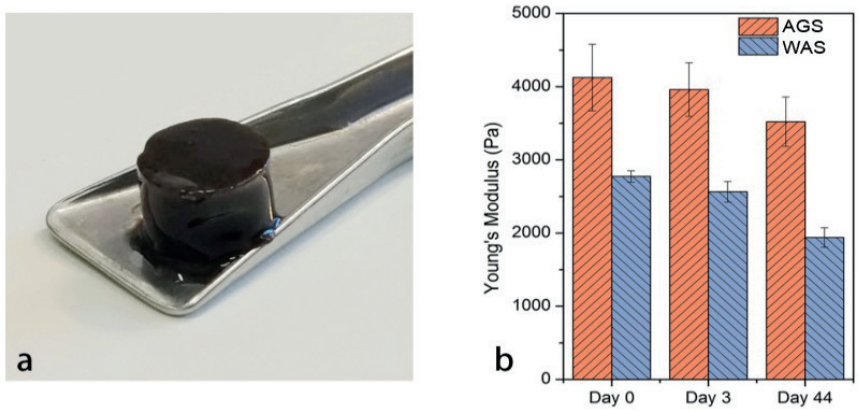

Figure 6.5 (a) SEPS hydrogel formed with Ca^{2+}, and (b) changes of gel-forming property of $SEPS_{AGS}$ and $SEPS_{WAS}$ during anaerobic digestion of AGS and WAS

To prove this assumption, the shifts in particle size distribution of both types of sludge after 44 days of AD were determined and are shown in Figure 6.6. Both AGS and WAS experienced deterioration of their particle sizes: the fraction particles larger than 100 µm decreased by 30% in WAS while it decreased only 23% in AGS. The fraction above 250 µm is defined as granules (de Kreuk et al., 2007). Although this fraction in AGS reduced 44%, going from 54 to only 24% during AD, the fraction of big particles especially larger than 2 mm remained present in AGS after 44 days AD. This observation is in line with the differences in gel-forming properties of $SEPS_{WAS}$ and $SEPS_{AGS}$ as discussed above.

6.3.4 Structural changes of SEPS in EPS matrix

This study revealed that the structural morphology of AGS and WAS changed during the AD process. Besides the deterioration of sludge dewatering properties due to these structural changes (Lu et al., 2015; Novak et al., 2003), the gel-forming EPS matrix within the sludge also weakened, resulting in degradation and shifts between the different EPS binding strength. Therefore, the content of SEPS in slime,

loosely bound-EPS (LB-EPS) and tightly bound-EPS (TB-EPS) before and after AD was determined for both types of sludge. As shown in Figure 7, initially, the slime fraction of the SEPS was very low. The $SEPS_{TB\text{-}EPS}/SEPS_{LB\text{-}EPS}$ ratio was highest in the AGS, while both sludge types were dominated by TB-EPS, which was in line with previous studies claiming that TB-EPS plays an important role in maintaining the matrix structure of both aerobic granular sludge and activated sludge (Chen et al., 2010; Yuan et al., 2014).

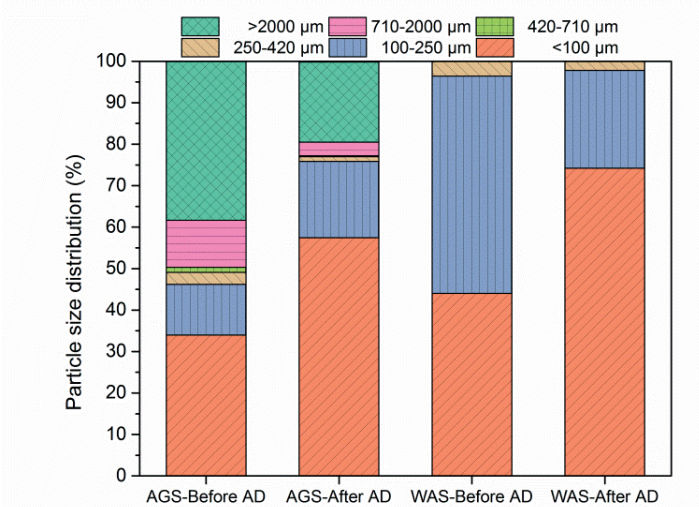

Figure 6.6 Particle size distribution of sludge before and after anaerobic digestion of AGS and WAS

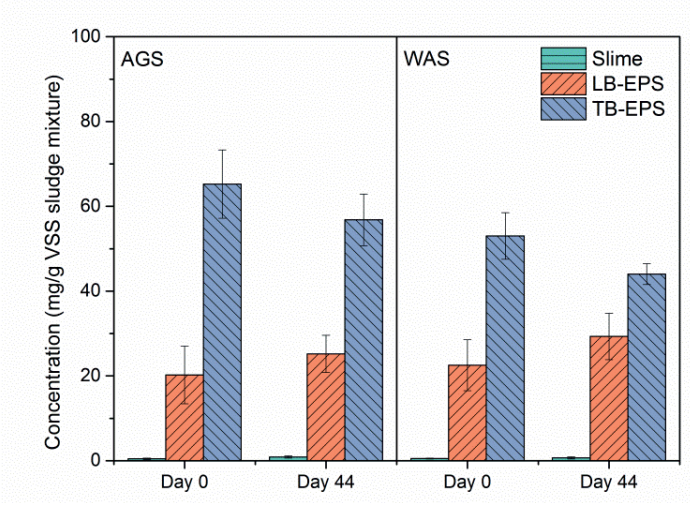

Figure 6.7 The content of $SEPS_{AGS}$ and $SEPS_{WAS}$ in slime, loosely and tightly bound EPS before and after anaerobic digestion of both sludges

Even though the content of SEPS in TB-EPS remained high, a shift of SEPS from TB-EPS to LB-EPS was observed during AD: The $SEPS_{LB\text{-}EPS}$ fraction increased by 23% and 25% for AGS and WAS respectively, while the $SEPS_{TB\text{-}EPS}$ fraction decreased with 13% and 20%, respectively (Figure 6.7). This transition is likely due to the loss of binding capacity between SEPS and cations as a result of enzymatic hydrolysis (Yu et al., 2010). In contrast, the slime fraction of SEPS remained very low, indicating that the SEPS shifted from the LB-EPS to the slime fraction during AD might be converted to methane during this process.

The presence of LB-EPS and TB-EPS are reported to exhibit different sludge dewaterability (Chen et al., 2010; Yuan et al., 2014): deterioration of dewaterability during AD is associated with a shift of polymers from TB-EPS to LB-EPS (Ye et al., 2014). In the current study, a substantial difference in CST was observed between AGS and WAS at different moments during AD (Figure 6.8), which could be explained by the larger SEPS shifts in WAS than in AGS during AD. We used the normalised CST method as an indicative analysis for the sludge dewaterability. Although this method has been accepted by several researchers to characterise dewaterability, it might not be the optimal method to study dewaterability of AGS: the CST of AGS is usually very short (16-19 s) (Basuvaraj et al., 2015; Lotito et al., 2014), because the free water around the granules is loosely bound. However, the water that is captured within the granules is not released during a CST measurement and therefore CST might not represent the overall dewaterability of AGS. In the current study, the AGS and WAS were both mixed with digestate: the latter determined the overall suction time, which was much higher than that of sole AGS and WAS. The dewaterability of digestate is determined by the particle size distribution and the polymer fraction in the matrix. Therefore, in this research it is reasonable to compare the dewaterability of AGS and WAS (sludge-inoculum mixture) by CST as a qualitative parameter.

6.3.5 SEPS degradation mechanism and implications

In the anaerobic degradation of both sludge types, considering the observed changes in SEPS, the following mechanism is proposed for SEPS degradation (Figure 6.9): before the AD process, the SEPS was mainly aggregated in TB-EPS and exhibited a strong gel-forming capacity with cations such as Ca^{2+}. Nevertheless, AD negatively influences the gel-forming strength of the Ca^{2+}-SEPS hydrogel, due to the degradation of key polysaccharides and proteins and related to this, due to the transition of SEPS from TB-EPS to LB-EPS. The lower degradation of $SEPS_{AGS}$ compared to $SEPS_{WAS}$, resulted in a higher remaining SEPS fraction in AGS structure during the whole AD process, leading to a lower overall biodegradability of AGS compared to WAS.

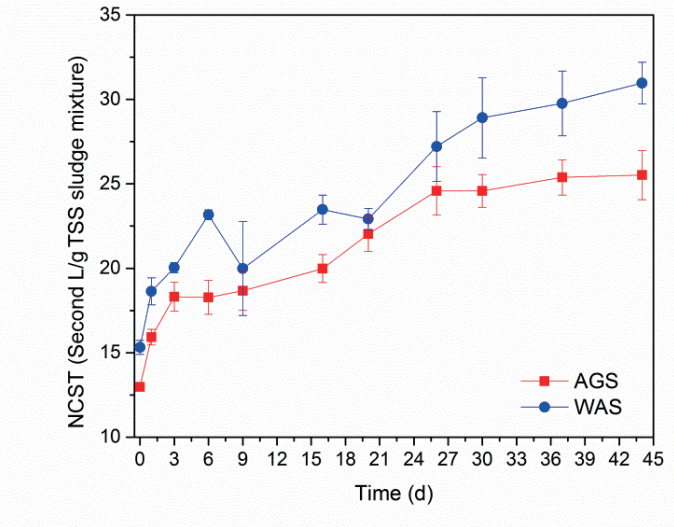

Figure 6.8 Changes in normalized CST of sludge during anaerobic digestion of AGS and WAS

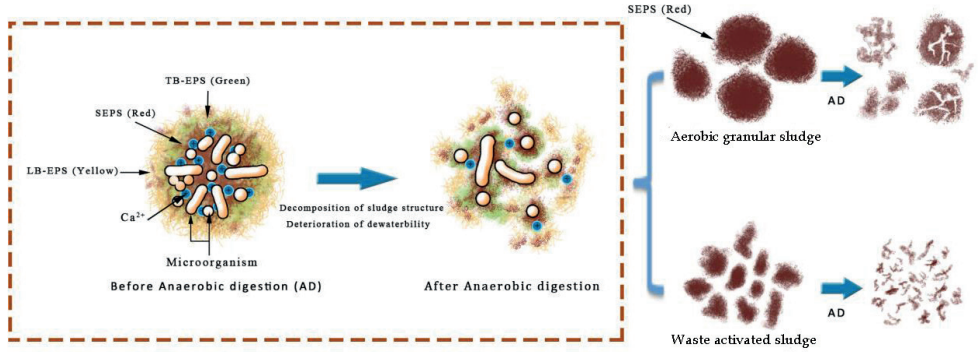

Figure 6.9 SEPS degradation mechanism in anaerobic digestion of AGS and WAS

VS removal in both types of sludge during anaerobic digestion was around 30% and therefore relatively low. Considering that only 20-40% of SEPS can be biodegraded, a possible strategy for enhancing the biodegradability of sludge, especially AGS, could be the acceleration of the decomposition or degradation of the SEPS structure. This could be done through destructive mechanical methods, such as crushing or ultrasound treatment, in combination with the addition of specific enzymes targeting the SEPS polymers. It can be speculated that this pre-treatment would liberate biodegradable compounds of the SEPS matrix, leading to enhanced methane production. Besides, the gel-forming SEPS are useful biopolymers in industrial applications (Lin et al., 2015), and recovery of SEPS from AGS is studied at pilot scale

(Kaumera®, Royal HaskoningDHV, The Netherlands). The extraction process for SEPS can be regarded as an effective pre-treatment method to entirely destroy the sludge matrix and remove the non-easily biodegradable SEPS polymers from the sludge simultaneously. The methane production after SEPS extraction and the application potential of "SEPS extraction + AD" for AGS treatment requires further investigation.

6.4 Conclusions

SEPS isolated from AGS and WAS followed similar degradation steps: (1) degradation of polysaccharides and proteins, (2) reduction of hydrogel stiffness, (3) transition of SEPS from TB-EPS to LB-EPS to slime and (4) further conversion of the slime fraction to methane. $SEPS_{AGS}$ revealed a lower degradation rate and extent than $SEPS_{WAS}$, in combination with a lower reduction in mechanical stiffness upon AD, owing to the lower degradation efficiency of key organic fractions especially polysaccharides. The perseverance of $SEPS_{AGS}$ resulted in an undisrupted residue structure of AGS after AD. In conclusion, it can be claimed that SEPS is a major constituent that resulted in the distinct digestibility between AGS and WAS in AD.

Supplementary data

Table S1 Excitation and emission (Ex/Em) wavelengths of the different fluorescence regions that can be distinguished with 3D-EEM

Region	Substance	Ex/Em wavelengths (nm)
Region I	Aromatic protein-like region	240-250/280-380
Region II	Fulvic acid-like region	240-250/380-550
Region III	Soluble microbial by-product-like region	250-340/280-380
Region IV	Humic acid-like region	250-400/380-550

Table S2 FT-IR spectra band

Frequencies (cm^{-1})	**Band assignment**
Over 3000	O–H bond stretching vibrations of polysaccharides
2927	C-H bonds associated with polysaccharides
1654	C=O stretching (amide I) and C=N stretching associated with proteins
1539	N–H and C–N stretching in amide II associated with proteins
1400	Symmetric stretching of carboxylic O-C-O vibration for polysaccharides
1240	C-N stretch associated with secondary amides of proteins (amide III)
1080	C–O and C–O–C stretching vibration of hydroxyl in polysaccharides
700-950	Fingerprint (or anomeric) region

References

APHA, 2005. Standard methods for the examination of water and wastewater, 21st Edn. American Public Health Association, Washington, DC. USA

Appels, L., Baeyens, J., Degreve, J., Dewil, R., 2008. Principles and potential of the anaerobic digestion of waste-activated sludge. Progress in Energy and Combustion Science, 34(6), 755-781.

Badireddy, A.R., Chellam, S., Gassman, P.L., Engelhard, M.H., Lea, A.S., Rosso, K.M., 2010. Role of extracellular polymeric substances in bioflocculation of activated sludge microorganisms under glucose-controlled conditions. Water Research, 44(15), 4505-4516.

Basuvaraj, M., Fein, J., Liss, S.N., 2015. Protein and polysaccharide content of tightly and loosely bound extracellular polymeric substances and the development of a granular activated sludge floc. Water Research, 82, 104-117.

Bernat, K., Cydzik-Kwiatkowska, A., Wojnowska-Baryla, I., Karczewska, M., 2017. Physicochemical properties and biogas productivity of aerobic granular sludge and activated sludge. Biochemical Engineering Journal, 117, 43-51.

Bolzonella, D., Pavan, P., Battistoni, P., Cecchi, F., 2005. Mesophilic anaerobic digestion of waste activated sludge: influence of the solid retention time in the wastewater treatment process. Process Biochemistry, 40(3-4), 1453-1460.

Chen, H.A., Zhou, S.G., Li, T.H., 2010. Impact of extracellular polymeric substances on the settlement ability of aerobic granular sludge. Environmental Technology, 31(14), 1601-1612.

Chen, W., Westerhoff, P., Leenheer, J.A., Booksh, K., 2003. Fluorescence excitation-emission matrix regional integration to quantify spectra for dissolved organic matter. Environmental Science & Technology, 37(24), 5701-10.

Das, D., Ara, T., Dutta, S., Mukherjee, A., 2011. New water resistant biomaterial biocide film based on guar gum. Bioresource Technology, 102(10), 5878-83.

Davis, B.G. and Fairbanks, A.J., 2002. Carbohydrate Chemistry. Oxford University Press. The United Kingdom.

de Kreuk, M.K., Kishida, N., van Loosdrecht, M.C.M., 2007. Aerobic granular sludge - state of the art. Water Science and Technology, 55(8-9), 75-81.

del Rio, A.V., Morales, N., Isanta, E., Mosquera-Corral, A., Campos, J.L., Steyer, J.P., Carrere, H., 2011. Thermal pre-treatment of aerobic granular sludge: Impact on anaerobic biodegradability. Water Research, 45(18), 6011-6020.

del Rio, A.V., Palmeiro-Sanchez, T., Figueroa, M., Mosquera-Corral, A., Campos, J.L., Mendez, R., 2014. Anaerobic digestion of aerobic granular biomass: effects of thermal pre-treatment and addition of primary sludge. Journal of Chemical Technology and Biotechnology, 89(5), 690-697.

Dignac, M.F., Urbain, V., Rybacki, D., Bruchet, A., Snidaro, D., Scribe, P., 1998. Chemical description of extracellular polymers: Implication on activated sludge floc structure. Water Science and Technology, 38(8-9), 45-53.

Dubois, M., Gilles, K. A., Hamilton, J. K., Rebers, P. T., & Smith, F., 1956. Colorimetric method for determination of sugars and related substances. Analytical chemistry, 28(3), 350-356.

Felz, S., Al-Zuhairy, S., Aarstad, O.A., van Loosdrecht, M.C., Lin, Y.M., 2016. Extraction of Structural Extracellular Polymeric Substances from Aerobic Granular Sludge. J Vis Exp(115), e54534.

Felz, S., Kleikamp, H., Zlopasa, J., van Loosdrecht, M.C., Lin, Y.M., 2019a. Impact of Metal Ions on Structural EPS Hydrogels from Aerobic Granular Sludge. Biofilm, in press, DOI: https://doi.org/10.1016/j.bioflm.2019.100011

Felz, S., Vermeulen, P., van Loosdrecht, M.C., Lin, Y.M., 2019b. Chemical characterization methods for the analysis of structural extracellular polymeric substances (EPS). Water Research, 157, 201-208.

Felz, S., Neu, T. R., van Loosdrecht, M. C., & Lin, Y.M., 2020. Aerobic granular sludge contains Hyaluronic acid-like and sulfated glycosaminoglycans-like polymers. Water research, 169, 115291.

Frolund, B., Griebe, T., Nielsen, P.H., 1995. Enzymatic-Activity in the Activated-Sludge Floc Matrix. Applied Microbiology and Biotechnology, 43(4), 755-761.

Frolund, B., Palmgren, R., Keiding, K., Nielsen, P.H., 1996. Extraction of extracellular polymers from activated sludge using a cation exchange resin. Water Research, 30(8), 1749-1758.

Ghasimi, D.S.M., de Kreuk, M., Maeng, S.K., Zandvoort, M.H., van Lier, J.B., 2016. High-rate thermophilic bio-methanation of the fine sieved fraction from Dutch municipal raw sewage: Cost-effective potentials for on-site energy recovery. Applied Energy, 165, 569-582.

Guo, H., van Lier, J.B., de Kreuk, M., 2020. Digestibility of waste aerobic granular sludge from a full-scale municipal wastewater treatment system. Water Research, 173, 115617.

Guo, X., Wang, X., Liu, J.X., 2016. Composition analysis of fractions of extracellular polymeric substances from an activated sludge culture and identification of dominant forces affecting microbial aggregation. Scientific Reports, 6, 28391.

Li, X.W., Dai, X.H., Takahashi, J., Li, N., Jin, J.W., Dai, L.L., Dong, B., 2014. New insight into chemical changes of dissolved organic matter during anaerobic digestion of dewatered sewage sludge using EEM-PARAFAC and two-dimensional FTIR correlation spectroscopy. Bioresource Technology, 159, 412-420.

Li, X.Y., Yang, S.F., 2007. Influence of loosely bound extracellular polymeric substances (EPS) on the flocculation, sedimentation and dewaterability of activated sludge. Water Research, 41(5), 1022-1030.

Lin, Y., de Kreuk, M., van Loosdrecht, M.C.M., Adin, A., 2010. Characterization of alginate-like exopolysaccharides isolated from aerobic granular sludge in pilot-plant. Water Research, 44(11), 3355-3364.

Lin, Y.M., Nierop, K.G.J., Girbal-Neuhauser, E., Adriaanse, M., van Loosdrecht, M.C.M., 2015. Sustainable polysaccharide-based biomaterial recovered from waste aerobic granular sludge as a surface coating material. Sustainable Materials and Technologies, 4, 24-29.

Lin, Y.M., Sharma, P.K., van Loosdrecht, M.C.M., 2013. The chemical and mechanical differences between alginate-like exopolysaccharides isolated from aerobic flocculent sludge and aerobic granular sludge. Water Research, 47(1), 57-65.

Liu, H., Fang, H.H.P., 2002. Extraction of extracellular polymeric substances (EPS) of sludges. Journal of Biotechnology, 95(3), 249-256.

Lotito, A.M., De Sanctis, M., Di Iaconi, C., Bergna, G., 2014. Textile wastewater treatment: Aerobic granular sludge vs activated sludge systems. Water Research, 54, 337-346.

Lu, F., Zhou, Q., Wu, D., Wang, T.F., Shao, L.M., He, P.J., 2015. Dewaterability of anaerobic digestate from food waste: Relationship with extracellular polymeric substances. Chemical Engineering Journal, 262, 932-938.

Luo, J., Zhang, Q., Zhao, J., Wu, Y., Wu, L., Li, H., Tang M., Sun, Y., Guo, W., Feng, Q., Cao, J., Wang, D., 2020. Potential influences of exogenous pollutants occurred in waste activated sludge on anaerobic digestion: A review. Journal of hazardous materials, 383, 121176.

Mottet, A., Francois, E., Latrille, E., Steyer, J.P., Deleris, S., Vedrenne, F., Carrere, H., 2010. Estimating anaerobic biodegradability indicators for waste activated sludge. Chemical Engineering Journal, 160(2), 488-496.

Novak, J.T., Sadler, M.E., Murthy, S.N., 2003. Mechanisms of floc destruction during anaerobic and aerobic digestion and the effect on conditioning and dewatering of biosolids. Water Research, 37(13), 3136-3144.

Palmeiro-Sanchez, T., del Rio, A.V., Mosquera-Corral, A., Campos, J.L., Mendez, R., 2013. Comparison of the anaerobic digestion of activated and aerobic granular sludges under brackish conditions. Chemical Engineering Journal, 231, 449-454.

Pronk, M., de Kreuk, M.K., de Bruin, B., Kamminga, P., Kleerebezem, R., van Loosdrecht, M.C., 2015. Full scale performance of the aerobic granular sludge process for sewage treatment. Water Research, 84, 207-17.

Salama, Y., Chennaoui, M., Sylla, A., Mountadar, M., Rihani, M., Assobhei, O., 2016. Characterization, structure, and function of extracellular polymeric substances (EPS) of microbial biofilm in biological wastewater treatment systems: a review. Desalination and Water Treatment, 57(35), 16220-16237.

Sam, S.B., Dulekgurgen, E., 2016. Characterization of exopolysaccharides from floccular and aerobic granular activated sludge as alginate-like-exoPS. Desalination and Water Treatment, 57(6), 2534-2545.

Sardari, R.R., Kulcinskaja, E., Ron, E.Y., Bjornsdottir, S., Friethjonsson, O.H., Hreggviethsson, G.O., Karlsson, E.N., 2017. Evaluation of the production of exopolysaccharides by two strains of the thermophilic bacterium Rhodothermus marinus. Carbohydr Polym, 156, 1-8.

Seviour, T., Lambert, L.K., Pijuan, M., Yuan, Z.G., 2010. Structural Determination of a Key Exopolysaccharide in Mixed Culture Aerobic Sludge Granules Using NMR Spectroscopy. Environmental Science & Technology, 44(23), 8964-8970.

Seviour, T., Pijuan, M., Nicholson, T., Keller, J., Yuan, Z.G., 2009. Gel-forming exopolysaccharides explain basic differences between structures of aerobic sludge granules and floccular sludges. Water Research, 43(18), 4469-4478.

Seviour, T., Yuan, Z., van Loosdrecht, M.C., Lin, Y., 2012. Aerobic sludge granulation: a tale of two polysaccharides? Water Research, 46(15), 4803-13.

Sun, J., Guo, L., Li, Q., Zhao, Y., Gao, M., She, Z., Wang, G., 2016. Structural and functional properties of organic matters in extracellular polymeric substances (EPS) and dissolved organic matters (DOM) after heat pretreatment with waste sludge. Bioresource Technology, 219, 614-623.

Tajmir-Riahi, H. A., 1984. Infrared spectra of crystalline β-d-glucuronic acid and its Na+, K+, and Rb+ salts. Carbohydrate research, 125(1), 13-20.

Wang, Z.W., Wu, Z.C., Tang, S.J., 2009. Extracellular polymeric substances (EPS) properties and their effects on membrane fouling in a submerged membrane bioreactor. Water Research, 43(9), 2504-2512.

Ye, F.X., Liu, X.W., Li, Y., 2014. Extracellular polymeric substances and dewaterability of waste activated sludge during anaerobic digestion. Water Science and Technology, 70(9), 1555-1560.

Yu, G.H., He, P.J., Shao, L.M., Lee, D.J., Mujumdar, A.S., 2010. Extracellular Polymeric Substances (EPS) and Extracellular Enzymes in Aerobic Granules. Drying Technology, 28(7), 910-915.

Yuan, D.Q., Wang, Y.L., Feng, J., 2014. Contribution of stratified extracellular polymeric substances to the gel-like and fractal structures of activated sludge. Water Research, 56, 56-65.

Zhang, T.T., Wang, Q.L., Khan, J., Yuan, Z.G., 2015. Free nitrous acid breaks down extracellular polymeric substances in waste activated sludge. Rsc Advances, 5(54), 43312-43318.

Zhang, X.D., Hu, J.M., Spanjers, H., van Lier, J.B., 2014. Performance of inorganic coagulants in treatment of backwash waters from a brackish aquaculture recirculation system and digestibility of salty sludge. Aquacultural Engineering, 61, 9-16.

Zheng, Y.M., Yu, H.Q., Sheng, G.P., 2005. Physical and chemical characteristics of granular activated sludge from a sequencing batch airlift reactor. Process Biochemistry, 40(2), 645-650.

Zhu, L., Zhou, J.H., Lv, M.L., Yu, H.T., Zhao, H., Xu, X.Y., 2015. Specific component comparison of extracellular polymeric substances (EPS) in flocs and granular sludge using EEM and SDS-PAGE. Chemosphere, 121, 26-32.

Chapter 7

CONCLUDING REMARKS AND OUTLOOK

7.1 Aim of the research

The research described in this thesis demonstrates the feasibility of the application of a novel anaerobic digestion (AD) process by cascading CSTRs as a pretreatment method for waste sewage sludge digestion. Besides increasing knowledge about the mechanisms behind the observed improved performance of the CAD compared to conventional AD, the process control and potential feeding substrates, such as WAGS, the performed research also resulted in the scale-up of the laboratory set-up to a full-scale design, which was tested in practice.

7.2 Concluding Remarks

The conclusions are summarized with respect to the formulated research questions:

How does the CAD configuration affect the enzymatic hydrolysis and reduction of WAS compared to a conventional digester?

The CAD demonstrated an enhanced sludge treatment capacity of 30-35% compared to a conventional sludge digester of the same volume at a total SRT of only 12 days, indicating the potential for efficient and cost-effective excess sludge treatment. The tests for hydrolytic enzyme activity revealed higher enzyme activities in the CAD than in the conventional sludge digester particularly under short SRTs, which explained the overall accelerated specific hydrolysis rate in the CAD system. In addition, several enzymes that target hydrolysis of SEPS-related organic compounds displayed reversed distribution and higher activity in the CAD than in the conventional digester, indicating an additional degradation capacity of compounds that are commonly regarded refractory in single stage digesters. The increased relative abundance of key hydrolytic bacteria found in the first 3 reactors of the CAD and the structural shift from hydrogenotrophic methanogens to acetoclastic methanogens alongside the cascade under low SRTs suggested that cascading CSTRs imposed selective pressures on the microbial population. This contributed to achieving enhanced enzymatic hydrolysis and sludge reduction, particularly under low SRT conditions.

How does digestate recirculation regulates WAS digestion in a high-rate CAD system?

Operating a short-SRT CAD system with a 10% digestate recirculation ratio resulted in a stable total chemical oxygen demand (tCOD) reduction efficiency of 40% on average; reducing the recirculation ratio to 2% led to a 14% decrease in tCOD reduction efficiency. The decline in efficiency was attributed to lower hydrolysis rates rather than methanogenesis inhibition, as inferred from the results of specific methanogenic activity (SMA) and hydrolytic enzyme activity tests. Furthermore,

recovery of tCOD conversion efficiency was achieved when only the solids fraction of the digestate was recycled at a 10% ratio, underscoring the critical role of the solids fraction in the efficiency of WAS digestion in the CAD system. Returning trace metals from a later stage to the first reactor, might be a key factor in regulating WAS hydrolysis; Mn and Zn concentrations related to the molecular size fractions ranging from 10 kDa to 100 kDa, were extracted from the solids fraction of the sludge. These trace metals, apparently bound to larger molecules, revealed a descending trend over the successive CAD reactors. Conversely, Zn and Mn concentrations in the fraction below 10 kDa exhibited an increasing trend over the successive reactors of the CAD system. It was hypothesized that these trace elements were important in the accelerated enzyme production in the first reactors in the cascade, but only liberated from the sludge fraction downstream in the cascade. Recycling Zn and Mn with the sludge fraction could have enhanced its bioavailability for enzyme production in the first reactor. Meanwhile, comparative microbial analysis of the sludge at different recirculation ratios, indicated that the solids fraction of the digestate served as a source of active hydrolytic microorganisms from the third to the first reactor of the CAD system.

What are the sludge hydrolysis and sludge reduction efficacies of the CAD process at full-scale fed with a PS - WAS mixture with fluctuating compositions?

The full-scale CAD system was retrofitted from two previously existing CSTRs at Tollebeek WWTP, the Netherlands. A mixture of WAS, PS, and a small proportion of external sludge (ES) was used as the substrate with fluctuating loading rates. The retrofit involved dividing one CSTR into three small pie-shaped reactors operated in series with a low SRT and a small recycle between the third and first reactors, followed by one large CSTR in series. Long-term operation of the CAD system demonstrated a stable and obvious higher sludge reduction efficiency of approximately 56%, compared to the situation before the retrofit. Enhanced enzymatic activity of protease and cellulase was observed in the first reactors of the full-scale CAD system. Microbial population analysis revealed a dominance of fermentative bacteria in the first three reactors and a high abundance of *Methanosaeta* in all reactors. Unlike laboratory experiments that exhibited a distinct separation of microbial populations and related conversion processes, the full-scale CAD system showed a less pronounced separation. The latter observation might be related to the pie-shaped design of this first full-scale CAD system.

Can WAGS also be a potential substrate for treatment by the CAD process, considering the differences in physicochemical properties of sludge between WAGS and WAS?

The used WAGS consisted of two fractions, namely AGS-RTC and AGS-SD, from an aerobic granular sludge full-scale process. AGS-RTC revealed a significant lower BMP than WAS. Mechanically destroying the compact structure of AGS did not affect its BMP, but accelerated the degradation rate of rapidly biodegradable organics and liberated a fraction of slowly biodegradable ones, resulting in higher methane production rate. The BMP of AGS-SD was similar to the BMP of PS, and much higher than that of AGS-RTC. Observed results were attributed to the presence of highly biodegradable and poorly settleable cellulose-like fibres that end up in AGS-SD fraction of WAGS. The degradation pattern of SEPS isolated from AGS and WAS suggested that SEPS-AGS had a lower degradation rate and extent than SEPS-WAS. In addition, also a lower reduction in mechanical stiffness upon AD was observed for SEPS-AGS, which was attributed to the lower degradation efficiency of key organic compounds, especially polysaccharides. The SEPS-AGS persistency resulted in an undisrupted residual structure of AGS after AD. The researched CAD process can be one of potential technologies to accelerate the decomposition and/or degradation of the SEPS structure of AGS-RTC (chapter 2).

7.3 Outlook and recommendations for future research

The results from this thesis give a solid basis for future research and application of the technology; recommendations for future directions are discussed in this section.

7.3.1 Sludge hydrolysis kinetics using the cascade configuration

Hydrolysis enhancement during anaerobic WAS digestion was achieved by applying a cascade reactor configuration (this thesis). Hydrolytic enzyme activities were accelerated in each subsequent reactor in the cascade. The exact reasons for this increased enzyme activity, however, are not fully clear yet. Statistical analysis, reported in chapter 2, revealed that the calculated specific hydrolysis rates were strongly dependent on applied loading rates or SRTs. This suggests that the hydrolysis kinetics in the subsequent CSTRs seemed to be more complex than the standard first-order hydrolysis model, which assumes that the only two dependencies of the hydrolysis rate are substrate concentration in the reactor and a sludge-dependent hydrolysis rate constant. It has been reported that the first-order hydrolysis rates very well fit for most easily degradable sludges and soluble substrates. However, for substrates that are more complex and more difficult to degrade, this mathematical description might need modifications (Miron et al., 2000). With the appearance of new sludge types, which are treated in new reactor systems, applied kinetic models likely need amendments to better explain the observed hydrolysis process in these systems, or for these sludges (Dharma Patria et al., 2022). A well-calibrated model may serve as a useful tool for optimization and scenario analysis to determine the performance limits

of a sludge treatment process. Therefore, increasing the understanding of hydrolysis kinetics for the CAD systems treating WAS will be of prime importance for reaching successful system control with an acceptable accuracy at full-scale.

7.3.2 Metals related to hydrolytic enzyme extract

Applying appropriate low-ratio digestate recirculation maintains efficient sludge hydrolysis of the CAD. Our results showed that suppletion of trace elements, such as Zn and Mn, via recirculation was very likely an important factor, determining the required recirculation flow (chapter 3). Fractionation of the extracted trace elements into two groups, e.g., < 10kDa and 10-100kDa, aimed to quantify the transition of metals from one group to the other group. However, the current research mainly focused on the metal fractions from the sludge-attached enzyme extract. In order to be able to obtain a mass balance for the essential metals, also the elements from the free enzyme extract has to be measured. In addition, experiments without sludge recycling but with the dosage of different (mixtures of) trace elements to study long-term reactor performance could increase our understanding of the impact of trace metals on regulating enzymatic hydrolysis.

7.3.3 CAD process at full-scale

Efficient enhancement of sludge hydrolysis by the CAD system has gained great interests in the potential usage of the system at full scale WWTPs. The proposed full-scale configuration is currently marketed by RHDHV as the Ephyra® system. At present, there are 74 Ephyra® systems in operation worldwide and various other implementation projects are being studied at pilot-scale, or full-scale reactors are being designed. Further information can be found at the company website below:

https://www.royalhaskoningdhv.com/en/services/ephyra.

Studying the conversion processes, kinetics, and microbial consortia in these full-scale applications, along the proposed different configurations, will give more insights in the process performance and optimal operational conditions.

Besides WAS, a large fraction of sludge that requires stabilization consists of PS as well. The results from chapter 4 reveal that the presence of PS in WAS led to a significant difference in, not only the performance, but also the enzymatic hydrolysis and microbial community structure of each reactor along the full-scale cascade. The degree of mixing and applied residence time in the cascade reactors affect the degree of completion of reactions, and thus biomethane potential, within the reactor. However, the impact of the unique pie-shape reactor configuration (chapter 4),

was not further investigated in this study. Therefore, it was rather difficult to determine if the observed differences in full-scale compared to lab-scale were due to the presence of PS or other differences in substrate composition, or to the differences in mixing in the pie shape reactors compared to the lab-reactors. Tracer studies that evaluate the hydraulics of the process could help to understand the effect of the different mixing regimes on the performance of full-scale CAD system.

Pipe clogging is one of main technical issues occurring in conventional full-scale sludge digesters because of extensive precipitation of struvite (Bergmans et al., 2014). In the CAD system, we observed that the majority of phosphorus and ammonia was released in the first reactor of the process (chapter 2). This phenomenon gives the possibility of controlled struvite precipitation in an early stage of the process to avoid clogging in pipelines or onto moving parts, hence minimizing maintenance costs.

7.3.4 WAGS management applying the CAD process

AD is widely used in excess sludge treatment, and AD technology is seemingly also appropriate for WAGS stabilization, converting the complex organic polymers (EPS) into methane. Nowadays there is no AD system solely fed with WAGS, but there is always co-digestion of WAS and WAGS. Very likely, this explains why the AD of WAGS was not studied in detail so far. Our present results showed rather intriguing results applying AD on the different fractions of WAGS. BMP results (chapter 5) clearly showed that AGS-SD is far less stabilized than AGS-RTC, possibly attributable to the higher amount of readily biodegradable lipids and carbohydrates in AGS-SD.

Although currently flocculent AGS-SD is the main fraction that is wasted from the Nereda® system, also the aerobic granules themselves (AGS-RTC) need to be removed from the reactor to keep the granule concentration at the required 8 to 10 g/L (Pronk et al., 2015). The differences in biodegradation kinetics between these two sludge fractions likely call for differences in AD design (Figure 7.1). A rapid direct fermentation of the easily biodegradable AGS-SD could be used to generate VFA, to be added into the anaerobic period of the Nereda® cycle for boosting the activity of phosphate accumulating organisms (PAOs) (Ortega, 2023). Unlike AGS-SD, AGS-RTC contains a substantial fraction of structural EPS, of which only 25% is anaerobically biodegradable within 20 days (chapter 6). Thus, technologies to accelerate the decomposition or degradation of this SEPS structure is highly recommended for enhancing the biogas production. Results presented in this thesis clearly showed that the CAD process enhanced the conversion of structural EPS of WAS by around 30% (chapter 2). Conversely, results indicate the potential of the cascade digestion system to effectively digest AGS-RTC, with or without AGS-SD co-digestion. Moreover, VFAs

produced in the first stage of the cascade could be used to boost the bio-P, whilst the assumed higher structural EPS degradation in the later stages could keep the biomethane production high. Possibly, a combination with destructive mechanical methods, such as crushing or ultrasound treatment, could be advantageous to quickly destroy the sludge structure and accelerate the AD process.

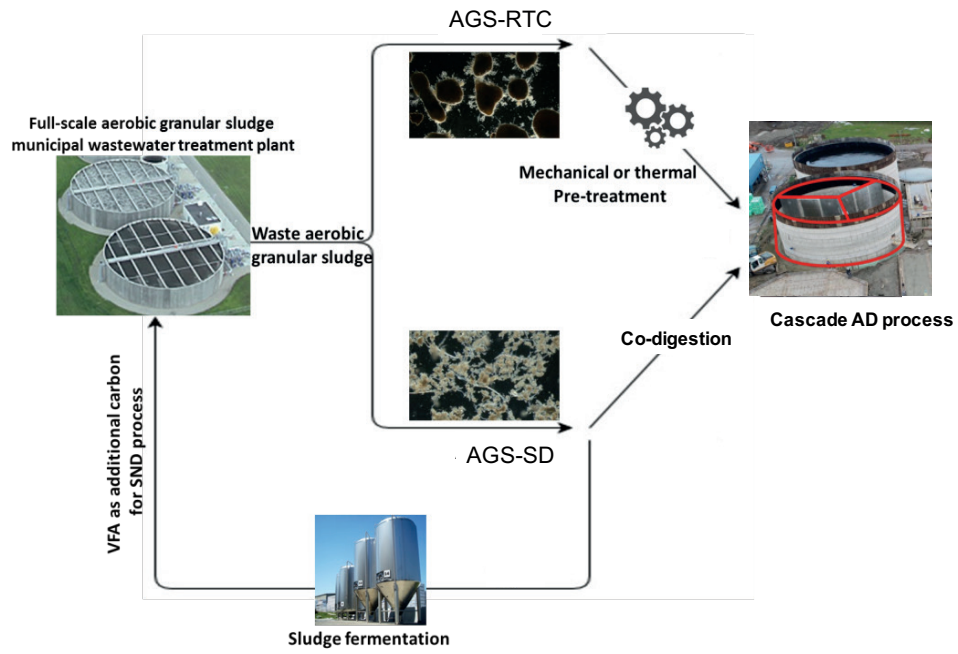

Figure 7.1 The role of the CAD process in future WAGS management

References

Miron, Y., Zeeman, G., Van Lier, J.B., Lettinga, G. 2000. The role of sludge retention time in the hydrolysis and acidification of lipids, carbohydrates and proteins during digestion of primary sludge in CSTR systems. Water Research, 34(5), 1705-1713.

Dharma Patria, R., Rehman, S., Vuppaladadiyam, A.K., Wang, H., Lin, C.S.K., Antunes, E., Leu, S.Y. 2022. Bioconversion of food and lignocellulosic wastes employing sugar platform: A review of enzymatic hydrolysis and kinetics. Bioresour Technol, 352, 127083.

Bergmans, B.J.C., Veltman, A.M., van Loosdrecht, M.C.M., van Lier, J.B., Rietveld, L.C. 2014. Struvite formation for enhanced dewaterability of digested wastewater sludge. Environmental Technology, 35(5), 549-555.

Toja Ortega, S. 2023. Conversion of Polymeric Substrates by Aerobic Granular Sludge. Ph.D. Dissertation, TU Delft